

広島大学学術情報リポジトリ  
Hiroshima University Institutional Repository

Title	Geometry and Internal Structures of Flexural Folds ( I ) Folding of a Single Competent Layer Enclosed in Thick Incompetent Layer
Author(s)	HARA, Ikuo; UCHIBAYASHI, Seiji; YOKOTA, Yuji; UMEMURA, Hayao; ODA, Masanobu
Citation	Journal of science of the Hiroshima University. Series C, Geology and mineralogy , 6 ( 1 ) : 51 - 113
Issue Date	1968-05-31
DOI	
Self DOI	<a href="https://doi.org/10.15027/53038">10.15027/53038</a>
URL	<a href="https://ir.lib.hiroshima-u.ac.jp/00053038">https://ir.lib.hiroshima-u.ac.jp/00053038</a>
Right	
Relation	



# Geometry and Internal Structures of Flexural Folds

## (I) Folding of a Single Competent Layer Enclosed in Thick Incompetent Layer

By

**Ikuo HARA, Seiji UCHIBAYASHI, Yuji YOKOTA,  
Hayao UMEMURA and Masanobu ODA**

---

*with 14 Tables, 61 Text-figures and 11 Plates*

---

(Received April 25, 1968)

**ABSTRACT:** Some problems on folding of a single competent layer enclosed in thick incompetent layer, with regard to the variation in competency difference between the related rocks, have been examined on natural flexural folds, *i. e.*, folds of quartz-rich layers in pelitic schist in the Kune district and the Oboke district, folds of quartz-rich layers in psammitic schist in the Oboke district, and folds of psammitic schist in pelitic schist in the Oboke district.

Shape and orientation of the strain ellipsoid of mean strain of small domain in the Oboke and the Kune district, at the time when the buckle folding of competent layers and the cleaving (the formation of strain-slip cleavage) of incompetent matrix in that domain occurred, have been determined. The strain-slip cleavage in the incompetent matrix is correlated with the plane normal to the direction of maximum shortening, *i. e.*, the principal plane XY of the mean strain ellipsoid.

Geometric relationships between the strain ellipsoid of mean strain of a domain and geometric elements of buckle folds have been examined, especially where the enveloping surfaces of folded competent layers are inclined at angles of between 50° and 60° to the principal plane XY. At the initial stage of folding the axial surface shows a tendency to be normal to the layer being folded. For some folds the axial surfaces are completely rotated toward the principal plane XY when the interlimb angle becomes 90°-100°, but for some other folds they remain normal to the layer even when the interlimb angle becomes 70°-80°. When the interlimb angle becomes smaller than 70°-80°, the axial surfaces of all folds tend to rotate toward the principal plane XY. Although geometric relationship between the fold axes and the mean strain ellipsoid has not been strictly determined, the former does not appear to lie on the principal plane XY.

The intensity of folding of competent layers, which is estimated by interlimb angle, is maximum for the layers parallel to the schistosity of the incompetent matrix and to the principal axis Z, and minimum for those normal to the schistosity and parallel to the axis Z, that showing the competency difference between different directions in the incompetent matrix, that is, the maximum competency in a direction parallel to the schistosity and the minimum in a direction normal to it.

It has been clarified that for the folds of quartz-rich layers in pelitic schist of the Kune district and the Oboke district and those in psammitic schist of the Oboke district a linear relationship exists between the length of arc (L) and the thickness of the quartz-rich layer (T). In the former cases, the average L/T ratios are 14.9 (Kune) and 16.2 (Oboke), and the minimum L/T ratios are 9.1 and 11.6, while in the latter case the average L/T ratio is 11.6 and the minimum L/T ratio 5.8, respectively. Folds of psammitic layers in pelitic schist show frequently L/T ratios smaller than 1.00.

On the assumption that during the folding pelitic schist, psammitic schist and quartz-rich layer behaved mechanically as Newtonian substance, the ratios of viscosity coefficient between those rocks have been estimated by using the average L/T ratios according to the wavelength equation of BIOT (1961). In the Oboke district, the viscosity ratio between the quartz-rich layer and the psammitic schist is ca. 38, that between the quartz-rich layer and the pelitic schist ca. 102, and that between the psammitic schist and the pelitic schist ca. 3 (indirectly estimated). In the Kune district, the viscosity ratio between the quartz-rich layer and the pelitic schist is ca. 80.

The relationship between the mechanisms of buckle folding and the internal structures, between the folding

mechanisms and the viscosity ratios of the related rocks and between the folding mechanisms and the orientational relation of the buckled layer to the mean strain ellipsoid of the domain concerned have also been examined.

Internal structure of buckle fold appears to be commonly characterized by the cleavage which is correlated with the principal plane  $XY$  of mean strain ellipsoid at any position of the fold. When buckled competent layer is a schistose rock, the cleavage is referred to the type of strain-slip cleavage, while for non-schistose rock it is referred to the type of flow cleavage.

The strain pictures developed during the buckle folding of competent layers which are parallel or subparallel to the principal axis  $Y$  (the intermediate axis = constant) have been classified into the following five types; Type I — the neutral axis is located at or near the middle part of fold knee, and the part of no-distortion is further developed at the inflection point and on the outermost side of the limbs. The principal axes  $X$  (the maximum extension axis) and  $Z$  (the maximum contraction axis) are oriented normal to the fold axis. Type II — the neutral axis is developed at the outermost part of fold knee, and the part of no-distortion is rarely developed on the limbs. The principal axes  $X$  and  $Z$  are oriented normal to the fold axis, and the principal axis  $X$  is radially arranged through the fold. Type III — the neutral axis is not developed within the layer. The principal axes  $X$  and  $Z$  are oriented normal to the fold axis, though at the outermost part of fold knee  $X=Y$ . The principal axis  $X$  is radially arranged through the fold. Type IV — the neutral axis is not developed within the layer. At any position of the fold the mean strain ellipsoid is of the triaxial type. The principal axes  $X$  and  $Z$  are oriented normal to the fold axis. The principal axis  $X$  is radially arranged through the fold. Type V — although the strain picture of this type may be essentially the same as that of Type IV, the angle  $\beta$  (angular deviation of the principal axis  $X$  between both limbs) for the former is much smaller than that for the latter. The change of the strain picture from Type I to Type V corresponds to the decrease of the angle  $\beta$ . The strain pictures of Type I, Type II, Type III, Type IV and Type V are never the end member.

The folds of quartz-rich layers in pelitic schist of the Kune district show the strain pictures of Type I, Type II and Type III, while those in psammitic schist show the strain pictures of Type II, Type III and Type IV. The folds of psammitic layers in pelitic schist show the strain picture of Type V. A definite relationship exists between the mechanisms of folding and the viscosity ratios of the related rocks, that is, the change of the strain picture from Type I to Type V corresponds to the decrease in the viscosity ratio, that showing a good agreement with RAMBERG's theory (1964). Namely, the decrease of viscosity ratio of the related rocks corresponds to the increase of distance of between the neutral axis and the bottom surface of fold knee of the competent layer, and to the decrease of the angle  $\beta$ , when compared between the folds with the same interlimb angle and the same initial thickness of layer. It has been pointed out that, if any fold is characterized the fan-like arrangement of cleavage with downward convergence, buckling instability played in general the by important role in the development of the fold.

The nature of change of layer-thickness due to buckling has also been examined. For folds which show orthorhombic or near orthorhombic symmetry and larger interlimb angles, the competent layers show generally a tendency to be thickened at all positions of the folds and the amount of thickening appears to be maximum at the fold knee and minimum at the inflection point. The nature of change of layer-thickness due to buckling appears to be closely related to the type of strain picture (Type I to Type V) which is controlled by the viscosity ratio of the related rocks: with respect to the whole amount of layer shortening, the amount of layer thickening at the fold knee and the inflection point, and the difference in the amount of layer thickening between these two positions, Type I < Type II < Type III < Type IV < Type V, when compared between the folds with the same interlimb angle. Roughly speaking, the layer shortening due to the folding (interlimb angle = ca.  $65^\circ$ ), which is characterized by the formation of the strain picture of Type I, may be less than ca. 10 per cent. That due to the folding for the strain picture of Type II may be between ca. 10 per cent and ca. 15 per cent. And, that due to the folding for the strain picture of Type IV—Type V may be larger than ca. 15 per cent. For the fold of competent layer, therefore, the present length of arc is not always equal to the initial fold wavelength. From the measurement of the layer shortening for the folds of quartz-rich layers in the Kune district and the Oboke district, the average  $L/T$  ratios and the viscosity ratios between the related rocks have been re-estimated.

## Geometry and Internal Structures of Flexural Folds

### CONTENTS

- I. Introduction
  - II. Geometric relationship between strain ellipsoid of mean strain of a system and geometric elements of buckle folds of competent layers involved
  - III. Relationship between fold wavelength and thickness of buckled competent layers
  - IV. Internal structures in buckled competent layers
  - V. Distribution of layer-thickness in buckle folds
- References

### I. INTRODUCTION

In folding of heterogeneously layered rocks under lateral compression, of which some layers are competent and others are incompetent, the mechanism of folding of competent layers involves buckling and material of incompetent layers adjusts itself to interspace by passive flow. Such folding of heterogeneously layered rocks, which is referred to the type of flexural folding, appears to be the most predominant in geologic deformation. Some problems on the flexural folding of this type will be examined in this paper.

Essential difference between various mechanisms of flexural folding of heterogeneously layered rocks appears to be mainly due to the competency difference between the competent layers and the surrounding incompetent layers combined with the spacing between the competent layers, according to theoretical and experimental studies on rock folding after BIOT (1961, 1964, 1965a, 1965b and 1965c, etc), RAMBERG (1959, 1960, 1963 and 1964, etc) and CURRIE, PATNODE and TRUMP (1962) and observations of natural flexural folds after the senior author (HARA, 1963, 1966b, 1966c and 1967). In the present paper (Part I), therefore, will be examined some problems on the folding of a single competent layer enclosed in a thick incompetent layer, with regard to the variation in the competency difference between the former and the latter layers, while problems on the folding of multilayered rock system will be examined in the following paper (Part II).

The authors wish to express their sincere thanks to Prof. G. KOJIMA for his critical review of the manuscript. The field works for this study have been supported in part by the Grant in Aid for Scientific Researches from the Ministry of Education.

### II. GEOMETRIC RELATIONSHIP between STRAIN ELLIPSOID of MEAN STRAIN of a SYSTEM and GEOMETRIC ELEMENTS of BUCKLE FOLDS of COMPETENT LAYERS INVOLVED.

It is very important to understand how the geometric elements of buckle folds of competent layers involved in a system are geometrically related to the strain ellipsoid of mean strain of the system. However, this problem has not so far been clarified on

natural flexural folds. Recently, theoretical and experimental studies on this problem have been made by RAMBERG (1959), FLINN (1962), MCBIRNEY and BEST (1961), GHOSH (1966) and RAMSAY (1967). According to the theoretical study after FLINN, the axis on which buckling of any competent layer involved in a system takes place can be predicted from the mean strain ellipsoid of the system, for it will be one of the two principal birections of a section (strain ellipse) in which the competent layer cuts that ellipsoid. If one principal direction in a section is a direction of shortening, then buckling can occur parallel to the other principal direction in that section. On the other hand, if one principal direction is the direction of extension, then boudinage can occur parallel to the other. He also says, "what cannot be predicted is the attitude of the axial plane in a newly generated fold. It is possible that the newly generated axial plane will be normal to the layer being folded. ...." (p. 424). The conclusions drawn by FLINN (1962) for the relationship between the geometric elements of buckle folds (fold axis and axial plane) and the mean strain ellipsoid agree with the results from model experiments after GHOSH (1966). While, model experiments after MCBIRNEY and BEST (1961) gave the conclusion that "the orientation of linear features and fold axes produced by deformation of viscous materials is determined by the intersection of the layered surface and a plane normal to the direction of maximum shortening and is independent of the minimum and intermediate bulk strain axes. ...." (p. 498), unlike the case of GHOSH.

In this chapter the above-described problem will be examined on two examples: folds of quartz-rich layers (quartz veins) enclosed in the psammitic schist of the Oboke district, Shikoku, and those in the pelitic schist of the Kune district, Shizuoka Prefecture.

Firstly, Some structural features of the psammitic schist of the Oboke district (in positions 1 and 2 in Fig. 1) will briefly be described. Fig. 1 shows the distribution and major structure of the psammitic schist in the Oboke district. The major structure is characterized by an anticline with open form, the Oboke anticline, and a syncline with open form, the Koboke syncline, (KOJIMA, 1951; KOJIMA and MITSUNO, 1966). The psammitic schist shows a distinct schistosity defined by preferred orientation of flaky minerals, which is parallel to the bedding plane. The schistosity ( $S_1$  in HARA *et al.* 1966) is markedly folded in various scales. Folds of all scales share the same fold axis and approximately the same axial plane, showing that they are referred

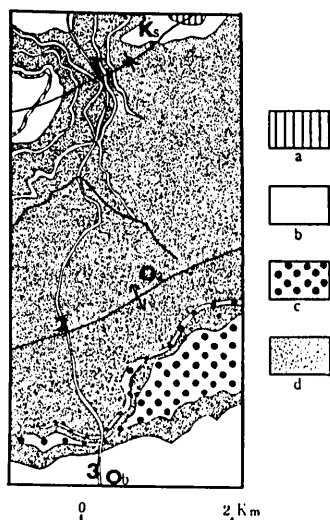


FIG. 1 Geological map of the Oboke district (after KOJIMA and MITSUNO, 1966).

- a: basic schist.
- b: pelitic schist.
- c: conglomerate schist.
- d: psammitic schist.
- Oa: Oboke anticline.
- Ks: Koboke syncline.
- Ob: Oboke.

to the type of parasitic fold in relation to the Oboke anticline and Koboke syncline, and appear to belong to the same generation. Folds of the smallest scale (here termed  $B_2^S$ -fold), which are shown by crenulation of flaky minerals, have generally wavelength of less than several millimeters, and they are frequently associated with microfault parallel to the axial surfaces. Therefore, it can be said that the structure in question is identical with a cleavage structure referred to the type of the strain-slip cleavage (KNILL, 1960; TURNER and WEISS, 1963;  $S_2$  in HARA *et al.* 1966). The  $B_2^S$ -folds appear to develop in all parts of the psammitic schist, though the intensity of development varies from place to place.

In the psammitic schist of the Oboke district Kink bands are rarely found. They are a structure of the latest stage of deformation, as well as jointing and faulting. Therefore, the tectonic history of the psammitic schist of the Oboke district (in positions 1 and 2 in Fig 1) can be roughly said in the order of younging as follows: 1) the deformation related to the  $S_1$ -schistosity (here termed  $S_1$ -deformation), 2) the deformation

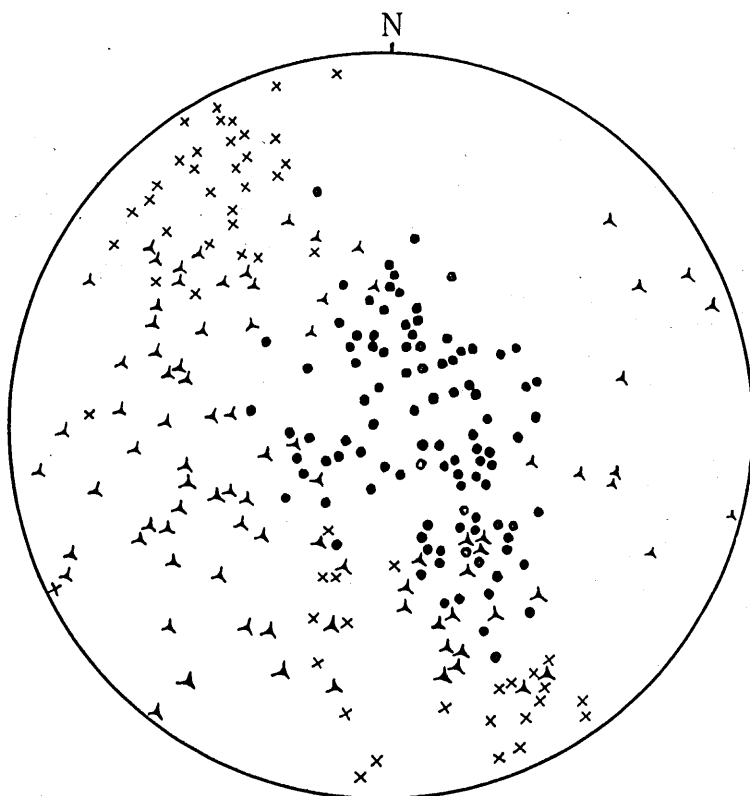


FIG. 2 Diagram for poles of folded and non-folded quartz-rich layers enclosed in the psammitic schist of the small domain (position 1 in Fig. 1) of the hinge zone of the Koboke syncline.

Crosses: non-folded quartz-rich layers. Triangles: weakly folded quartz-rich layers. Solid circles: intensely folded quartz-rich layers.

related to the  $B_2^S$ -fold (here termed  $B_2$ -deformation). 3) kinking, jointing and faulting.

In the psammitic schist there are many quartz-rich layers (quartz veins), which were formed after the  $S_1$ -deformation and suffered the  $B_2$ -deformation. Those layers are running parallel or oblique to the  $S_1$ -schistosity. Some quartz-rich layers appear to have been formed after the  $B_2$ -deformation. The folds of the quartz-rich layers which were formed during the  $B_2$ -deformation will be designated  $B_2^m$ -fold.

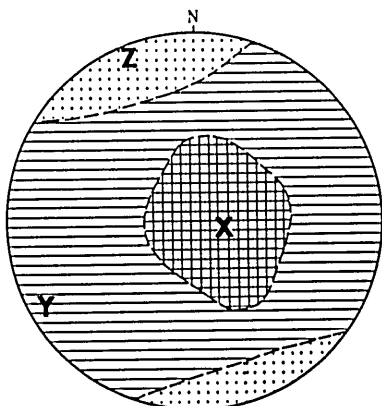


FIG. 3 Diagram showing the distribution of the non-folded area (stipled), weakly folded area and strongly folded area (crossed) drawn on the basis of Fig. 2. X, Y, and Z: The three principal axes of mean strain ellipsoid.

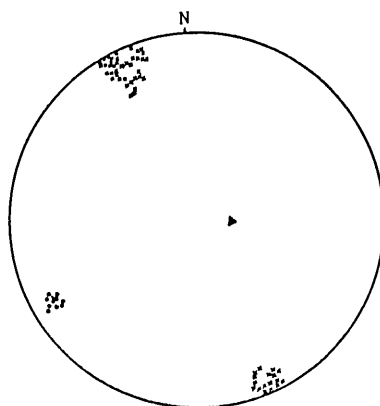


FIG. 4 Diagram showing orientation data of  $S_1$ -schistosity,  $S_2$ -cleavage and  $L_{1-2}$ -lincation in the psammitic schist of the small domain of the hinge zone of the Kobokey syncline. Crosses:  $S_2$ -cleavage. Solid circles:  $L_{1-2}$ -lincation. Triangle: general trend of  $S_1$ -schistosity.

The metamorphism of the Sambagawa belt in Shikoku belongs to the high-pressure intermediate group of the metamorphic facies series after MIYASHIRO (1965). The metamorphic grade of the psammitic schist of the Oboke district corresponds to that of the zone II of the Kotsu-Bizan district, east of Oboke, studied by IWASAKI (1963), according to his personal communication (IWASAKI, 1965).

In the psammitic schist involved in a small domain (ca. 30 m<sup>2</sup>) of the hinge zone of the Kobokey syncline (position 1 in Fig. 1) there are many quartz-rich layers which show various orientation (Plate 5). Within this small domain, geometric relationship between the geometric elements of buckle folds of the quartz-rich layers and the strain ellipsoid of mean strain of the psammitic schist has been examined. According to RAMBERG's (1959), FLINN's (1962) and RAMSAY's (1967) works on rock folding, the shape and orientation of the mean strain ellipsoid of the psammitic schist in this domain is determined by the analysis of the orientation of quartz-rich layers, some of which show folding of various intensity while others do not show folding.

Fig. 2 is the diagram for poles of quartz-rich layers in the psammitic schist in the

small domain in question. Some of these layers whose poles also are plotted in Fig. 2 appear to have been formed after the  $B_2$ -deformation. The folded quartz-rich layers are grouped into two types: 1) intensely folded quartz-rich layers which are folded with the interlimb angles of smaller than  $90^\circ$ , and 2) weakly folded quartz-rich layers which are folded with the interlimb angles of larger than  $90^\circ$ . The diagram (Fig. 2) may be schematically divided into three areas, that is, the non-folded area, the weakly folded area and the intensely folded area, as shown in Fig. 3. Thus, it will be concluded that the deformation of the psammitic schist within the domain in question is statistically homogeneous, that the principal axis Z (the direction of maximum contraction) of the mean strain ellipsoid of this domain is placed at the center of the non-folded area in Fig. 3 and that the principal axes X (the direction of maximum extension) and Y (the intermediate axis) are oriented on the girdle containing the weakly folded and the intensely folded areas.

Before the  $B_2$ -deformation occurred, the Oboke psammitic schist appears to have been structurally characterized by the development of a single set of schistosity parallel to the bedding plane which was defined by the preferred dimensional orientation of mineral grains such as mica, chlorite and quartz, associated with the preferred lattice orientation of those minerals. Therefore, it should be assumed that during the  $B_2$ -deformation the psammitic schist was never homogeneous and isotropic but strongly anisotropic, and so that the resistance which the psammitic schist offered against the contact strain set up by the folding of the quartz-rich layers was different in intensity between different directions. Such anisotropy of the psammitic schist would have influenced strongly the mechanism of folding of the quartz-rich layers. RAMBERG (1964, p. 307) says, "affected" by lateral compression, a "competent" sheet of rock enclosed in a less "competent" host, shortens by two unlike mechanisms; viz., (1) by buckling (buckle shortening) and (2) by uniform strain along the sheet (layer shortening). The relative rate of these two types of shortening depends chiefly upon the relative competency of the host and the enclosed sheet. The greater the contrast in competency (viscosity, rigidity), the higher the rate of buckle shortening relative to the rate of layer shortening. Therefore, if rock sheets with unlike competency are enclosed in a given host, ..... a given amount of compression is likely to result in quite unlike finite strain patterns of the several sheets. The least competent sheet ..... becomes shortened and thickened with only negligible folding, whereas the more competent sheet ..... responds to the compressive stress essentially by buckling. ...." The buckling of a competent layer enclosed in incompetent layer is resisted by two distinct forces, according to RAMBERG (1960): 1) the resistive force the competent layer itself offers against buckling, and 2) the resistance which the incompetent layer offers against the development of the contact sinusoidal strain due to folding of the competent layer. The general trend of the  $S_1$ -schistosity surface in the examined domain is parallel to the principal strain axis Z and the  $L_{1-2}$ -lineation (Fig. 4). Therefore, the difference in intensity of folding between the quartz-rich layers parallel to the principal axis Z and normal to the  $L_{1-2}$ -lineation (those normal to the bedding schistosity) and

those parallel to the axis Z and the  $L_{1-2}$ -lineation (those parallel or subparallel to the bedding schistosity), shown in Fig. 2, may be interpreted in terms that the resistance which the psammitic schist offered against the development of the contact strain due to the folding of the quartz-rich layers was maximum in a direction parallel to the  $L_{1-2}$ -lineation (for the former case) and minimum in that normal to the schistosity surface (for the latter case).

The strain distribution in the folded quartz-rich layers enclosed in the psammitic schist of the domain in question, which will be in details examined in the later pages, is quite different between those parallel or subparallel to the principal axis Z and the  $L_{1-2}$ -lineation and those normal or subnormal to the  $L_{1-2}$ -lineation. For the former case, generally, the shape and orientation of the mean strain ellipsoid of quartz aggregate at the fold knee will be explained as follows:  $X > Y > Z$ , and X and Z are oriented on the plane normal to the fold axis. While, for the latter case,  $X \approx Y > Z$ , and Z is oriented on the plane normal to the fold axis. Thus, it may be concluded that the mean strain ellipsoid of the psammitic schist within the domain in question is of the triaxial type and that the principal axes Y and X are oriented approximately parallel to the  $L_{1-2}$ -lineation, (therefore the axis Y coincides approximately with the center of the weakly folded area in Fig. 3), and normal to the  $L_{1-2}$ -lineation and the principal axis Z, (the axis X coincides approximately with the center of the strongly folded area in Fig 3), respectively.

Quartz-layers parallel or subparallel to the principal plane XY do not appear to show folding and boudinage. In the psammitic matrix there is no linear structure that is oblique to the  $L_{1-2}$ -lineation and belongs to the same generation as it. Therefore, it may be assumed that during the  $B_2$ -deformation the contraction (or extension) in a direction parallel to the principal axis Y was negligible.

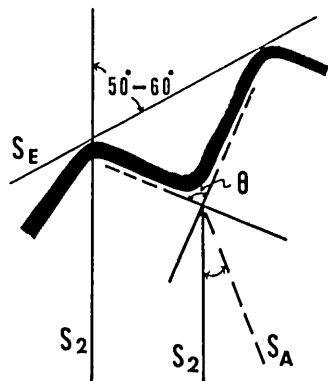


FIG. 5 Diagram illustrating the interlimb angle  $\theta$  and  $S_A \wedge S_2$  for a quartz-rich layer.

$S_E$ : enveloping surface of folded quartz-rich layer.  $S_A$ : axial surface.  $S_2$ :  $S_2$ -cleavage.

Fig. 4 shows the orientation patterns of the  $S_2$ -cleavage surface and the  $L_{1-2}$ -lineation. From Figs. 3 and 4, it can be further pointed out that the  $S_2$ -cleavage surface in the psammitic schist is parallel to the principal plane XY of the mean strain ellipsoid, that is, normal to the direction of the maximum shortening, and that  $L_{1-2}$ -lineation (=the axis of the Koboke syncline) is parallel to the principal axis Y. The strain-slip cleavage has been correlated either with the plane of shearing (e. g. WILSON, 1949) or with the plane of flattening (e. g. WILLIAMS, 1961). In the present case, the  $S_2$ -cleavage (= strain-slip cleavage) appears to be correlated with the plane of flattening.

Next, we are going to examine the geometric relationship between the above-analysed mean strain

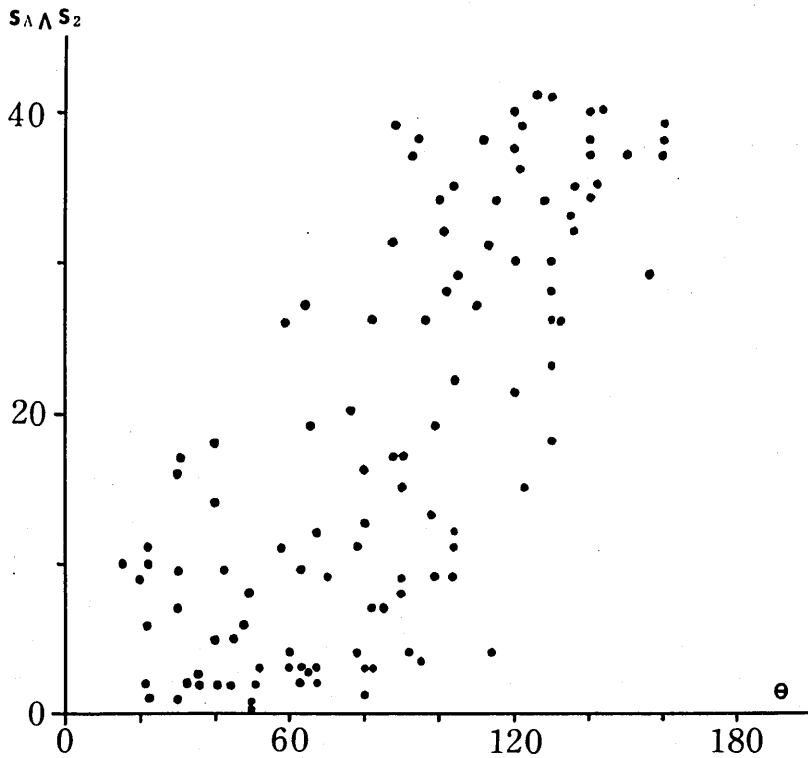


FIG. 6 Diagram showing the relationship between the angle  $S_A \wedge S_2$  and  $\theta$  for the folds of quartz-rich layers in the psammitic schist of the small domain of the hinge zone of the Koboike syncline, whose enveloping surfaces are inclined at angles of between  $50^\circ$  and  $60^\circ$  to the  $S_2$ -cleavage (=the principal plane XY of the mean strain ellipsoid of this domain).

ellipsoid of the psammitic schist and the axial surface of folds of the quartz-rich layers involved in that schist.

Especially, this problem will be examined on the folds whose enveloping surfaces are inclined at angles of between  $50^\circ$  and  $60^\circ$  to the  $S_2$ -surfaces (=the principal plane XY of the mean strain ellipsoid) and whose axes are parallel to the  $L_{1-2}$ -lineation (=the intermediate axis of the mean strain ellipsoid) (Fig. 5). In the present case, the axial surface of a fold corresponds to the bisecting surface of that fold, as shown in Fig. 5. Fig. 6 shows the relation of the angle between the axial surface and  $S_2$ -surface for a fold ( $S_A \wedge S_2$ ) to the interlimb angle ( $\theta$ ) for that fold. According to Fig. 6, for the folds of quartz-rich layers whose interlimb angles are larger than  $135^\circ$ , the axial surfaces show a tendency to be normal to the layer surface. This fact appears to show that at the initial stage of buckle folding generally the axial surfaces develop normal the layer being folded, that showing an agreement with the result from model experiment after RAMBERG (1959) and GHOSH (1966). Furthermore, Fig. 6 shows that for some folds the axial surfaces are completely rotated toward the principal plane XY

when  $\theta$  becomes less than  $100^\circ$ , but that for some other folds the axial surfaces remain normal to the layer surface even when  $\theta$  becomes  $80^\circ$ , and that, when  $\theta$  becomes less than  $80^\circ$ , the axial surfaces of all folds tend to rotate toward the principal plane XY.

Geometric relationship between the axes of folds of quartz-rich layers and the mean strain ellipsoid of the psammitic schist within the domain in question is illustrated in Fig. 7. The fold axes are plotted on a broad great-circle girdle normal to the principal axis Z of the mean strain ellipsoid. Strictly speaking, however, it is not apparent only from Fig. 7 whether the axes of folds of quartz-rich layers in question lie within the plane normal to the direction of the maximum shortening as is the case of model experiment after MCBIRNEY and BEST (1961) or they develop parallel to the principal direction of the strain ellipse on the enveloping surface of the quartz-rich layer as is the case of model experiment after GHOSH (1966). Although the  $L_{1-2}$ -lineation just outside the folded quartz-rich layers appears to be generally parallel to the fold axes

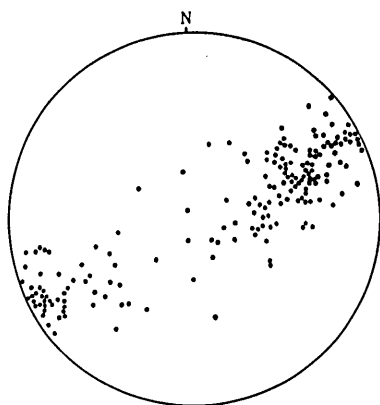


FIG. 7 Diagram showing the orientation of the axes of folds of quartz-rich layers in the psammitic schist of the small domain of the hinge zone of the Koboke syncline.

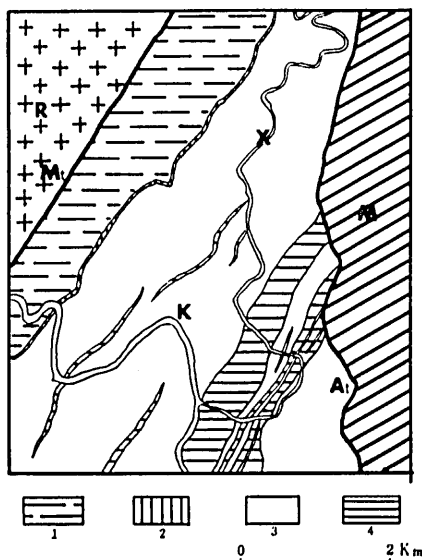


FIG. 8 Geological map of the Kune district (by the staff of the Furukawa Mining Company Ltd).

1: alternation of pelitic schist and basic schist. 2: crystalline limestone. 3: pelitic schist. 4: basic schist.

R: Ryoke metamorphic zone. M: Mesozoic rocks.  $M_1$ : Median tectonic line.  $A_1$ : Akaishi tectonic line. K: Kune.

of these layers, the width of the girdle in Fig. 7 does not appear to correspond to the range of variation in attitude of the  $S_2$ -cleavage in this domain. The former fact will be explained in terms that the cleavage-attitude just outside a competent layer is controlled by the development of contact strain due to the folding of the layer.

Therefore, it does not seem probable that the axes of folds of quartz-rich layers lie within the principal plane XY.

The same problems on the geometric relationship between the mean strain ellipsoid of a system and the geometric elements of buckle folds of competent layers involved have also been examined on the folds of quartz-rich layers (quartz veins) enclosed in the pelitic schist (micarich layer) in the Kune district. Fig. 8 is the geological map of the Sambagawa crystalline schists of the Kune district. The Sambagawa crystalline schist of this district tends to dip at moderate angles toward NW. In a small domain of the Kune district where the above-described problems have been examined (position X in Fig. 8), however, the schist shows a tendency to dip homoclinally at low to high angles toward SW.

The pelitic schist in this domain, as well as that in other domains of the Kune district, shows a distinct schistosity defined by preferred orientation of flaky minerals, which is parallel to the bedding plane. The schistosity ( $S_1$  in HARA, 1966a) is markedly folded in various styles and scales. The folds and related structures in the pelitic schist, observed on the scale of the outcrop, have been classified into the following three groups in the order of younging by the senior author (HARA, 1966a); 1)  $B_1$ -fold— intraforial folds, which occur as tectonic inclusions in the schistosity surfaces. The deformation related to the formation of the  $B_1$ -fold will be named  $B_1$ -deformation. 2) Folds and cleavages as designated  $B_2^l$ -fold,  $B_2^m$ -fold,  $S_{2q}$ -cleavage and  $S_{2m}$ -cleavage ( $B_2^s$ -fold)— flexural folds, whose axial surfaces are generally inclined at moderate to high angles to the schistosity surfaces, and cleavage structures as microfault associated with those flexural folds. The folds described in terms of  $B_2^l$ -fold and  $B_2^m$ -fold are the folds of quartz-rich layers enclosed in the pelitic schist which have wavelength of several centimeters to some tens centimeters and that of several millimeters to a few centimeters respectively. For the former is essentially the same as the latter (HARA,

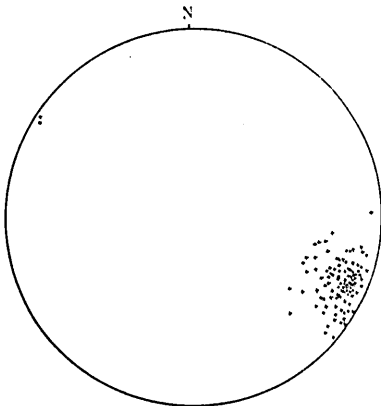


FIG. 9 Diagram showing the orientation of the  $S_{2m}$ -cleavage surfaces in the pelitic schist of the small domain at the position X in Fig. 8.

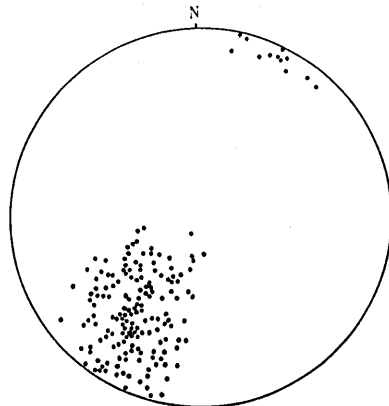


FIG. 10 Diagram showing the orientation of the  $L_{1-2}$ -lineation in the pelitic schist of the small domain at the position X in Fig. 8.

1966b), they will be collectively named  $B_2^m$ -fold in this paper. The  $S_{2,1}$ -cleavage is a cleavage structure formed by transposition of the quartz-rich layers on the limbs of  $B_2^m$ -folds. The  $S_{2,m}$ -cleavage ( $B_2^s$ -fold) is a cleavage structure referred to the type of the strain-slip cleavage, that is found only in the pelitic schist (see HARA, 1966a) (Plates 2 and 3). The  $S_{2,1}$ -cleavage and the  $S_{2,m}$ -cleavage, which belong to the same generation, are commonly parallel to each other. The deformation related to the formation of the  $B_2^m$ -fold,  $S_{2,1}$ -cleavage and  $S_{2,m}$ -cleavage will be named the  $B_2$ -deformation. And, 3) kink bands (HARA, 1965).

The  $B_2$ -deformation which the pelitic schist in the domain in question experienced appears to be divided into two separate episodes. The  $B_2^m$ -fold,  $S_{2,1}$ -cleavage and  $S_{2,m}$ -cleavage formed during the  $B_2$ -deformation of the first episode (here termed the  $B_{2-1}$ -deformation) are very pronounced, while the  $B_2$ -deformation of the second episode (here termed the  $B_{2-2}$ -deformation) is quite insignificant. During the  $B_{2-2}$ -deformation, only the  $S_{2,m}$ -cleavage appears to have been very weakly developed.

Figs. 9 and 10 show the orientation data for the  $S_{2,m}$ -cleavage in this domain, which

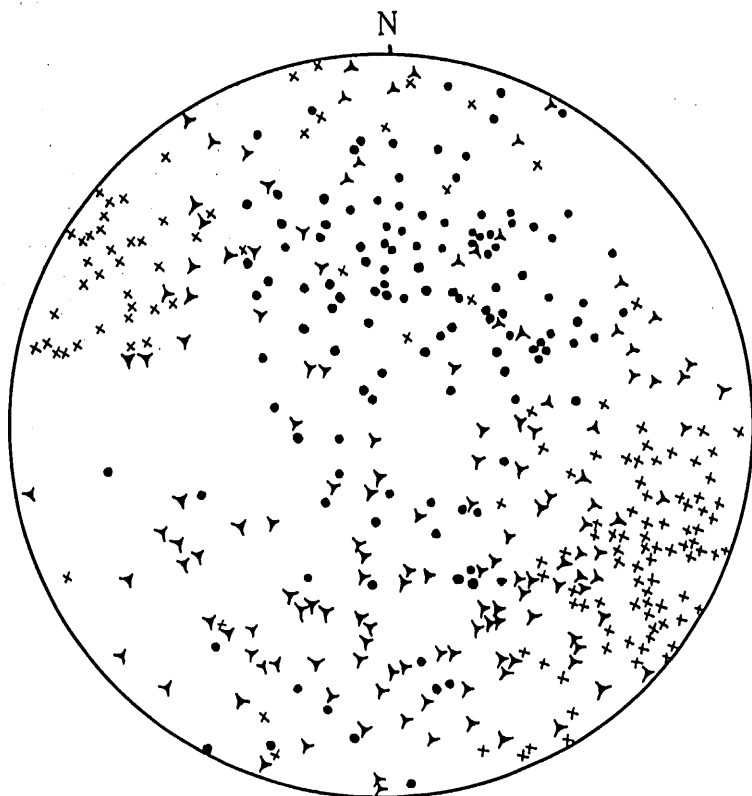


FIG. 11 Diagram for poles of folded and non-folded quartz-rich layers in the pelitic schist of the small domain at the position X in Fig. 8. Crosses: non-folded quartz-rich layers. Triangles: weakly folded quartz-rich layers. Solid circles: strongly folded quartz-rich layers.

was formed during the  $B_{2-1}$ -deformation. The  $S_{2m}$ -cleavage surfaces (Fig. 9) are constant in attitude and oriented with the inclination of ca.  $78^\circ$  toward  $N65^\circ W$ . While, the lines of intersection of the  $S_1$ -schistosity and the  $S_{2m}$ -cleavage (here termed the  $L_{1-2}$ -lineation) are preferably oriented with the plunges of various angles toward SW (Fig. 10), this variation in plunge being mainly due to the variation in initial attitude of the  $S_1$ -schistosity surfaces.

The metamorphism of the Sambagawa belt in the Chubu Province belongs to the high-pressure intermediate group of the metamorphic facies series after MIYASHIRO (1965). The metamorphic grade of the pelitic schist in this domain corresponds to that of the zone II of the Tenryū district, south of Kune, studied by SEKI (1961). That appears to be approximately the same as the metamorphic grade of the Oboke psammitic schist.

Fig. 11 is a diagram for poles of quartz-rich layers in the pelitic schist in this domain. Some of these quartz-rich layers whose poles also are plotted in Fig. 11 appear to have been formed after the  $B_{2-1}$ -deformation. The diagram may be schematically divided into three areas, as shown in Fig. 12, that is, the non-folded area, the weakly folded area and the strongly folded area, although even within the weakly folded area there are some poles of strongly folded quartz-rich layers and some poles of weakly folded quartz-rich layers are also found within the strongly folded area. Thus, it will be concluded that the  $B_{2-1}$ -deformation of the pelitic schist in this domain is statistically homogeneous, and the principal axis Z of the strain ellipsoid is placed at the center of the non-folded area in Fig. 12 and the principal axes X and Y are oriented on the great-circle containing the weakly folded and the strongly folded area, according to RAMBERG's (1959), FLINN's (1962) and RAMSAY's (1967) works on rock folding.

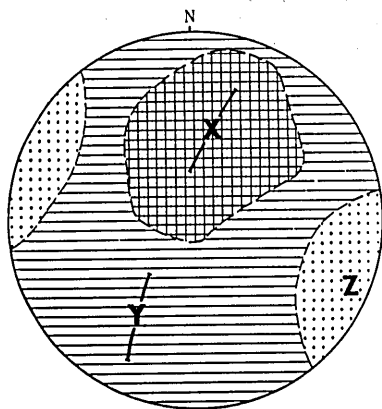


Fig. 12 Diagram showing the distribution of the non-folded area (stippled) weakly folded area and strongly folded area (crossed) drawn on the basis of Fig. 11.

X, Y and Z: The three principal axes of mean strain ellipsoid.

Many of the weakly folded quartz-rich layers show a tendency to incline at high angles to the  $S_1$ -schistosity, while most of the strongly folded quartz-rich layers are oriented parallel or sub-parallel to the  $S_1$ -schistosity. Before the  $B_{2-1}$ -deformation occurred, the pelitic schist in this domain would have been structurally characterized by the development of a single set of schistosity parallel to the bedding plane, for the  $B_1$ -fold is only rarely found in this domain. Therefore, the difference in intensity of folding between the quartz-rich layers parallel or sub-parallel to the  $S_1$ -schistosity and the  $L_{1-2}$ -lineation (strongly folded) and those normal or subnormal to the  $S_1$ -schistosity and the  $L_{1-2}$ -lineation (weakly folded), shown in Fig. 11, may be interpreted in terms that the resistance, which the pelitic schist offered against the development

and during the  $S_1$ -deformation. The  $S_2$ -cleavage surfaces (Fig. 9) are  
 tilted and oriented with the inclination of ca. 78° toward N 65° W.  
 The intersection of the  $S_1$ -schistosity and the  $S_2$ -cleavage formed  
 is probably oriented with the plunges of various angles toward  
 in plane being mainly due to the variation in initial

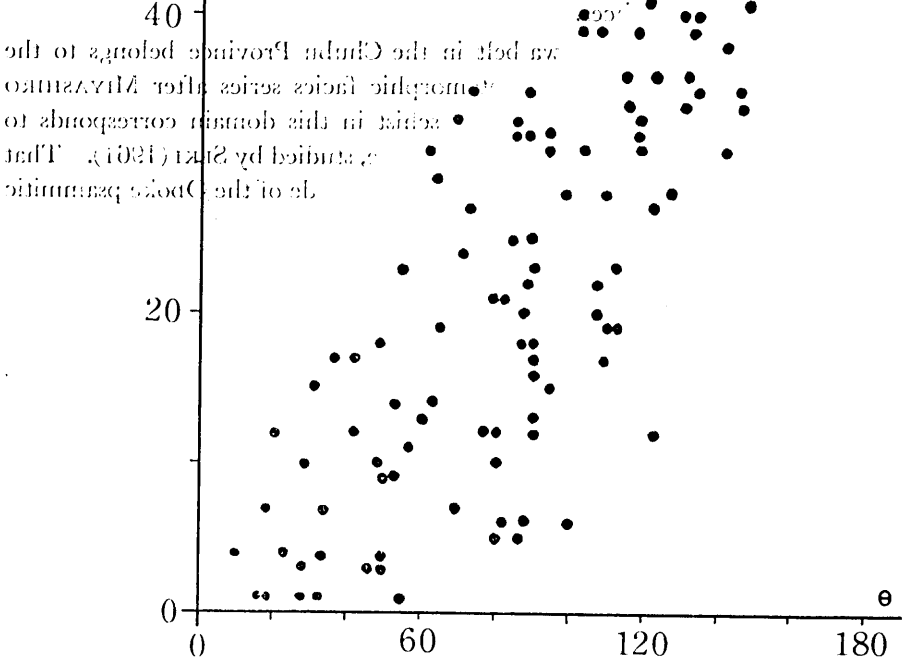


Fig. 13 Diagram showing the relationship between the angle  $S_A \wedge S_2$  and  $\theta$  for the folds of quartz-rich layers in the pelitic schist of the small domain at the position X in Fig. 8, whose enveloping surfaces are inclined at angles of between 50° and 60° to the  $S_{2m}$ -cleavage (=the principal plane XY of mean strain ellipsoid of this domain).

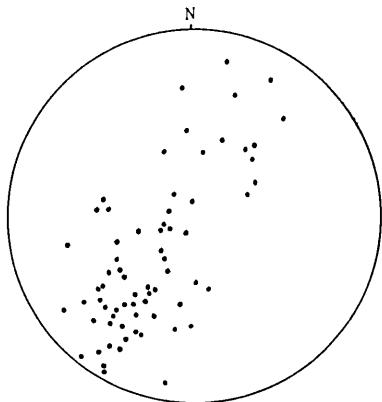


Fig. 14 Diagram showing the orientation of the axes of folds of quartz-rich layers in the pelitic schist at the position X in Fig. 8.

of the contact strain due to the folding of the quartz-rich layers, was minimum in a direction normal to the  $S_1$ -schistosity (for the former case) and maximum in that parallel to the  $S_1$ -schistosity (for the latter case), like in the case of the Oboke psammitic schist.

The orientation of the principal axes X and Y in this domain has been established on the basis of the shape and orientation of the strain ellipsoid of quartz aggregate in the quartz-rich layer parallel to the principal plane XY which will be in details described in the later pages. According to the result obtained, the principal axes Y and X are oriented parallel to and normal to the  $L_{1-2}$ -lineation, respectively. Therefore, the direction of those axes appears to change in a narrower range, as shown schematically in Fig. 12, which corresponds to the range of variation in trend of the  $S_1$ -schistosity, though the principal axis Z shows the constant direction.

Quartz-rich layers parallel or subparallel to the principal plane XY do not appear to show folding and boudinage. In the pelitic matrix there is no linear structure that is oblique to the  $L_{1-2}$ -lineation and belongs to the same generation as it. Therefore, it may be assumed that during the  $B_{2-1}$ -deformation the contraction (or extension) in a direction parallel to the principal axis Y was negligible.

From Figs. 9 and 12, it can be pointed out that the  $S_{2m}$ -cleavage surfaces (=strain-slip cleavage) in the pelitic schist in this domain tend to be parallel to the principal plane XY of the mean strain ellipsoid, that is, normal to the direction of the maximum shortening, like the  $S_2$ -cleavage in the Oboke psammitic schist.

Fig. 13 shows the variation in relation of  $S_A \wedge S_{2m}$  to  $\theta$  for the folds of quartz-rich layers in the pelitic schist in this domain whose enveloping surfaces are inclined at angles of between  $50^\circ$  and  $60^\circ$  to the  $S_m$ -cleavage (=the principal plane XY) and whose axes are parallel or subparallel to the  $L_{1-2}$ -lineation. According to Fig. 13, it will be pointed out that, for the folds whose interlimb angles  $\theta$  are larger than  $120^\circ$ , the axial surfaces show a tendency to be normal to the layer surface, that for some folds the axial surfaces are completely rotated toward the principal plane XY when  $\theta$  becomes  $90^\circ$  but for some other folds the axial surfaces remain normal to the layer surface even when  $\theta$  becomes  $70^\circ$ , and that when  $\theta$  becomes less than  $70^\circ$  the axial surfaces of all folds tend to rotate toward the principal plane XY. The data of Fig. 13 appears to be essentially the same as that of Fig. 6 for the folds of quartz-rich layers in the Oboke psammitic schist. Generally speaking, at the initial stage of buckle folding the axial surfaces appear to develop normal to the layer being folded, showing an agreement with the result from model experiment after RAMBERG (1959) and GHOSH (1966).

Fig. 14 is a diagram for the axes of folds of quartz-rich layers in the pelitic schist in this domain. The fold axes are plotted on a broad great-circle girdle normal to the principal axis Z of the mean strain ellipsoid. The width of the girdle in Fig. 14 is not equal to that for the  $L_{1-2}$ -lineation in Fig. 10, though, generally, the  $L_{1-2}$ -lineation just outside the folded quartz-rich layers appear to be parallel to the fold axes for them. Roughly speaking, therefore, it does not seem probable that the axes of folds

of quartz-rich layers in question lie within the principal plane XY, like in the case of the Oboke psammitic schist.

### III. RELATIONSHIP between FOLD WAVELENGTH and THICKNESS of BUCKLED COMPETENT LAYERS

For a long time it has been stated by many structural geologists that the size of a flexural fold in a multilayered system consisting of alternating competent layers and incompetent layers is controlled by both relative competency of the former and the latter and the thickness of the former, i. e., the greater the competency difference and the thicker the competent layer involved, the larger the size of the flexural fold. Sometimes, this empirical relation has been called the competence law (FAIRBAIRN, 1949). However, this relation has not precisely been examined for natural flexural folds until CURRIE *et al.* (1962) fixed attention to the relationship between fold wavelength (that developed at the early stage of folding) and thickness of dominant competent member in the folded sedimentary strata. CURRIE *et al.* (1962, p. 672) found that "a linear relationship exists between fold wave length and dominant member thickness. This relationship, although tested in a limited number of cases, is approximated by structures whose spacing ranges from a foot to several miles; the thickness of the dominant member that controls this wave length ranges from a fraction of an inch to about 1500 feet." Recent progress in theoretical and experimental investigations of folding in rheologically heterogeneous body after BIOT (1957, 1961, 1964, 1965a, 1965b and 1965c, etc), BIOT, ODÉ and ROEVER (1961), RAMBERG (1960, 1961, 1963 and 1964, etc) and CURRIE *et al.* (1962) indicated that for flexural folds in a multilayered rock system may commonly exist a certain linear relationship between initial fold wavelength and thickness of buckled competent layers involved, and that detailed observation of this relationship is very important in order to understand the physical conditions and mechanisms of formation of flexural folds.

In flexural folding of multilayered rock system, in which competent layers involved are widely spaced, these layers are independently buckled in a disharmonic, fashion, while, where competent layers involved in the system are closely spaced, these layers show a tendency to buckle in phase with one another. RAMBERG says, "the aforementioned unlike behaviour of multilayers is due to interference between the buckling layers, and this interference is determined by the extent to which the fields of contact strain and stress of neighbour competent layers penetrate one another. Now the width of the contact strain along a buckling sheet in a infinite medium equals about one wavelength  $\lambda_{\infty}$  ..... Thus if the spacing is greater than  $2\lambda_{\infty}$  the interference should be completely negligible and each competent layer should buckle as if surrounded by an infinite medium. At decreasing spacing the interference will increase in significant, the layers should show increasing tendency to buckle in phase with one another, ....." (RAMBERG, 1963, p. 493). According to theoretical and experimental studies after BIOT (1961, etc), RAMBERG (1964, etc) and CURRIE *et al.* (1962), the stable initial fold

wavelength developed where the competent layers involved in the system are independently buckled in a disharmonic fashion is generally different from that developed where those layers buckle in phase with one another, that is, the former is less than the latter. In order to determine the relationship between initial wavelength and thickness of buckled competent layers in a multilayered system, therefore, it must firstly be determined whether each of these layers independently buckles as if surrounded by an infinite medium or these layers show a combined action giving an increased fold wavelength.

In this chapter, for small-scale folds ( $B_2^m$ -fold) of quartz-rich layers (quartz veins) enclosed in psammitic schist of the Oboke district and for those ( $B_2^m$ -fold) in pelitic schist of the Kune district and the Oboke district, the relationship between fold wavelength and layer-thickness will be described. Especially, this relationship will be examined for the quartz-rich layers which appear to be folded under the condition in which the interference between neighbour quartz-rich layers is negligible, that is, the spacing between these layers is larger than  $\lambda_1 + \lambda_2$  ( $\lambda_1$  is the initial fold wavelength for a quartz-rich layer and  $\lambda_2$  is that for another quartz-rich layer just adjacent to that layer), according to the above-cited information after Ramberg. For the folded quartz-rich layers thicker than about 1cm, however, the measurement of fold wavelength has been done even where the spacing between the layer in question (with  $\lambda_1$ ) and the adjacent layer (with  $\lambda_2$ ) is narrower than  $\lambda_1 + \lambda_2$ , only if the former and the latter are independently folded to each other in disharmonic fashion. Because the initial wavelength for the folds of quartz-rich layers in question can not directly be measured, in the present cases, it is replaced by the length of arc for these folds. According to RAMBERG (1964), when, under lateral compression, competent layer enclosed in incompetent layers is folded, buckle shortening and layer shortening take place simultaneously but usually with different rates. For natural flexural folds, therefore, the present length of arc will not be commonly equal to the initial fold wavelength. This seems to be true for the folds of quartz-rich layers in question, judging from the dimensional fabric of quartz in those which will be examined in the later pages. Roughly speaking, difference in length between the initial fold wavelength and the present length of arc appears to be less than 20 per cent for the folds of quartz-rich layers enclosed in the Oboke psammitic schist, while it appears to be less than 15 per cent for those in the Kune pelitic schist (fuller explanation is given in the later pages).

Relationship between the length of arc and layer-thickness for the folds of quartz-rich layers in the Oboke psammitic schist has been examined on those developed within small domains of the hinge zones of the Oboke anticline and the Koboke syncline (positions 1 and 2 of Fig. 1). Especially, measurement has been done on the  $B_2^m$ -folds whose  $L-W/L$  values are larger than 0.05 ( $L$  = length of arc, and  $W$  = fold wavelength), whose axes are parallel or subparallel to the  $L_{1-2}$ -lineation, whose enveloping surfaces are inclined at angles larger than  $45^\circ$  to the  $S_2$ -cleavage, and through each of which variation in the layer-thickness is less than 20 per cent. The result is shown

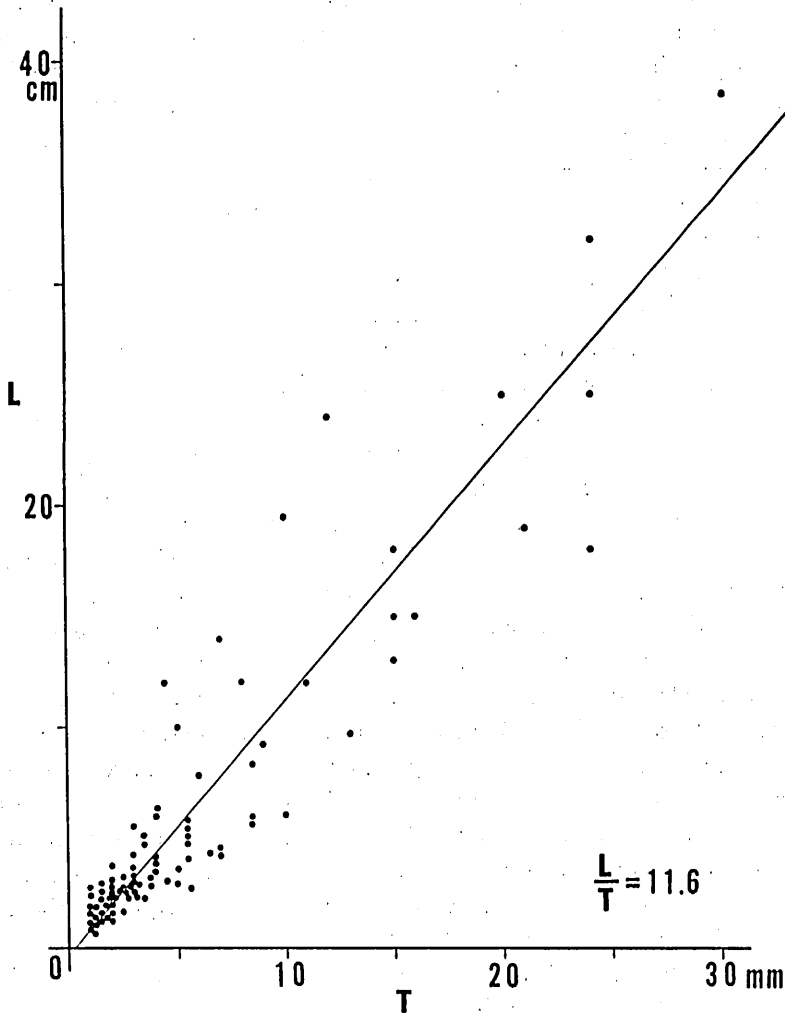


FIG. 15 Diagram showing the relationship between the length of arc and layer thickness for the folds of quartz-rich layers in the psammitic schist in two small domains (positions 1 and 2 in Fig. 1) of the Oboke district. L=length of arc of a fold. T=layer-thickness.

in Fig. 15. The diagram shows a close relationship between the length of arc and the layer-thickness. There is shown a general tendency that, as the thickness of quartz-rich layer increases, the length of arc increases, like in the case of CURRIE *et al.* (1962). Roughly speaking, the value of  $L/T$  approximates to 11.6 ( $T$ =layer-thickness). The minimum value of  $L/T$  is 5.8.

The relationship in question has also been examined on folds of four quartz-rich layers which are found in the pelitic schist on the southern limb of the Oboke anticline (position 3 of Fig. 1). Structural features of the pelitic schist within the outcrop where

the folds were measured are as follows; It shows a distinct schistosity defined by preferred orientation of flaky minerals, which is parallel to the bedding plane. The schistosity in the pelitic schist corresponds to the  $S_1$ -schistosity in the psammitic schist with respect to their generation. The schistosity is markedly folded in small-scales (less than several centimeters). All folds appear to share the same fold axis and the same axial plane and belong to the same generation. These folds are frequently associated with microfaults parallel to the axial surfaces. Therefore, the structure is identical with a cleavage structure referred to the type of the strain-slip cleavage, and

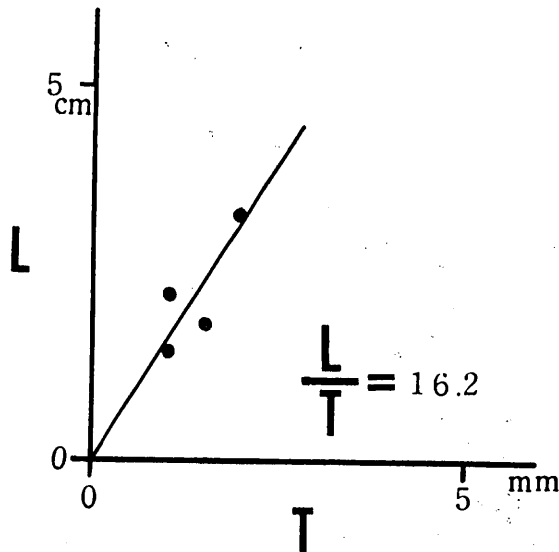


FIG. 16 Diagram showing the relationship between the length of arc and layer-thickness for the folds of quartz-rich layers in the pelitic schist in the small domain (position 3 in Fig. 1) on the southern limb of the Oboke anticline.

it appears to be essentially the same as the  $B_2^0$ -fold (the  $S_2$ -cleavage) in the psammitic schist and the  $S_{2m}$ -cleavage in the Kune pelitic schist. The cleavage structure in the pelitic schist belongs to the same generation as that in the psammitic schist.

The folds in question were formed during the  $B_2$ -deformation. For those folds,  $L-W/L$  values are between 0.09 and 0.27. The variation in layer-thickness through each fold is less than 15 per cent. Their axes are parallel to the  $L_{1-2}$ -lineation, and their enveloping surfaces are inclined at angles larger than  $60^\circ$  to the cleavage in the pelitic schist. Relationship between the length of arc and the layer-thickness for those folds is illustrated in Fig. 16. The average  $L/T$  ratio is 16.2, and the minimum  $L/T$  ratio is 11.6.

Relationship between the length of arc and the layer-thickness for the  $B_2^m$ -folds of quartz-rich layers in the pelitic schist in a small domain of the Kune district (position X of Fig. 8), where was examined the geometric relationship between the mean strain

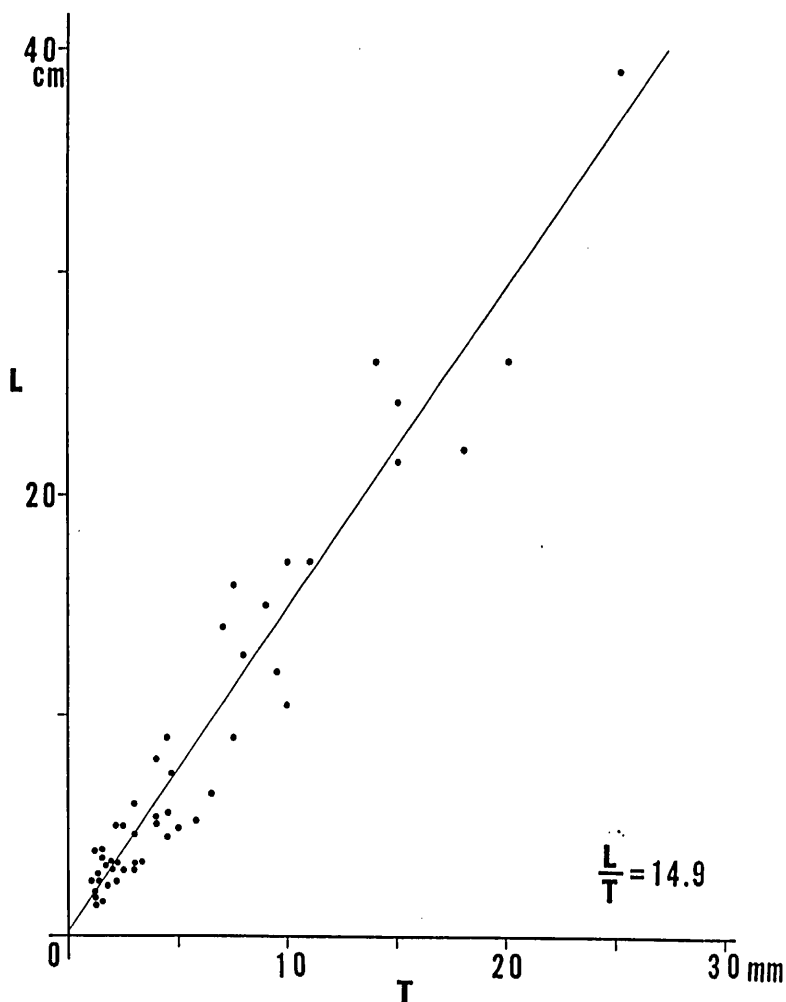


FIG. 17 Diagram showing the relationship between the length of arc and layer-thickness for the folds of quartz-rich layers in the peritic schist in the small domain (position X in Fig. 8) of the Kunc district.

ellipsoid of the pelitic schist and geometric elements of the  $B_2^m$ -folds involved, has been examined. Especially, it has been examined on the folds, whose  $L-W/L$  values are between 0.13 and 0.58, through each of which variation in layer-thickness is less than 20 per cent, and whose enveloping surfaces are inclined at angles larger than  $50^\circ$  to the  $S_{2m}$ -cleavage. The result is illustrated in Fig. 17. The diagram shows a close relationship between the length of arc and the layer-thickness. The average value of  $L/T$  is 14.9. The minimum  $L/T$  ratio is 9.1. The average  $L/T$  ratio and the minimum  $L/T$  ratio are, respectively, slightly less than those (16.2 and 11.6) for the folds of quartz-rich layers in the Oboke pelitic schist, but they are larger than those (11.6 and 5.8) for the  $B_2^m$ -folds in the Oboke psammitic schist. It is clear that there

is difference in the average  $L/T$  ratio between the folds of quartz-rich layers in the pelitic schist and those in the psammitic schist (Figs. 15, 16 and 17), that is, the average  $L/T$  ratio for the former is larger than that for the latter.

Recently, BIOT (1957, 1961, 1964, 1965a, 1965b, and 1965c, etc), RAMBERG (1960, 1961, 1963 and 1964) and CURRIE *et al.* (1962) have investigated the problems on the deformation of rheologically heterogeneous layered body, making attempts to deduce theoretically the wavelength of the folds produced by buckling. BIOT (1957 and 1961) has shown that, when an elastic layer of thickness  $T$  enclosed in an infinite viscous medium is subjected to compression in a direction parallel to the layer, the dominant wavelength  $L_d$  of buckle folding of the elastic layer, for which the rate of increase of the amplitude is maximum, is given by

$$L_d = \pi T \sqrt{\frac{E}{(1-\nu^2)P}},$$

where  $P$  is the axial compression,  $E$  is the Young's modulus and  $\nu$  is the Poisson's ratio for the layer. In this case, the dominant wavelength is independent of the viscosity of the medium surrounding the elastic layer, but depends on the axial compression. On the other hand, BIOT (1957 and 1961) has also shown that, in buckling of a viscous layer of thickness  $T$  enclosed in an infinite viscous medium of lower viscosity under layer-parallel compression, the dominant wavelength is given by

$$L_d = 2\pi T \sqrt[3]{\frac{\mu_1}{6\mu}}$$

where  $\mu_1$  and  $\mu$  are the viscosity coefficient for the layer and the medium respectively. RAMBERG (1960 and 1963) has also given a similar wavelength equation. According to BIOT and RAMBERG, therefore, it can be pointed out that in buckling of a viscous layer in an infinite viscous medium of lower viscosity the fold wavelength depends on both the viscosity ratio of the former and the latter and the thickness of the former, but is independent of the axial compression. Model experiments on buckle folding of the viscous layer enclosed in a viscous medium of lower viscosity have also been done by BIOT *et al.* (1961) and MCBIRNEY *et al.* (1961). The result after Biot *et al.* appears to be in good agreement with the theoretical predictions after BIOT and RAMBERG. While, MCBIRNEY *et al.* appear to have shown a large discrepancy between the experiments and the theory. According to RAMBERG (1963, p. 490), however, "the large deviations between experiments and theory reported by MCBIRNEY *et al.*, 1961, indicate that the material used did not have the rheological character specified for the theoretical model, or that the experiments were not performed according to the premises of the models of Biot and the present writer" (RAMBERG).

Our knowledge on the rheological state of rock materials during the geologic deformation which is associated with the formation of flexural folds is quite inadequate at present. However, RAMSAY (1967, p. 374) says, "it seems that as first approximation we can consider them as fluids (Newtonian) with high viscosities (perhaps of the order

of  $10^{17}$  to  $10^{22}$  poises).” Also some other authors appear to have assumed that rock materials under the physical conditions, in which the metamorphism can occur, mechanically behaved as Newtonian substance. If it would be assumed that during the B<sub>2</sub>-deformation in the Oboke district and in the Kune district the psammitic schist, pelitic schist and quartz-rich layers behaved mechanically as Newtonian substance, the ratio of the viscosity coefficient of the quartz-rich layer and the psammitic schist or the pelitic schist may be estimated on the basis of the data of the average L/T ratio in Figs. 15, 16 and 17, according to the wavelength equation of Biot; In the Oboke district, the viscosity ratio between the quartz-rich layer and psammitic schist=ca. 38, and that between the quartz-rich layer and pelitic schist=ca. 102. In the Kune district, the viscosity ratio between the quartz-rich layer and pelitic schist=ca. 80. If, according to the data of the average L/T ratio in Figs 15 and 16, the viscosity ratio of the psammitic schist and the pelitic schist of the Oboke district is indirectly estimated, it would amount to about 3.

In the present cases, however, the difference between the initial wavelength and the present length of arc for the folds of quartz-rich layers comes into question, in order to make exact estimates of the viscosity ratio between those rocks. Roughly speaking, the difference in question appears to be less than 20 per cent for the folds of quartz-rich layers enclosed in the psammitic schist, while it appears to be less than 15 per cent for those in the pelitic schist of the Kune district. Because some other factors are related to the interpretation of the data of the L/T ratio in Figs. 15, 16 and 17, however, it will be again done in the later pages.

According to BIOT (1961), when the folding of a viscous layer enclosed in an infinite viscous medium of lower viscosity under layer-parallel compression proceeds, the rate of increase of amplitude is a function of the wavelength (the concept of amplification), and the wavelength for which it is maximum becomes predominant after an interval of time, giving a certain regularity in the wavelength (the concept of selectivity). The degree of amplification  $A_d$  which occurs for the dominant wavelength after an interval of time  $t$  is given by

$$\log_e A_d = \frac{t}{t_1} \left( \frac{\mu_1}{6\mu} \right)^{\frac{1}{2}}$$

where  $t_1$  is a time when the compressive strain corresponds to a shortening of 25 per cent. “Beyond a certain amplification, the amplitude of folding will increase at an explosive rate. This happens when  $A_d=1000$ , and we can adopt this value as a standard. .... This time ratio for explosive amplification is a function only for the viscosity ratio. .... good selectivity also begins to appear for amplifications of about 1000; .... Another important feature .... is the small amplification exhibited for viscosity ratios smaller than 100. Larger amplification would, of course, appear for times  $t$  larger than  $t_1$ . However, this would imply a shortening of the layer larger than 25 per cent. Such a large compressive strain would overshadow the folding itself. We can conclude, therefore, that a clearcut folding with sharp definition requires that the

viscosity of the layer be at least 100 times that of the medium." (BIOT, 1961, p. 1606-1607). If the material is nonlinear, however, "appreciable folding may occur for effective viscosity ratios smaller than 100. Hence, when nonlinearity is introduced, significant folding may still occur for dominant wavelengths which are smaller than about 15 times the thickness." (BIOT, 1961, p. 1611). According to the above cited informations after BIOT, the linear relationship between the length of arc and the layer-thickness for the folds of quartz-rich layers enclosed in the psammitic schist of the Oboke district (Fig. 15), where the viscosity ratio of the quartz-rich layers and the psammitic schist is between 38 and 126.9, appears to be very interesting. The folds of psammitic schist enclosed in the pelitic schist of the Oboke district, where the viscosity ratio of the related rocks is about 3, show frequently the ratio of the length of arc and the layer-thickness smaller than 1.00. That the mechanisms of formation of folds of psammitic layers in the pelitic schist are understood with reference to the internal structures seems to be very important. Generally, relationship between the characters of the internal structures which corresponds to the mechanisms of folding and the viscosity ratios of the related rocks must be clarified.

#### IV. INTERNAL STRUCTURES in BUCKLE FOLDS

In this chapter dimensional fabrics of quartz in the folds of quartz-rich layers (quartz veins) enclosed in the pelitic schist of the Kune district and those in the psammitic schist of the Oboke district, will be described and discussed,\* with regard to the relationships between the mechanisms of buckle folding and the related internal structures (movement and strain pictures), between the mechanisms of buckle folding and the viscosity ratios of related rocks, and between the mechanisms of buckle folding and the orientational relation of the buckled layer to the mean strain ellipsoid of a system concerned. Firstly, quartz dimensional fabrics in folds of quartz-rich layers in the Kune district will be examined on four selected specimens.

Specimen I (H65 I2014): Some macroscopic characters of the fold observed in the specimen are enumerated as follows. 1) The fold is referred to the type of cylindrical plane fold with reference to its geometric property (cf. TURNER *et al.*, 1963). 2) The form is nearly symmetric bilaterally across the axial surface. The fold has a near orthorhombic symmetry. 3) The angle between the limbs is about 60°. 4) In the surrounding mica-rich layers (pelitic schist) is found the  $S_{2m}$ -cleavage in one set, as axial plane cleavage which is referred to the Type II, Type III and Type IV (cf. HARA, 1966a). 5) The enveloping surface of the folded quartz-rich layer is nearly normal to the  $S_{2m}$ -cleavage and parallel to the  $L_{1-2}$ -lineation.

\* Quartz grains in those quartz-rich layers (quartz veins) appear to have been commonly produced by fragmentation of coarse-grained quartz (vein quartz) during the folding. They are essentially the same as quartz grains in a quartz vein in deformed rhyolite pebble in the Oboke psammitic schist previously described by the senior author (HARA *et al.*, 1966).

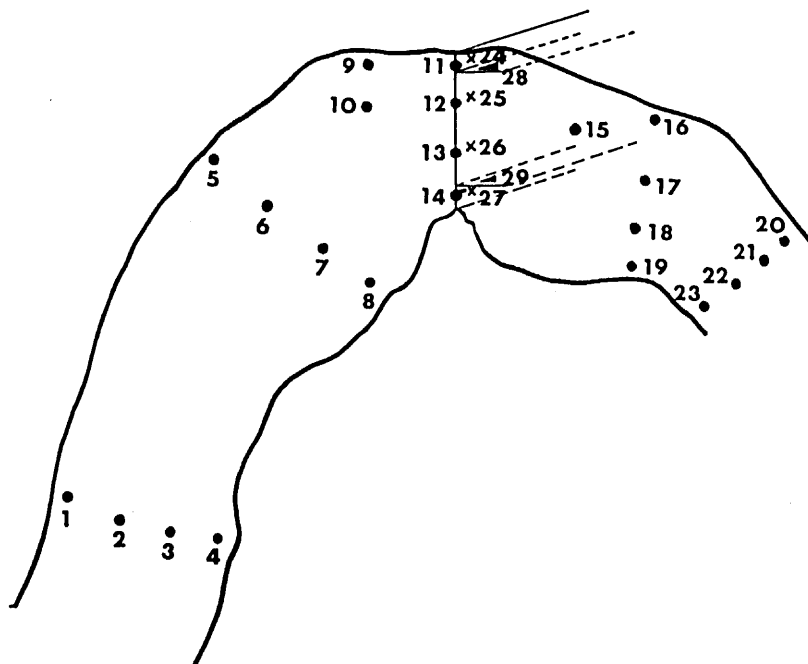


FIG. 18 Diagram showing the positions for the measurement of directions and degrees of grain orientation of quartz in the fold of the specimen I. Solid circles: positions on the ac-section. Crosses: position on the bc-section. Triangles: positions on the ab-sections.

The grain orientation of quartz in the fold of the quartz-rich layer has been examined at 29 positions, as shown in Fig. 18, according to the method of analysis used in the previous papers of the senior author (HARA, 1966b, 1966c and 1967; HARA *et al.*, 1966). The results are illustrated in Fig. 19 and Table 1 (cf. Plate 8). The quartz dimensional fabric will also be interpreted according to the rule used in the papers of the senior author (HARA, 1966b, 1966c and 1967), that was established with reference to the data and the idea given by OFTEDAHL (1948), FAIRBAIRN (1950), FLINN (1956), BRACE (1955 and 1961), TURNER *et al.* (1963) and CARTER, CHRISTIE and GRIGGS (1964).

On the basis of the results of measurement of grain orientation in selected positions and the complementary microscopic observation of remaining parts, the pattern of the grain orientation on the plane normal to the fold axis (the plane of the ac-section) will be illustrated as follows; At the inner side of fold knee, the directions of preferred grain orientation are radially arranged, while, at the outer side of fold knee they are subparallel to the layer surface. And, at the middle part of fold knee, the grain orientation is not statistically significant. On both limbs the directions of preferred grain orientation stand generally at high angles on the layer surface, though at the outer parts of both limbs the grain orientation is not statistically significant.

The degree of the grain orientation (vector magnitude) on the ac-section is very

Geometry and Internal Structures of Flexural Folds

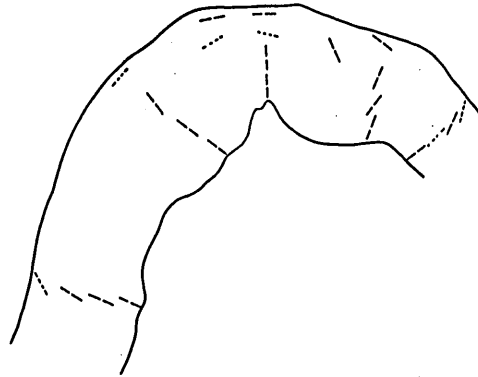


Fig. 19 Diagram showing the directions of preferred grain orientation of quartz at 23 positions on the ac-section for the fold of the specimen I.  
Dotted lines: direction of grain orientation which is not statistically significant.

TABLE 1. Summary of grain orientation data for the specimen I.

Position Nos.	Vector Magnitude (%)	Probability	Significant	The angle between fold axis and vector mean (degrees)
1	23.6	>0.05	No	
2	37.2	<10 <sup>-3</sup>	Yes	
3	43.6	<10 <sup>-3</sup>	Yes	
4	52.2	<10 <sup>-5</sup>	Yes	
5	21.6	>0.10	No	
6	37.2	<10 <sup>-3</sup>	Yes	
7	38.0	<10 <sup>-3</sup>	Yes	
8	65.4	<10 <sup>-5</sup>	Yes	
9	42.6	<10 <sup>-3</sup>	Yes	
10	15.2	>0.30	No	
11	25.2	<0.05	Yes	
12	20.8	>0.10	No	
13	39.4	<10 <sup>-3</sup>	Yes	
14	67.2	<10 <sup>-5</sup>	Yes	
15	34.8	<0.01	Yes	
16	26.6	<0.04	Yes	
17	42.6	<10 <sup>-3</sup>	Yes	
18	46.2	<10 <sup>-4</sup>	Yes	
19	53.0	<10 <sup>-5</sup>	Yes	
20	23.5	>0.05	No	
21	28.5	<0.02	Yes	
22	20.4	>0.10	No	
23	44.4	<10 <sup>-4</sup>	Yes	
24	24.1	>0.05	No	3
25	2.8	>0.85	No	88
26	26.2	<0.04	Yes	87
27	27.0	<0.03	Yes	87
28	15.7	>0.30	No	86
29	87.8	<10 <sup>-15</sup>	Yes	3

variable (Table 1). The area of the largest vector magnitude appears to be located at the innermost side of fold knee, and at the outer side of fold knee and the middle to inner sides of both limbs the grain orientation has low to moderate vector magnitude.

The direction and degree of the grain orientation of quartz have also been examined on the thin section (the bc-section) cut along the axial surface of the fold (Fig. 18 and Table 1). At the innermost side of fold knee the direction of grain orientation is normal to the fold axis. However, at the middle to outer part of fold knee the grain orientation is not statistically significant.

On the thin sections parallel to the layer surface at the innermost side and the outermost side of fold knee (the ab-section I and ab-section II, respectively), the grain orientation has been examined (Fig. 18 and Table 1). The direction of preferred grain orientation on the ab-section I is parallel to the fold axis, having a large vector magnitude, while that on the ab-section II is normal to the fold axis, though the grain orientation is not statistically significant.

The direction of grain orientation of the position 14 on the ac-section and that of the position 27 on the bc-section are approximately parallel to the line of intersection of those two sections, which is normal to the fold axis (Table 1). While, at the position 29 (ab-section I), that is parallel to the fold axis, namely, parallel to the line of intersection of the ab-section and the bc-section (Table 1). Therefore, it can be concluded that, in the vicinity of the positions 14, 29 and 27 (the innermost part of fold knee), the planes of ac-section, bc-section and ab-section are identical with the three principal

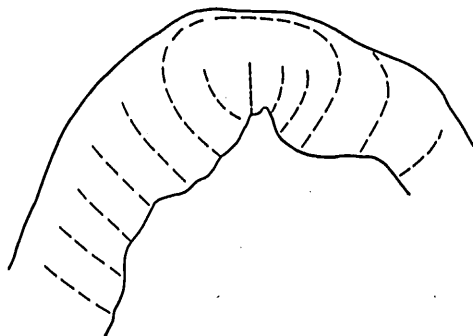


FIG. 20 Diagram showing the trajectories of the principal axis X through the fold of the specimen I.

plane of the mean strain ellipsoid, and that the principal strain axis X is parallel to the line of intersection of the ac-section and the bc-section, the principal axis Z parallel to the line of intersection of the ac-section and the ab-section and the principal axis Y parallel to the fold axis.

The direction of grain orientation of the position 11 on the ac-section and that of the position 24 on the bc-section, though the latter is not statistically significant, are parallel to the trace of the layer surface on each section, and that of the position 28.

on the ab-section II is normal to the fold axis, though not statistically significant (vector magnitude=15.7). Therefore, it may be concluded that at the vicinity of the positions 11, 24 and 28 (the outermost part of fold knee) the principal axis X is parallel to the layer surface and normal to the fold axis, and that the principal axes Y and Z are nearly equal (the former may be parallel to the fold axis and the latter normal to the layer surface).

At the positions 12 and 25 (the middle part of fold knee), the grain orientation is not statistically significant. Therefore, the three principal strain axis may be nearly equal in the vicinity of the positions 12 and 25.

The pattern of the dimensional fabric of quartz in the fold knee of the present specimen is quite similar to that of the specimen previously described by the senior author (Hara, 1966c).

It may be concluded that, in the axial zone of the fold, the principal axes X and Z are oriented on the plane of the ac-section and that the principal axis Y is parallel to the fold axis. While, it is impossible to define strictly the principal axes at other positions of the fold only on the basis of the data of Table 1. If it is assumed that, at any position of the fold the principal axes X and Z are oriented on the plane normal to the fold axis and the principal axis Y is parallel to the fold axis, the trajectories of

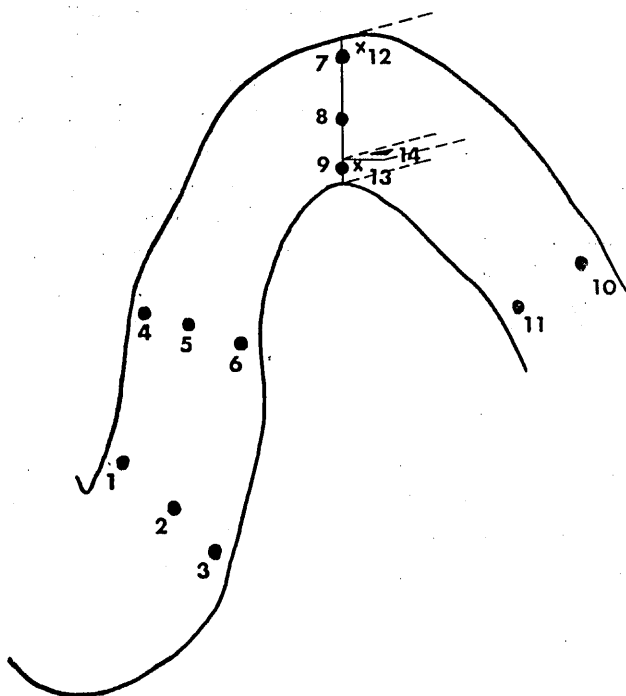


FIG. 21 Diagram showing the positions for the measurement of directions and degrees of grain orientation of quartz in the fold of the specimen II.

the principal axis  $X$  through the fold will be drawn on the basis of Fig. 19 as shown in Fig. 20. From this figure, it may be said that the outer side of fold knee was subjected to extension parallel to the layer surface and the inner side of fold knee underwent compression in the same direction, and that the neutral axis dividing between the former and the latter was developed in the middle part of fold knee. The strain picture in question will be designated Typy I.

Specimen II (H65I2016): Some macroscopic characters of the fold observed in the specimen are enumerated as follows. 1) The fold is referred to the type of cylindrical plane fold with reference to its geometric property. 2) The form is nearly symmetric bilaterally across the axial surface. The fold has a near orthorhombic symmetry. 3) The angle between the limbs is about  $50^\circ$ . 4) In the surrounding mica-rich layers is found the  $S_{2m}$ -cleavage in one set as axial plame clewage, which is referred to the Type II and Type III. 5) The enveloping surface of the folded quartzrich layer is nearly normal to the  $S_{2m}$ -cleavage and subparallel to the  $L_{1-2}$ -lineation.

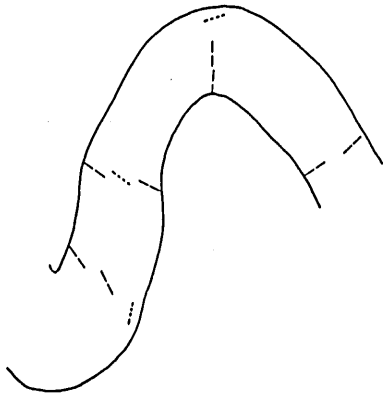


FIG. 22 Diagram showing the directions of preferred grain orientation of quartz at 11 positions on the ac-section for the fold of the specimen II.

The grain orientation of quartz in the fold of quartz-rich layer has been examined at 14 positions, as shown in Fig. 21. The results are illustrated in Fig. 22 and Table 2. On the basis of the results of measurement of grain orientation and the complementary microscopic observation of remaining parts, the pattern of the grain orientation on the ac section will be illustrated as follows; The directions of preferred grain orientation are radially arranged throughout the fold. The area of the largest vector magnitude and that of the smallest vector magnitude appear to be located at the innermost side and the outermost side of fold knee, respectively (Table 2). Especially, the grain orientation at the outermost side of fold knee is not

statistically significant.

The direction and the degree of grain orientation of quartz have also been examined on the bc-section cut along the axial surface at the fold knee (Fig 21). At the innermost side of fold knee (position 13) the direction of grain orientation is normal to the fold axis, while at the outermost side (position 12) the grain orientation is not statistically significant.

On the ab-section at the innermost side of the fold knee (position 14), the direction of preferred grain orientation is parallel to the fold axis, showing a large vector magnitude.

Therefore, it will be concluded that, in the vicinity of the positions 9, 13 and 14 (the innermost part of fold knee), the planes of ac-section, bc-section and ab-section

Geometry and Internal Structures of Flexural Folds

TABLE 2. Summary of grain orientation data for the specimen II.

position Nos.	Vector Magnitude (%)	Probability	Significant	The angle between fold axis and vector mean (degrees)
1	62.2	$<10^{-5}$	Yes	
2	43.6	$<10^{-4}$	Yes	
3	22.8	$>0.05$	No	
4	34.6	$<0.01$	Yes	
5	21.4	$>0.05$	No	
6	37.2	$<0.01$	Yes	
7	19.6	$>0.10$	No	
8	63.4	$<10^{-5}$	Yes	
9	83.8	$<10^{-10}$	Yes	
10	34.2	$<0.01$	Yes	
11	27.4	$<0.03$	Yes	
12	11.2	$>0.50$	No	16
13	32.4	$<0.01$	Yes	86
14	61.8	$<10^{-5}$	Yes	5

are identical with the three principal planes of the mean strain ellipsoid, and that the principal axis X is parallel to the line of intersection of the ac-section and the bc-section, the principal axis Z parallel to the line of intersection of the ac-section and the ab-section and the principal axis Y parallel to the fold axis. At the positions 7 and 12 (the outermost part of fold knee) the grain orientation is not statistically significant. Therefore, the three principal axes of the mean strain ellipsoid at the outermost part of fold knee may be nearly equal.

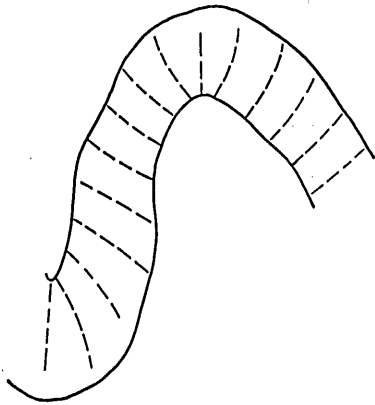


FIG. 23 Diagram showing the trajectories of the principal axis X through the fold of the specimen II.

Now, if it is assumed that, at any position of the fold, the principal axes X and Z are oriented on the plane normal to the fold axis, the trajectories of the principal axis X through the fold will be drawn on the basis of Fig. 22 as shown in Fig. 23. From this figure and Table 2, it may be said that during the folding of the quartz-rich layer the extension zone was not developed even at the outermost side of fold knee, but, showing the development of the neutral axis at the outermost side of fold knee, the layer

underwent compression as a whole, unlike the specimen I. The strain picture in question will be named Type II.

Specimen III (H6511809): Some macroscopic characteristics of the fold observed in the specimen are listed as follows. 1) The fold is referred to the type of cylindrical

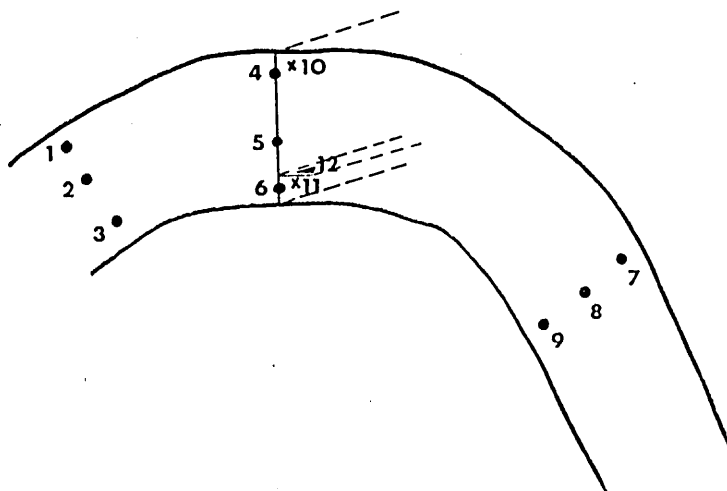


FIG. 24 Diagram showing the positions for the measurement of directions and degrees of grain orientation of quartz in the fold of the specimen III.

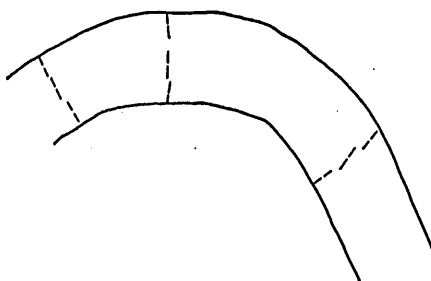


FIG. 25 Diagram showing the directions of preferred grain orientation of quartz at 9 positions on the ac-section for the fold of the specimen III.

TABLE 3. Summary of grain orientation data for the specimen III.

Position Nos.	Vector Magnitude (%)	Probability	Significant	The angle between fold axis and vector mean (degrees)
1	32.0	$<0.01$	Yes	
2	59.4	$<10^{-5}$	Yes	
3	54.2	$<10^{-5}$	Yes	
4	33.2	$<0.01$	Yes	
5	64.0	$<10^{-5}$	Yes	
6	84.2	$<10^{-15}$	Yes	
7	36.0	$<0.01$	Yes	
8	59.0	$<10^{-5}$	Yes	
9	65.8	$<10^{-5}$	Yes	
10	23.2	$>0.05$	No	86
11	34.5	$<0.01$	Yes	87
12	67.8	$<10^{-5}$	Yes	6

plane fold with reference to its geometric property. 2) The form is nearly symmetric bilaterally across the axial surface. The fold has a near orthorhombic symmetry. 3) The angle between the limbs is about  $90^\circ$ . 4) In the surrounding mica-rich layers is found the  $S_{2m}$ -cleavage in one set, as axial plane cleavage which is referred to the Type II, Type III and Type IV. 5) The enveloping surface of the folded quartz-rich layer is nearly normal to the  $S_{2m}$ -cleavage and slightly oblique to the  $L_{1-2}$ -lineation.

The grain orientation of quartz in the fold of quartz-rich layer has been examined at 12 position, as shown in Fig. 24. The results are illustrated in Fig. 25 and Table 3. On the basis of the results of measurement of grain orientation and the complementary microscopic observation of remaining parts, the pattern of the grain orientation on the ac-section will be illustrated as follows; The directions of preferred grain orientation are radially arranged throughout the fold. The degree of grain orientation appears to decrease from the inner side to the outer side of fold. The area of the largest vector magnitude and that of the smallest vector magnitude appear to be located at the innermost side and the outermost side of fold knee, respectively (Table 3).

The direction and the degree of grain orientation of quartz have also been examined on the bc-section cut along the axial surface (Fig. 24 and Table 3). At the innermost side of fold knee (position 11) the direction of grain orientation is normal to the fold axis, while at the outermost side (position 10) the grain orientation is not statistically significant. On the ab-section at the innermost side of fold knee (position 12), the direction of grain orientation is parallel to the fold axis (Fig. 24 and Table 3).

Therefore, it will be concluded that, in the vicinity of the positions 6, 11 and 12 (the innermost part of fold knee), the planes of ac-section and ab-section are identical with the three principal planes of the mean strain ellipsoid, and that the principal axis X is parallel to the line of intersection of the ac-section and the bc-section, the principal axis Z parallel to the line of intersection of the ac-section and the ab-section and the principal axis Y parallel to the fold axis, like in the cases of the specimens I and II and the previously described specimens of the senior author (HARA, 1966b\* and c).

Now, if it is assumed that, at any position of the fold, the principal axes X and Z are oriented on the plane normal to the fold axis, the trajectories of the principal axis X through the fold will be drawn on

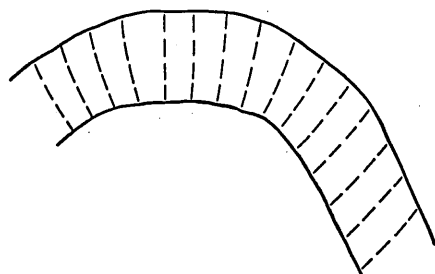


FIG. 26 Diagram showing the trajectories of the principal axis X through the fold of the specimen III.

\* In the fold I of the specimen (HG511707 — here called specimen IV) previously described by the senior author, the grain orientation on the bc-section cut along the axial surface and the ab-section at the innermost side of fold knee has been also examined, in addition to the previous examination of the grain orientation on the ac-section (Fig. 27). The results are illustrated in Fig. 28 and Table 4. The shape and orientation of the mean strain ellipsoid at the innermost part of fold knee will be clearly established on the basis of the obtained data. The nature of mean strain at the innermost part of fold knee appears to be essentially the same as the cases of the specimens I and II.

the basis of Fig. 25 as shown in Fig. 26. From this figure, it may be said that during the folding of the quartz-rich layer the neutral axis was not developed even at the outermost side of fold knee but the layer underwent as a whole compression, unlike the cases of the specimens I, II and IV. It must be further noted that the shape of the mean strain ellipsoid at the outermost part of fold knee is  $X \approx Y > Z$ . The strain picture in question will be designated Type III.

It will be safely pointed out that the strain picture in the quartz-rich layer developed during the folding is quite different between the specimens I, II and III, on the basis of the pattern of dimensional fabric of quartz, e. g., with respect to the position of the neutral axis in fold knee, for the specimen I the neutral axis is developed near the middle part of fold knee, for the specimen II that is located at the outermost side of fold knee and for the specimen III that is not developed within the layer, and, with

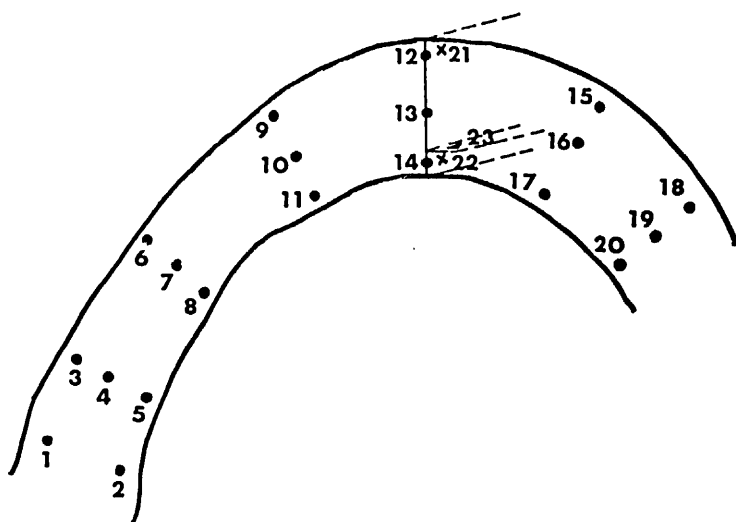


FIG. 27 Diagram showing the positions for the measurement of directions and degrees of grain orientation of quartz in the fold of the specimen IV.

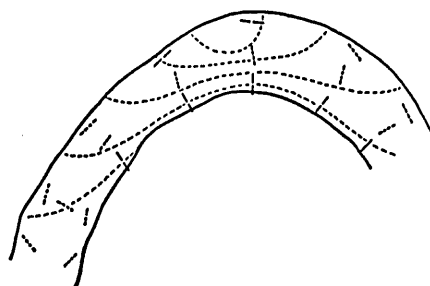


FIG. 28 Diagram showing the directions of preferred grain orientation of quartz at 20 positions on the ac-section and the trajectories of the principal axis Z through the fold of the specimen IV.

## Geometry and Internal Structures of Flexural Folds

TABLE 4. Summary of grain orientation data for the specimen IV.

Position Nos.	Vector Magnitude (%)	Probability	Significant	The angle between fold axis and vector mean (degrees)
1	12.2	>0.40	No	
2	10.8	>0.50	No	
3	15.0	>0.30	No	
4	18.5	>0.10	No	
5	8.6	>0.60	No	
6	18.7	>0.10	No	
7	21.2	>0.10	No	
8	51.3	<10 <sup>-5</sup>	Yes	
9	45.3	<10 <sup>-4</sup>	Yes	
10	6.4	>0.80	No	
11	78.2	<10 <sup>-10</sup>	Yes	
12	24.6	<0.05	Yes	
13	14.2	>0.30	No	
14	73.3	<10 <sup>-10</sup>	Yes	
15	22.3	>0.05	No	
16	19.9	>0.10	No	
17	68.2	<10 <sup>-10</sup>	Yes	
18	21.2	>0.10	No	
19	17.2	>0.20	No	
20	48.2	<10 <sup>-5</sup>	Yes	
21	16.6	>0.20	No	6
22	33.8	<0.01	Yes	87
23	38.8	<10 <sup>-3</sup>	Yes	4

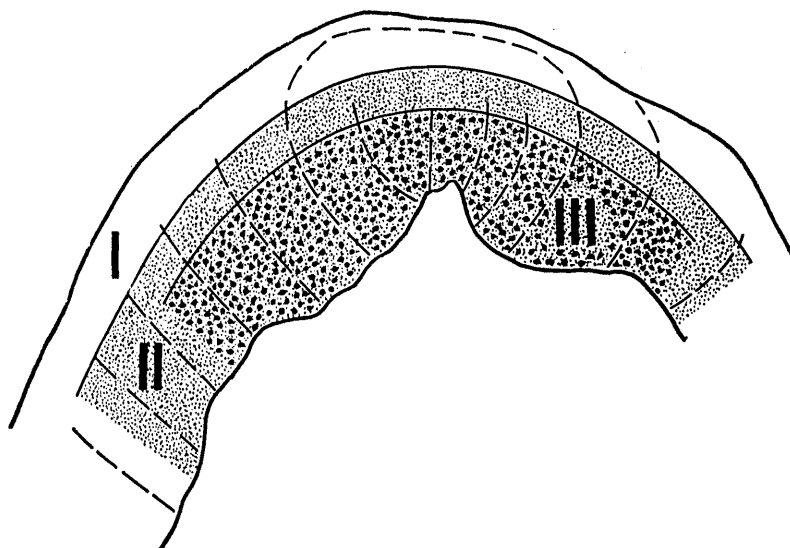


FIG. 29 Diagram showing the relationship between the strain pictures of Type I, Type II and Type III.

I: Type I. II: Type II. III: Type III.

Dashed lines: trajectories of the principal axis X of the strain ellipsoid through the fold of the specimen I.

respect to the strain picture on the limbs, for the specimen I the part of no-distortion (grain orientation is not statistically significant) is developed in the inflection point and the outside of limb, while for the specimens II and III the part of no-distortion is not developed on the limbs. Roughly speaking, the strain picture in the fold of quartz-rich layer of the specimen II (Fig. 23) appears to be correlated with that in the middle to inner side of the fold of quartz-rich layer in the specimen I (Fig. 20), and that in the fold of the specimen III (Fig. 26) with that in the inner side of the fold of the specimen I, as shown schematically in Fig. 29.

Microscopic observation of the dimensional fabrics of quartz in many folds of quartz-rich layers (quartz veins) enclosed in the pelitic schist of the Kune district, which have orthorhombic symmetry or near orthorhombic symmetry and whose axes are parallel or subparallel to the  $L_{1-2}$ -lineation, indicate that they do not always possess the same fabric pattern but many of them appear to be grouped into the above-described three types.

Specimen V (H64IIX1904): Some macroscopic characteristics of the fold observed in the specimen are listed as follows. 1) The fold is referred to the type of cylindrical plane fold with reference to its geometric property. 2) The form is nearly symmetric bilaterally across the axial surface. The fold has a near orthorhombic symmetry. 3) The angle between the limbs is about  $80^\circ$ . 4) In the mica-rich layers outside the fold is found the  $S_{2m}$ -cleavage in one set, as axial plane cleavage which is referred to

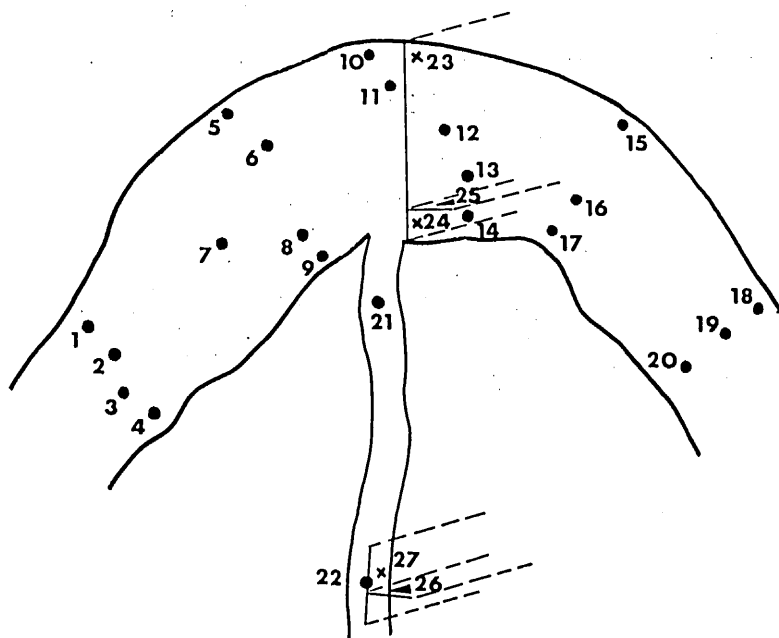


FIG. 30 Diagram showing the positions for the measurement of directions and degrees of grain orientation of quartz in the folded and non-folded quartz-rich layers in the specimen V.

Geometry and Internal Structures of Flexural Folds

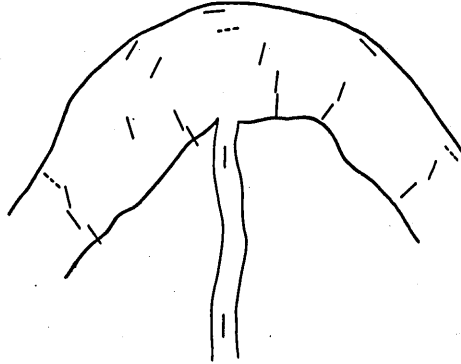


FIG. 31 Diagram showing the directions of preferred grain orientation of quartz at 22 positions on the ac-section for the specimen V.

TABLE 5. Summary of grain orientation data for the specimen V.

Position Nos.	Vector Magnitude (%)	Probability	Significant	The angle between fold axis and vector mean (degrees)
1	23.0	>0.05	No	
2	37.8	<10 <sup>-3</sup>	Yes	
3	70.6	<10 <sup>-10</sup>	Yes	
4	50.8	<10 <sup>-5</sup>	Yes	
5	55.4	<10 <sup>-5</sup>	Yes	
6	36.6	<0.01	Yes	
7	37.0	<10 <sup>-3</sup>	Yes	
8	71.8	<10 <sup>-10</sup>	Yes	
9	77.8	<10 <sup>-10</sup>	Yes	
10	34.8	<0.01	Yes	
11	22.8	>0.05	No	
12	44.8	<10 <sup>-4</sup>	Yes	
13	60.4	<10 <sup>-5</sup>	Yes	
14	73.5	<10 <sup>-10</sup>	Yes	
15	52.2	<10 <sup>-5</sup>	Yes	
16	25.2	<0.04	Yes	
17	28.2	<0.02	Yes	
18	23.8	>0.05	No	
19	50.2	<10 <sup>-5</sup>	Yes	
20	51.8	<10 <sup>-5</sup>	Yes	
21	66.6	<10 <sup>-5</sup>	Yes	
22	87.6	<10 <sup>-15</sup>	Yes	
23	6.4	>0.80	No	18
24	53.6	<10 <sup>-5</sup>	Yes	88
25	89.0	<10 <sup>-15</sup>	Yes	4
26	65.8	<10 <sup>-5</sup>	Yes	4
27	34.7	<0.01	Yes	85

the Type II and Type III. 5) In the mica-rich layer outside the concave zone of the fold is found a quartz-rich layer (quartz vein) running nearly along the axial surface and  $S_{2m}$ -cleavage, which is not folded, but the layer does not continue into the mica-rich layer outside the convex zone. For convenience' sake, the folded quartz-rich layer will be named the layer I and the quartz-rich layer subparallel to the axial surface the layer II. 6) The enveloping surface of the folded quartz-rich layer is normal to the  $S_{2m}$ -cleavage and parallel to the  $L_{1-2}$ -lineation.

The grain orientation of quartz in the layers I and II has been analysed at 27 positions as shown in Fig. 30. The results are illustrated in Fig. 31 and Table 5 (cf. Plate 9). With regard to the dimensional fabric pattern of quartz grains in the fold knee which is inferred from the orientation data on the ac-section, bc-section and ab-section, it will be assumed that, at any position of the fold, the principal axes X and Z are oriented parallel to the plane normal to the fold axis and that the principal axis Y is parallel to the fold axis. The trajectories of the principal axis X through the fold will be drawn as shown in Fig. 32. The strain picture in the fold appears to be essentially the same as that in the fold of the specimens I and IV.

The direction of preferred grain orientation of quartz in the layer II, as observed on the ac-section, appears to be generally parallel to the layer surface rather than to

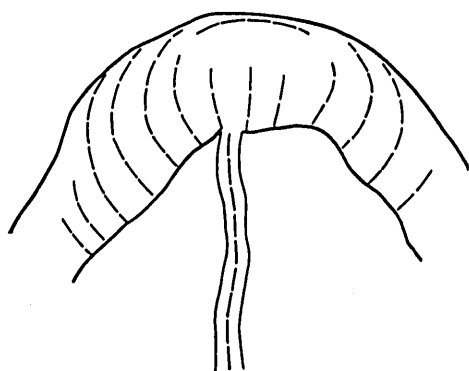


FIG. 32 Diagram showing the trajectories of the principal axis X of strain ellipsoid through the folded and non-folded quartz-rich layers in the specimen V.

the axial surface, though the former is approximately parallel to the latter (Plate 9). On a thin section (position 27) parallel to both the fold axis and the layer surface, quartz grain in the layer II are preferably oriented normal to the fold axis, while, on another thin section (position 26) parallel to the fold axis and normal to the layer surface, they are preferably oriented parallel to the fold axis. Therefore, the shape and orientation of the mean strain ellipsoid at any position of the layer II will be generally illustrated as follows: The strain ellipsoid is of the triaxial type. The principal axis X is parallel to the layer surface and normal to the fold axis, the

principal axis Z is normal to the layer surface and the fold axis, and the principal axis Y is parallel to the fold axis.

As mentioned in the preceding page, the  $S_{2m}$ -cleavage is parallel to the principal plane XY of the mean strain ellipsoid of the system concerned. The layer II is running subparallel to the  $S_{2m}$ -cleavage, while the enveloping surface of the layer I is approximately normal to the  $S_{2m}$ -cleavage. Therefore, it seems probable that the strain picture of the layer I (fold form and dimensional fabric of quartz) and that of the layer II (even form and dimensional fabric of quartz) were developed under the

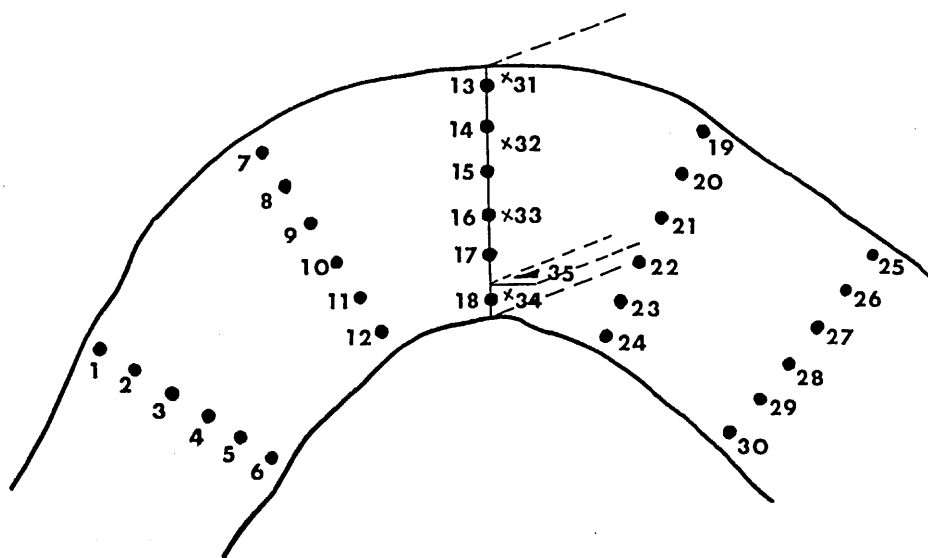


FIG. 33 Diagram showing the positions for the measurement of directions and degrees of grain orientation of quartz in the fold of the specimen VI.

same stress field, that is, the former corresponds to the deformation style of competent layer inclined at high angles to the principal plane XY and the latter corresponds to that of competent layer inclined at low angles to the principal plane XY, with regard to RAMBERG's (1959), FLINN's (1962) and RAMSAY's (1967) works on rock folding and boudinage.

Next, dimensional fabrics of quartz in the folds of quartz-rich layers enclosed in the psammitic schist of the Oboke district will be examined on four specimens.

Specimen VI (H67V0213): Some macroscopic characters of the fold observed in the specimen are enumerated as follows. 1) The fold is referred to the type of cylindrical plane fold with reference to its geometric property. 2) The form is nearly symmetric bilaterally across the axial surface. The fold has a near orthorhombic symmetry. 3) The angle between the limbs is about  $70^\circ$ . 4) In the surrounding psammitic schist is found the  $S_2$ -cleavage in one set as axial plane cleavage. 5) The enveloping surface of the folded quartz-rich layer is approximately normal to the  $S_2$ -cleavage and parallel to the  $L_{1-2}$ -lineation.

The grain orientation of quartz in the fold has been analysed at 35 positions as shown in Fig. 33. The results are shown in Fig. 34 and Table 6 (cf. Plate 10). With regard to the dimensional fabric of quartz grains in fold knee, it will be assumed that, at any position of the fold, the principal axes X and Z are oriented parallel to the plane normal to the fold axis and that the principal axis Y is parallel to the fold axis. The trajectories of the principal axis X through the fold will be drawn as shown in Fig. 35. The neutral axis appears to be located at the outermost side of fold knee. That strain picture in the fold in question is essentially the same as that in the fold of quartz-rich layer enclosed in the pelitic schist of the specimen II, that is, the Type II

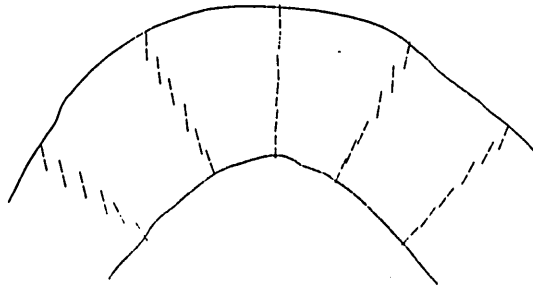


FIG. 34 Diagram showing the directions of the preferred grain orientation of quartz at 30 positions on the ac-section for the specimen VI.

TABLE 6. Summary of grain orientation data for for the specimen IV.

Position Nos.	Vector Magnitude (%)	Probability	Significant	The angle between fold axis and vector mean (degrees)
1	41.0	$<10^{-3}$	Yes	
2	53.0	$<10^{-5}$	Yes	
3	48.4	$<10^{-5}$	Yes	
4	48.2	$<10^{-5}$	Yes	
5	54.4	$<10^{-5}$	Yes	
6	62.8	$<10^{-5}$	Yes	
7	30.2	$<0.02$	Yes	
8	36.2	$<0.01$	Yes	
9	37.2	$<10^{-3}$	Yes	
10	41.6	$<10^{-3}$	Yes	
11	67.0	$<10^{-5}$	Yes	
12	72.4	$<10^{-10}$	Yes	
13	24.5	$<0.05$	Yes	
14	23.4	$>0.05$	No	
15	41.4	$<10^{-3}$	Yes	
16	55.2	$<10^{-5}$	Yes	
17	66.8	$<10^{-5}$	Yes	
18	87.4	$<10^{-15}$	Yes	
19	31.6	$<0.01$	Yes	
20	42.2	$<10^{-3}$	Yes	
21	60.2	$<10^{-5}$	Yes	
22	69.4	$<10^{-10}$	Yes	
23	75.4	$<10^{-10}$	Yes	
24	73.4	$<10^{-10}$	Yes	
25	53.2	$<10^{-5}$	Yes	
26	56.6	$<10^{-5}$	Yes	
27	53.6	$<10^{-5}$	Yes	
28	66.0	$<10^{-5}$	Yes	
29	78.4	$<10^{-10}$	Yes	
30	72.8	$<10^{-10}$	Yes	
31	14.6	$>0.30$	No	30
32	15.2	$>0.30$	No	10
33	21.2	$>0.10$	No	87
34	26.6	$<0.04$	Yes	85
35	80.6	$<10^{-10}$	Yes	3

of strain picture.

Specimen VII (H67V0204): Some macroscopic characteristics of the fold observed in the specimen are listed as follows. 1) The fold is referred to the type of cylindrical plane fold with reference to its geometric property. 2) The fold has a near orthorhombic symmetry. 3) The angle between the limbs is about  $120^\circ$ . 4) In the surrounding psammitic schist is found the  $S_2$ -cleavage in one set, showing such orientation pattern as shown in Fig. 37. 5) The enveloping surface of the folded quartz-rich layer is inclined at an angle ca.  $55^\circ$  to the  $S_2$ -cleavage and parallel to the  $L_{1-2}$ -lineation. The axial surface of the fold which is geometrically established as the bisecting surface of both limbs is normal to the enveloping surface of the layer.

The grain orientation of quartz in the fold has been examined at 18 positions as shown in Fig. 36. The results are illustrated in Fig. 37 and Table 7 (cf. Plate 11). The strain picture in the fold appears to be essentially the same as that in the fold of

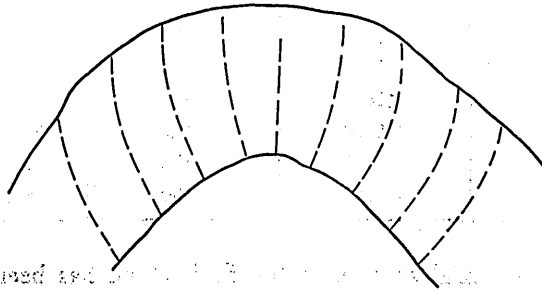


FIG. 35 Diagram showing the trajectories of the principal axis X of strain ellipsoid through the fold of the specimen VI.

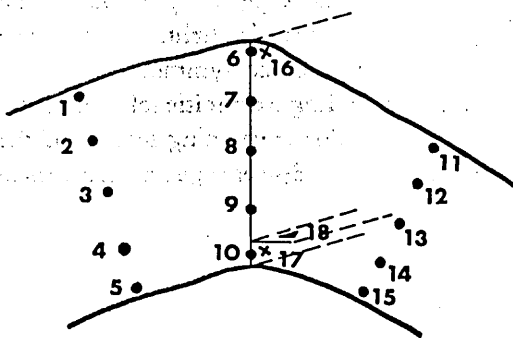


FIG. 36 Diagram showing the positions for the measurement of directions and degrees of grain orientation of quartz in the fold of the specimen VII.

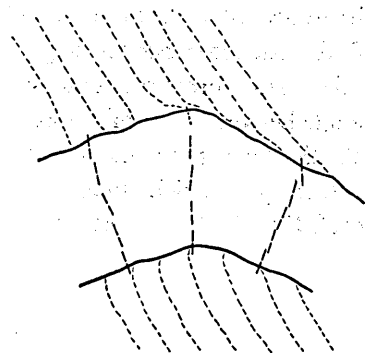


FIG. 37 Diagram showing the direction of preferred grain orientation of quartz at 15 positions on the ac-section for the fold of the specimen VII and the attitude of the  $S_2$ -cleavage in the surrounding mica-rich layers.

TABLE 7. Summary of grain orientation data for the specimen VII.

Position Nos.	Vector Magnitude (%)	Probability	Significant	The angle between fold axis and vector mean (degrees)
1	33.6	<0.01	Yes	
2	41.2	<10 <sup>-3</sup>	Yes	
3	44.4	<10 <sup>-4</sup>	Yes	
4	57.4	<10 <sup>-5</sup>	Yes	
5	63.4	<10 <sup>-5</sup>	Yes	
6	12.2	>0.40	No	
7	49.2	<10 <sup>-5</sup>	Yes	
8	64.8	<10 <sup>-5</sup>	Yes	
9	78.6	<10 <sup>-10</sup>	Yes	
10	85.8	<10 <sup>-15</sup>	Yes	
11	29.4	<0.02	Yes	
12	36.8	<0.01	Yes	
13	37.8	<10 <sup>-3</sup>	Yes	
14	68.4	<10 <sup>-10</sup>	Yes	
15	91.2	<10 <sup>-15</sup>	Yes	
16	21.4	>0.10	No	77
17	32.0	<0.01	Yes	85
18	61.5	<10 <sup>-5</sup>	Yes	4

the specimen VI. The axial surface of the fold which has been established on the basis of the dimensional fabric of quartz (see Fig. 38) coincides with that geometrically defined.

Specimen VIII (H67V0206): Some characteristics of the fold observed in the specimen are listed as follows. 1) The fold is referred to the type of cylindrical plane fold with reference to its geometric property. 2) The form is slightly asymmetric bilaterally across the axial surface. The fold has a monoclinic symmetry. 3) The angle between the limbs is about 100°. 4) In the surrounding psammitic schist is found the S<sub>2</sub>-cleavage in one set as axial plane cleavage. 5) The enveloping surface of the folded quartz-rich layer is inclined at an angle ca. 70° to the S<sub>2</sub>-cleavage and at an angle ca. 20° to the L<sub>1-2</sub>-lineation.

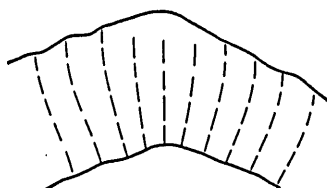


FIG. 38 Diagram showing the trajectories of the principal axis X of strain ellipsoid through the fold of the specimen VII.

Geometry and Internal Structures of Flexural Folds

The grain orientation of quartz in the fold has been analysed at 17 positions as shown in Fig. 39. The results are illustrated in Fig. 40 and Table 8. The neutral axis is not developed within the layer. The strain picture in the fold appears to be essentially the same as that in the fold of the quartz-rich layer enclosed in the pelitic schist of the specimen III, that is, the Type III of strain picture, as is obvious in Fig. 41 and Table 8.

Specimen IX (H66VII1001): Some macroscopic characteristics of the fold observed in the specimen are enumerated as follows. 1) The fold is referred to the type of cylindrical plane fold with reference to its geometric property. 2) The fold has a near orthorhombic symmetry. 3) The angle between the limbs is about  $90^\circ$ . 4) In the surrounding psammitic schist is found the  $S_2$ -cleavage in one set as axial plane cleavage. 5) The enveloping surface of the folded quartz-rich layer is inclined at an angle

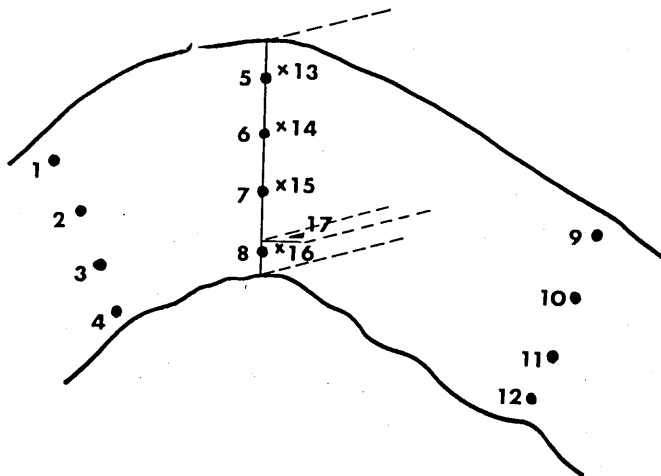


FIG. 39 Diagram showing the positions for the measurement of directions and degrees of grain orientation of quartz in the fold of the specimen VIII.

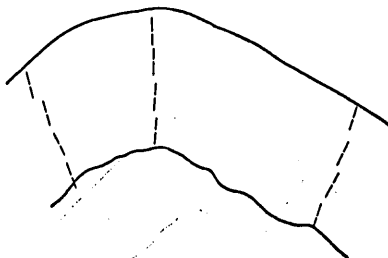


FIG. 40 Diagram showing the directions of preferred grain orientation of quartz at 12 positions on the section for the fold of the specimen VIII.

Table 8. Summary of grain orientation data for the specimen VIII.

Position Nns.	Vector Magnitude (%)	Probability	Significant	The angle between fold axis and vector mean (degrees)
1	55.4	$<10^{-5}$	Yes	
2	63.8	$<10^{-5}$	Yes	
3	81.2	$<10^{-10}$	Yes	
4	83.2	$<10^{-10}$	Yes	
5	44.2	$<10^{-4}$	Yes	
6	64.6	$<10^{-5}$	Yes	
7	85.2	$<10^{-15}$	Yes	
8	88.6	$<10^{-15}$	Yes	
9	63.0	$<10^{-5}$	Yes	
10	66.0	$<10^{-5}$	Yes	
11	86.0	$<10^{-15}$	Yes	
12	91.0	$<10^{-15}$	Yes	
13	23.6	$>0.05$	No	84
14	12.2	$>0.40$	No	82
15	25.4	$<0.05$	Yes	88
16	31.8	$<0.01$	Yes	87
17	45.2	$<10^{-4}$	Yes	2

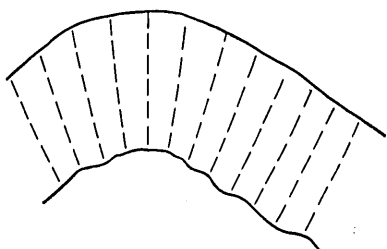


FIG. 41 Diagram showing the trajectories of the principal axis X of strain ellipsoid through the fold of the specimen VIII.

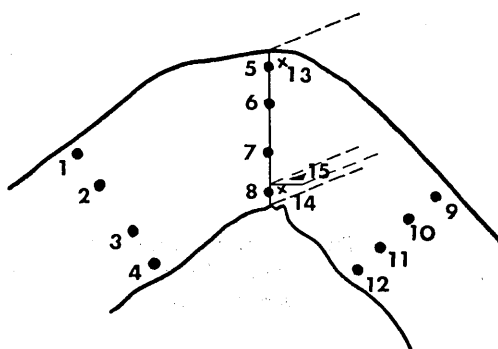


FIG. 42 Diagram showing the positions for the measurement of directions and degrees of grain orientation of quartz in the fold of the specimen IX.

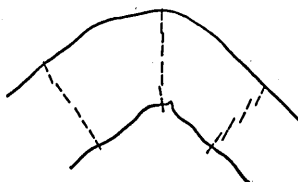


FIG. 43 Diagram showing the directions of preferred grain orientation of quartz at 12 positions on the ac-section for the fold of the specimen IX.

Geometry and Internal Structures of Flexural Folds

TABLE 9. Summary of grain orientation data for the specimen IX.

Position Nos.	Vestor Magnitude (%)	Probability	Significant	The angle between fold axis axis and vector mean (degrees)
1	26.0	<0.04	Yes	
2	56.2	<10 <sup>-5</sup>	Yes	
3	67.1	<10 <sup>-5</sup>	Yes	
4	69.6	<10 <sup>-10</sup>	Yes	
5	28.4	<0.02	Yes	
6	43.8	<10 <sup>-4</sup>	Yes	
7	64.4	<10 <sup>-5</sup>	Yes	
8	93.4	<10 <sup>-15</sup>	Yes	
9	46.3	<10 <sup>-4</sup>	Yes	
10	51.2	<10 <sup>-5</sup>	Yes	
11	63.7	>10 <sup>-5</sup>	Yes	
12	78.8	<10 <sup>-10</sup>	Yes	
13	26.4	<0.03	Yes	83
14	47.0	<10 <sup>-4</sup>	Yes	89
15	52.4	<10 <sup>-5</sup>	Yes	6

ca. 70° to the S<sub>2</sub>-cleavage and parallel to the L<sub>1-2</sub>-lineation.

The grain orientation of quartz in the fold has been analysed at 15 positions as shown in Fig. 42. The results are illustrated in Fig. 43 and Table 9 (cf. Plate 12). The pattern of the trajectories of the principal axis X through the fold appears to be essentially the same as that in the fold of the specimen VIII, as is obvious in Fig. 44. In the present specimen, however, even at the outermost part of fold knee the principal axes X and Y is not equal, the strain ellipsoid being of the triaxial type, and the principal axis X is oriented on the plane normal to the fold axis and the principal axis Y is parallel to the fold axis. Strictly speaking, therefore, the strain picture in the fold in question may be different from that in the fold of the specimen VIII. The strain picture in question will be named Type IV.

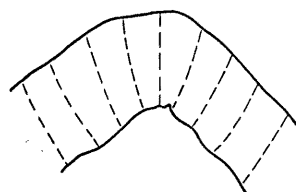


FIG. 44 Diagram showing the trajectories of the principal axis X of strain ellipsoid through the fold of the specimen IX.

It will be safely said that the strain picture in the quartz-rich layer developed during the folding is different between the specimens VI (and VII), VIII and IX, on the basis of the pattern of the dimensional fabric of quartz, e. g., with respect to the position of the neutral axis in the fold, for the specimens VI and VII the neutral axis is developed at the outermost side of fold knee, and for the specimens VIII and IX that is not developed within the layer, and, with respect to the shape of the mean strain ellipsoid at the outermost side of fold knee, for the specimen VIII X=Y>Z and for the specimen IX X>Y>Z. Roughly speaking, the strain picture in the fold of the specimens VI and VII (Figs. 35 and 38) appears to be correlated with that in the middle to inner side of the fold of the specimen I (Fig. 20), that in the fold of the specimen VIII (Fig. 41) with that in the outer to inner side of the fold of the specimen VI, and that in the

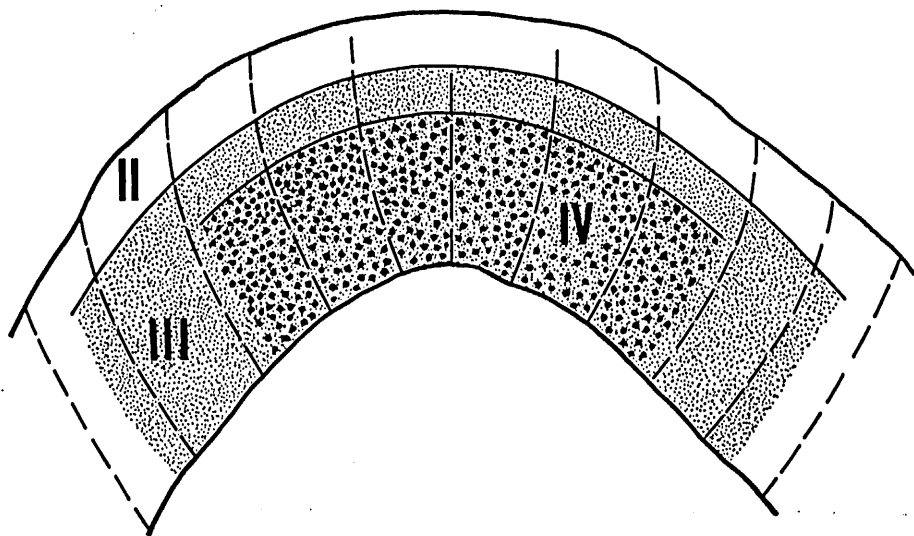


FIG. 45 Diagram showing the relationship between the strain pictures of Type II, Type III and Type IV.

II: Type II. III: Type III. IV: Type IV.

Dashed lines: the trajectories of the principal axis X of strain ellipsoid through the fold of the specimen VI.

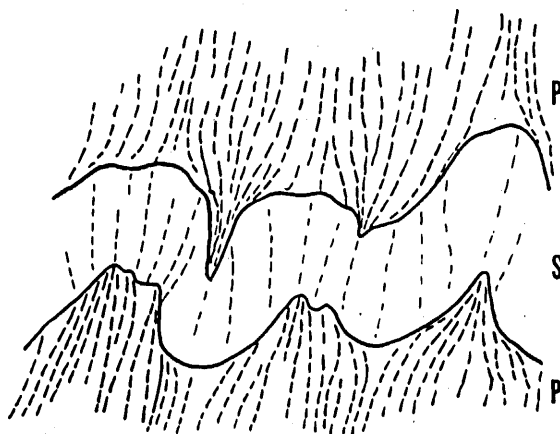


FIG. 46 Fold of a thin layer of psammitic schist enclosed in the pelitic schist.

Dashed lines: attitude of the  $S_2$ -cleavage in the fold.

p: pelitic schist. S: psammitic schist.

fold of the specimen IX (Fig. 44) with that in the middle to inner side of the fold of the specimen VI, as shown schematically in Fig. 45.

It appears to be pointed out that the dimensional fabrics of quartz in many folds of quartz-rich layers enclosed in the psammitic schist of the Oboke district, whose axes are parallel or subparallel to the  $L_{1-2}$ -lineation, are grouped into the above-described

three types, and that the development of the extension zone is not found in any one of the observed folds, unlike the case of the folds of quartz-rich layers enclosed in the pelitic schist of the Kune district.

Fig. 46 shows a fold of a thin layer of psammitic schist enclosed in the pelitic schist of the Oboke district, that was formed during the  $B_2$ -deformation. In both the psammitic and pelitic schists is found the cleavage structure in one set, which appears to be referred to the  $S_2$ -cleavage previously defined. The cleavage is uniformly developed through the fold of psammitic layer, though its development is rather weaker in the top of fold knee than in the bottom, showing a fan-like arrangement with downward convergence (Fig. 46). It has been clarified that the  $S_2$ -cleavage in the psammitic schist of the Koboke syncline coincides with the plane of flattening. If so also in the present case, the cleavage traces on the plane normal to the fold axis may be regarded as representing the trajectories of the principal axis X through the fold. The neutral axis does not appear to be developed within the layer. The strain picture in question appears to be fairly similar to that in the fold of quartz-rich layer of specimen IX, as is obvious in Figs. 46 and 44. With respect to the angle between the cleavage surface (the principal plane XY) and the layer surface at the middle part of a limb (the angle  $\alpha$  in Fig. 47) and that between the cleavage surfaces at the middle parts of both limbs (the angle  $\beta$  in Fig. 47), however,  $\alpha$  and  $\beta$  for the folds of psammitic layers enclosed in the pelitic schist are generally smaller than  $\alpha$  and  $\beta$  for

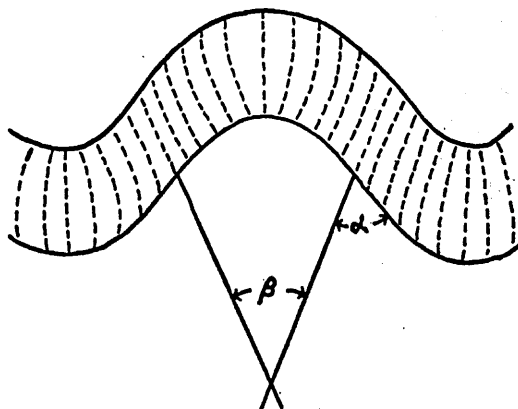


FIG. 47 Diagram illustrating the relationship between the angles  $\alpha$  and  $\beta$  and the cleavage-attitude in a fold.

the folds of quartz-rich layers in the psammitic schist, when compared between the folds with the same interlimb angle. For convenience' sake, the strain picture in the fold of psammitic layer, shown in Fig. 46, will be named Type V. Analogous strain picture is also equally obvious for many folds of psammitic layers enclosed in the Oboke pelitic schist.

Fig. 48 shows the cleavage-attitude in the fold of the multilayered system consisting

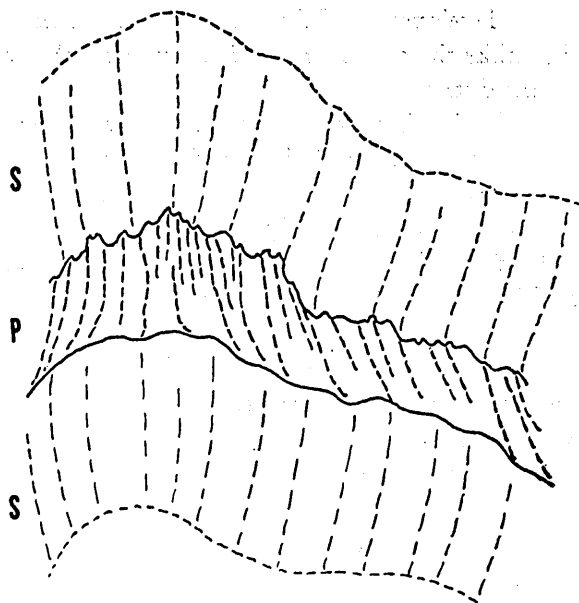


FIG. 48 The cleavage-attitude in the fold of the multilayered system consisting of alternating psammitic layers and pelitic layers.  
P: pelitic layer. S: psammitic layer.

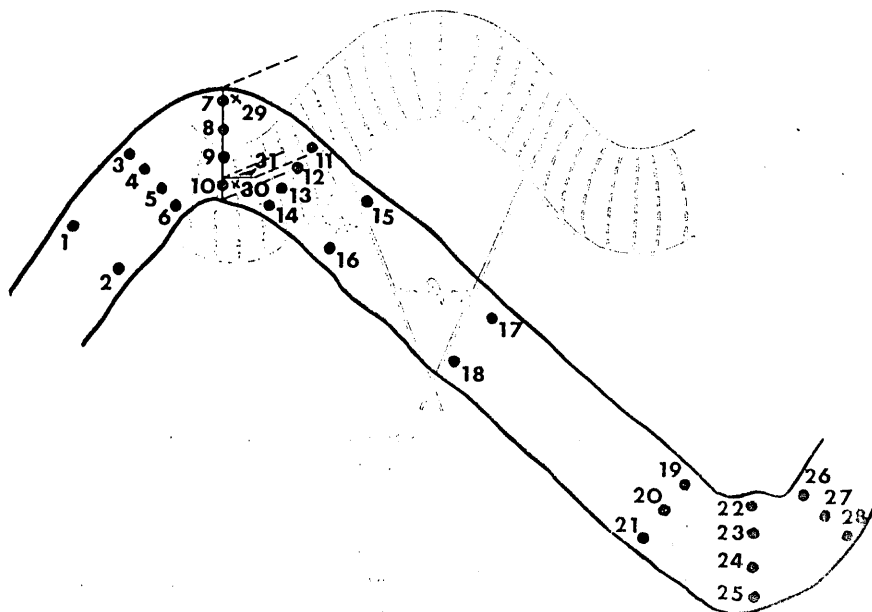


FIG. 49 Diagram showing the positions for the measurement of directions and degrees of grain orientation of quartz in the fold of the specimen X.

## Geometry and Internal Structures of Flexural Folds

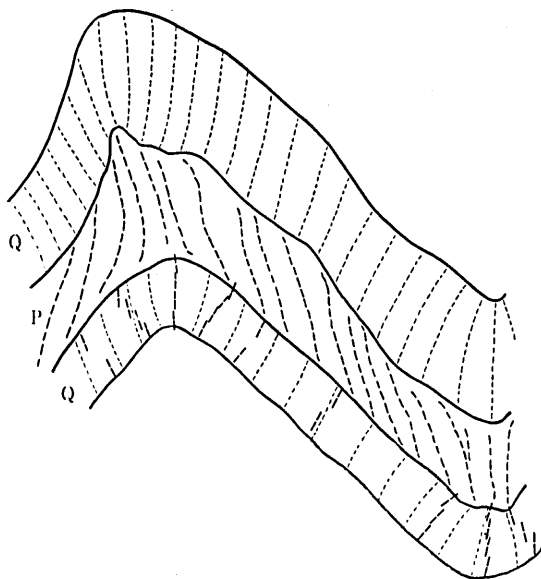


FIG. 50 Diagram showing the directions of preferred grain orientation of quartz at 28 positions on the ac-section for the fold of the specimen X, the trajectories of the principal axis X through the fold and the cleavage-attitude in the psammitic layer.  
Q: quartz-rich layer. P: psammitic layer.

of alternating psammitic layers and pelitic layers. The cleavage surfaces in the psammitic layers tend to converge toward the bottom of fold knee in such an attitude as to form a fan-like arrangement, while the cleavage-attitude in the folds of pelitic layers is as to form a fan-like arrangement with upward convergence. The cleavage in the pelitic layers shows commonly the weakest intensity at the bottom of fold knee (Fig. 48). Analogous relationship for the cleavage-attitude in the fold is commonly found in the folds of the multilayered system made of the alternation of psammitic layers and pelitic layers in the Oboke district. Fig. 50 (Specimen X) shows the cleavage-attitude which is commonly found in the folds of the multilayered system made of the alternation of quartz-rich layers and psammitic layers, though the cleavage in the quartz-rich layer is defined by the preferred orientation of quartz grains (= the principal plane XY) (Figs. 49 and 50, Table 10 and Plates 13 and 14). The orientation pattern of the cleavage in the fold of the latter condition (quartz-rich layer/psammitic layer), shown in Fig. 50 and Plate 13, appears to be essentially the same as that of the former condition (psammitic layer/pelitic layer), shown in Fig. 48.

Some points of discrepancies in the strain picture between the folds of quartz-rich layers enclosed in the pelitic schist, those of quartz-rich layers in the psammitic schist and those of psammitic layers in the pelitic schist will be again mentioned as follows\*

\* In all cases, the fold axis is parallel or subparallel to the principal axis Y of the mean strain ellipsoid of the system concerned.

TABLE 10. Summary of grain orientation data for the specimen X.

Position Nos.	Vector Magnitude (%)	Probability	Significant	The angle between fold axis and vector mean (degrees)
1	62.8	$<10^{-5}$	Yes	
2	77.8	$<10^{-10}$	Yes	
3	60.8	$<10^{-5}$	Yes	
4	65.0	$<10^{-5}$	Yes	
5	73.8	$<10^{-10}$	Yes	
6	78.6	$<10^{-10}$	Yes	
7	36.2	$<0.01$	Yes	
8	52.6	$<10^{-5}$	Yes	
9	69.4	$<10^{-10}$	Yes	
10	95.6	$<10^{-15}$	Yes	
11	57.0	$<10^{-5}$	Yes	
12	62.0	$<10^{-5}$	Yes	
13	67.4	$<10^{-5}$	Yes	
14	68.2	$<10^{-5}$	Yes	
15	57.0	$<10^{-5}$	Yes	
16	62.2	$<10^{-5}$	Yes	
17	78.0	$<10^{-10}$	Yes	
18	78.8	$<10^{-10}$	Yes	
19	73.0	$<10^{-10}$	Yes	
20	77.6	$<10^{-10}$	Yes	
21	60.0	$<10^{-5}$	Yes	
22	90.9	$<10^{-15}$	Yes	
23	81.2	$<10^{-10}$	Yes	
24	62.4	$<10^{-5}$	Yes	
25	42.8	$<10^{-3}$	Yes	
26	73.8	$<10^{-10}$	Yes	
27	68.0	$<10^{-5}$	Yes	
28	62.2	$<10^{-5}$	Yes	
29	27.4	$<0.03$	Yes	87
30	32.7	$<0.01$	Yes	89
31	57.3	$<10^{-5}$	Yes	5

(cf, Plate 4); The strain pictures in the folds of quartz-rich layers in the pelitic schist can be generally referred to the Type I, Type II and Type III, those in the folds of quartz-rich layers in the psammitic schist to the Type II, Type III and Type IV, and those of psammitic layers in the pelitic schist to the Type V. The development of the extension zone in the fold knee is frequently found in the folds of quartz-rich layers in the pelitic schist but not in other conditions. For some folds of quartz-rich layers in the psammitic schist, the neutral axis is developed at the outermost side of fold knee, but, for the folds of psammitic layers in the pelitic schist, that does not appear to be developed within the layer. Roughly speaking, the angle  $\beta$  is larger for the folds which

show the development of the extension zone within the layer (strain picture of Type I) than for the folds which do not show the development of the neutral axis within the layer (strain pictures of Type III, Type IV and Type V), when compared between the folds with the same interlimb angle. The minimum angle of  $\beta$  can be measured in the folds of psammitic layers enclosed in the pelitic schist, which show the strain picture of Type V, while the maximum angle of  $\beta$  in the folds of quartz-rich layers in the pelitic schist, which show the strain picture of Type I. The change of the strain picture from Type I to Type V may show the corresponding decrease of the angle  $\beta$ . Generally, the angle  $\beta$  should increase with increase of the angle  $\alpha$ . The maximum angle of  $\alpha$ , which will be measured in the fold showing the strain picture of Type I, appears to be about  $90^\circ$ , that corresponding to the case in which the principal axis X is normal to the layer surface.

According to RAMBERG (1964), under lateral compression, competent layers enclosed in incompetent layers shortens by two unlike mechanisms; 1) by buckle shortening and 2) by layer shortening. Buckle shortening and layer shortening take place simultaneously but usually with different rates. The relationship between the rate of buckle shortening ( $\dot{\lambda}/\lambda$ ) and that of the layer shortening ( $\dot{\epsilon}$ ) is

$$\frac{\dot{\lambda}/\lambda}{\dot{\epsilon}} = \frac{4}{3} \pi^2 \sqrt[3]{6 \left( \frac{\mu_1}{\mu} \right)^2 \left( \frac{y}{\lambda} \right)^2},$$

where  $y$  is amplitude of fold and  $\lambda$  is wavelength. "..... the significant information contained in this equation is that the rate of buckle shortening relative to the rate of layer shortening increases with increasing viscosity contrast between the layer and the surrounding material (at a given initial amplitude/wavelength ratio). It is also important that the ratio between the rates of buckle shortening and layer shortening increases rapidly as the amplitude increases." (RAMBERG, 1964, p. 310). If so, it will be assumed that the strain picture in a competent layer folded under lateral compression is considerably controlled by the viscosity ratio between the layer and the surrounding incompetent layers. Both the magnitude of uniform compressive strain along the layer and the amplitude of the fold, which are achieved before the tensile stress is developed at the outermost side of fold knee, appear to decrease with increase of the viscosity ratio between the layer and the surrounding incompetent layer. It is therefore possible that, for the folding of a multilayered system with smaller viscosity ratio, the neutral axis is not developed within the competent layers involved, whose fold form is of an acute type. "If the viscosity ratio between a layer and its host is small enough, buckling is apt to be completely masked by layer shortening. BIOT (1957, p. 451) assumes a  $\mu_1/\mu$  value of 60 as the limit below which buckling is negligible relative to layer shortening" (RAMBERG, 1964, p. 311).

Thus, the characteristics of the strain pictures in the folds of quartz-rich layers in the pelitic schist, in those of quartz-rich layers in the psammitic schist and in those of psammitic layers in the pelitic schist and the differences in the strain picture between the folds of those three different conditions may be clearly explained by the above-

cited informations after BIOT and RAMBERG. The change of the strain picture in the fold from the Type I to the Type V appears to correspond to that the rate of layer shortening relative to the rate of buckle shortening becomes gradually predominant with decreasing viscosity ratio between the competent layer (quartz-rich layer or psammitic layer) and the surrounding incompetent layer (psammitic layer or pelitic layer), that is, the strain pictures of Type III, Type IV and Type V correspond to those in the folds which were produced by buckling instability under the physical condition in which the ratio between the rate of buckle shortening and the rate of layer shortening shows smaller values through the whole stage of the folding, while the strain pictures of Type I and Type II correspond to those of the folds produced by buckling instability under the condition in which the ratio in question shows larger values. It will be very important that the fan-like arrangement of the cleavage (= the principal plane XY) is found even in the folds of the multilayered system consisting of alternating psammitic schist and pelitic schist, as shown in Figs. 46 and 48, in which the viscosity ratio between those rocks is about 3, showing the effect of buckling instability for the formation of the folds of psammitic layers and the effect of passive flow of the pelitic layers. Such assumption that the mechanism of buckling played an important role in the formation of the folds of psammitic layers appears to be supported also by the facts that in the folds of multilayered system consisting of alternating psammitic layers and pelitic layers, generally, the cleavage in the latter tends to develop with the weakest intensity at the bottom of fold knee, as well as the fan-like arrangement with upward convergence, showing the development of the contact strain due to the folding of the former. If the viscosity ratio between the layers in a multilayered system approximates to 1, for any layer in that system buckling will be completely masked by layer shortening. At this time, the cleavage will have the same direction through all the layers involved in the folds of the multilayered system, that is, the angle  $\beta$  will be 0. It may be concluded that, if any fold shows the fan-like arrangement of the cleavage as shown in Figs. 26, 41, 44, 46 and 48, generally, buckling instability played the important role in the formation of the fold. Measurements of the angle  $\beta$  (or  $\alpha$ ) in any fold with a given amplitude/wavelength ratio appear to lead us to the estimation of the ratio between the rate of buckle shortening and that of layer shortening and so the viscosity ratio between the competent layer and the surrounding incompetent layer under the physical condition in which the fold was produced. Now, theoretical solution of the strain picture (trajectories of the principal axis X) in a fold of competent layer, with regard to the variation in the viscosity ratio between the related rocks, will be required.

That the folds of quartz-rich layers in the pelitic schist show the strain pictures of Type I, Type II and Type III and those in the psammitic schist show the strain pictures of Type II, Type III and Type IV appear to show wide range of viscosity ratio of the related rocks in the system concerned. The average  $L/T$  ratios in Figs. 15, 16 and 17 are not correlated with the  $L_d/T$  ratio in the sense of BIOT (1961). Even within a given system the  $L_d/T$  ratio will be different between the folds with the different

types of strain picture, showing a relation that Type I > Type II > Type III > Type IV > Type V. In Fig. 17, therefore, the average L/T ratio for the folds with the strain picture of Type I, that of Type II and that of Type III must be shown by different three lines, and also in Fig. 15 that of Type II, that of Type III and that of Type IV by different three lines, though this problem is not examined in this paper. Only on the basis on the average L/T ratio obtained on the folds with the strain picture of a definite type, the viscosity ratio of the related rocks and its range in the system concerned will be exactly estimated.

The folds of quartz-rich layers in the Kune pelitic schist show the strain pictures of Type I, Type II and Type III. If most of them show the strain picture of Type III, the average L/T ratio 14.9 corresponds approximately to that for the folds with the strain picture of Type III. If it will be assumed that the layer shortening of quartz-rich layers during the folding, which is characterized by the formation of the strain picture of Type III, is less than ca. 15 per cent on the basis of the data described in the later page, then the ratio of the initial wavelength and the initial layer-thickness is 20.5 and the viscosity ratio of the related rocks is 207.9. Now, it will be pointed out that the folding for the strain picture of Type III occurs under the condition in which the viscosity ratio of the related rocks is not larger than 207.9. If most of the folds in the Kune pelitic schist show the strain picture of Type I, then the ratio of the initial wavelength and the initial layer-thickness approximates to 14.9 and the viscosity ratio of the related rocks to 80, for the layer shortening of quartz-rich layers during the folding, which is characterized by the formation of the strain picture of Type I, is less than several per cent. If most of the folds in the Oboke psammitic schist show the strain picture of Type II, then the ratio of the initial wavelength and the initial layer-thickness is 15.5 and the viscosity ratio of the related rocks is 89.3, for the layer shortening of quartz-rich layers during the folding, which is characterized by the formation of the strain picture of Type II, is about 14 per cent. Now, it will be pointed out that the folding for the strain picture of Type I occurs under the condition in which the viscosity ratio of the related rocks is larger than 89.3. If most of the folds in the Oboke psammitic schist show the strain picture of Type IV, then the ratio of the initial wavelength and the initial layer-thickness is 18.1 and the viscosity ratio of the related rocks is 141.7, for the layer shortening of quartz-rich layers during the folding, which is characterized by the formation of the strain picture of Type IV, is less than about 20 per cent for the observed folds in the Oboke psammitic schist. Therefore, it will be said that the folding for the strain picture of Type IV occurs under the condition in which the viscosity ratio of the related rocks is not larger than 141.7.

DONATH and PARKER (1964, p. 56) say, "passive folds can be characterized by rudely planar parallel surface (cleavage or other secondary foliation) inclined to the original layering even though the acting flow or slip surfaces . . . . may not be mutually parallel. Relative displacement of layering parallel to those surfaces determines the portion positions of fields of greatest curvature, i. e., the hinges of the fold. Thus, cleavage

commonly parallels the axial surface in passive folds. .... The relationship does not hold strictly in rock sequences having high ductility contrast, as, for example, passively folded limestone and dolomite; cleavage may have different attitudes in adjacent rock layers of contrasting behavior—the so-called “refraction” of cleavage.” Analogous opinion on the formation of the fold with axial plane cleavage has been presented by many other authors. According to the above-described data, however, the present authors will assume that for the formation of the folds with fan-like arrangement of axial plane cleavage (perhaps, that will be referred to any one of the strain pictures of Type II, Type III, Type IV, and Type V), generally, the mechanism of buckling played the important role, and that even in the multilayered rock system with low viscosity ratio (e. g. ca. 3) it did the important role in the formation of the fold of competent layer involved, being associated with passive flow of materials in incompetent layer. Therefore, the South Mountain fold examined in detail by CLOOS (1947) will also be referred to the type of the buckle fold and its strain picture, which is understood by the shape and orientation of deformed ooids, appears to be essentially the same as that of Type IV—Type V. In the mechanisms of formation of fold in nature, generally, buckling appears to be more important than passive folding.

The problem on the relationship between mechanisms of buckle folding and the orientational relation of the buckled layer to the mean strain ellipsoid of the system concerned will be examined on the folds of quartz-rich layers enclosed in the Oboke psammitic schist. Firstly, dimensional fabrics of quartz in some folds of quartz-rich layers, which show various orientations to the mean strain ellipsoid in the small domain of the hinge zone of the Kobokey syncline, will be described, with regard to the strain distribution in those folds.

Specimen XI (H66VII1004): The hinge line of the fold of quartz-rich layer observed in the specimen is inclined at an angle ca.  $35^\circ$  to the  $L_{1-2}$ -lineation and parallel to the  $S_2$ -cleavage. Some macroscopic characteristics of the fold are listed as follows. 1) The fold is referred to the type of cylindrical plane fold with reference to its geometric property. 2) The fold has a near orthorhombic symmetry. 3) The angle between the limbs is about  $100^\circ$ . 4) In the surrounding psammitic schist is found the  $S_2$ -cleavage in one set as axial plane cleavage. 5) The enveloping surface of the folded quartz-rich layer is subnormal to the  $S_2$ -cleavage.

The grain orientation of quartz in the fold has been examined at 14 positions as shown in Fig. 51. The results are illustrated in Fig. 52 and Table 11. The strain picture in the fold appears to be referred to the Type III, that is, at the inner part of fold knee the shape of the mean strain ellipsoid is of the triaxial type and the principal axes X and Z are oriented on the plane normal to the fold axis, while at the outermost part of fold knee  $X \approx Y > Z$  and the principal axis Z is oriented on the plane normal to the fold axis.

Specimen XII (H66VII1105): The hinge line of the fold of quartz-rich layer observed in the specimen is inclined at an angle ca.  $60^\circ$  to the  $L_{1-2}$ -lineation and parallel to the  $S_2$ -cleavage. Some macroscopic characteristics of the fold are listed as

Geometry and Internal Structures of Flexural Folds

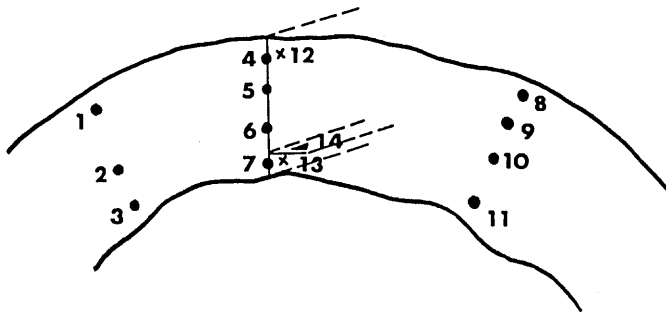


FIG. 51 Diagram showing the positions for the measurement of directions and degrees of grain orientation of quartz in the fold of the specimen XI.

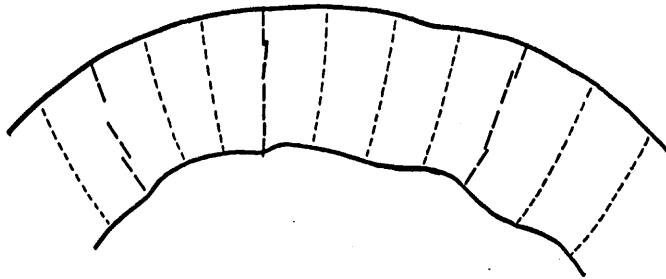


FIG. 52 Diagram showing the directions of preferred grain orientation of quartz at 11 positions on the ac-section for the fold of the specimen XI and the trajectories of the principal axis X through the fold.

TABLE 11. Summary of grain orientation data for the specimen XI.

Position Nos.	Vector Magnitude (%)	Probability	Significant	The angle between fold axis and vector mean (degrees)
1	44.0	$<10^{-4}$	Yes	
2	51.0	$<10^{-5}$	Yes	
3	63.4	$<10^{-5}$	Yes	
4	45.6	$<10^{-4}$	Yes	
5	63.4	$<10^{-5}$	Yes	
6	66.4	$<10^{-5}$	Yes	
7	82.2	$<10^{-10}$	Yes	
8	42.2	$<10^{-3}$	Yes	
9	51.2	$<10^{-5}$	Yes	
10	55.8	$<10^{-5}$	Yes	
11	75.6	$<10^{-10}$	Yes	
12	19.2	$>0.1$	No	84
13	38.6	$<10^{-3}$	Yes	83
14	68.2	$<10^{-5}$	Yes	3

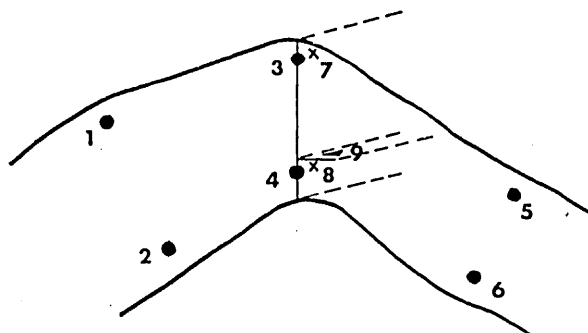


FIG. 53 Diagram showing the positions for the measurement of directions and degrees of grain orientation of quartz in the fold of the specimen XII.

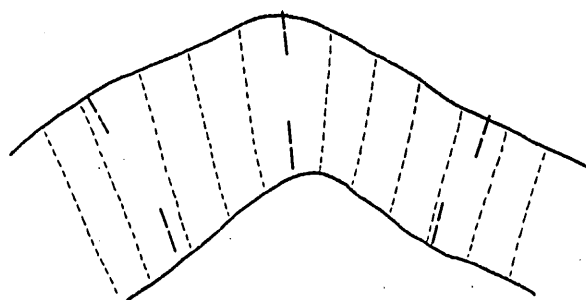


FIG. 54 Diagram showing the directions of preferred grain orientation of quartz on the ac-section for the fold of the specimen XII and the trajectories of the principal axis X through the fold.

TABLE 12. Summary of grain orientation data for the specimen XII.

Position Nos.	Vector Magnitude (%)	Probability	Significant	The angle between fold axis and vector mean (degrees)
1	46.0	$<10^{-4}$	Yes	
2	49.6	$<10^{-5}$	Yes	
3	38.1	$<10^{-3}$	Yes	
4	62.0	$<10^{-5}$	Yes	
5	42.7	$<10^{-3}$	Yes	
6	54.8	$<10^{-5}$	Yes	
7	15.2	$>0.3$	No	8
8	20.0	$>0.1$	No	5
9	68.3	$<10^{-5}$	Yes	2

follows. 1) The fold is referred to the type of cylindrical plane fold with reference to its geometric property. 2) The fold has a near orthorhombic symmetry. 3) The angle between the limbs is about  $105^\circ$ . 4) In the surrounding psammitic schist is found the  $S_2$ -cleavage in one set as axial plane cleavage. 5) The enveloping surface of the folded quartz-rich layer is inclined at an angle ca.  $60^\circ$  to the  $S_2$ -cleavage.

The grain orientation of quartz in the fold has been examined at 9 positions as shown in Fig. 53. The results are illustrated in Fig. 54 and Table 12. The shape of the mean strain ellipsoid of quartz aggregate appears to be  $X \approx Y > Z$  at all places of fold knee, even at the innermost side of fold knee. The principal axis  $Z$  must be oriented on the plane normal to the fold axis throughout the fold. The orientation pattern of the principal axis ( $X \approx Y$ ) on the plane normal to the fold axis is similar to the cases of the strain pictures of Type III and Type IV.

Specimen XIII (H66VIII108): The hinge line of the fold of quartz-rich layer observed in the specimen is inclined at angle ca.  $80^\circ$  to the  $L_{1-2}$ -lineation and parallel to the  $S_2$ -cleavage. Some macroscopic characteristics of the fold are listed as follows. 1) The fold is referred to the type of cylindrical plane fold with reference to its geometric property. 2) The fold has a near orthorhombic symmetry. 3) The angle between the limbs is about  $60^\circ$ . 4) In the surrounding psammitic schist is found the  $S_2$ -cleavage in one set as axial plane cleavage. 5) The enveloping surface of the folded quartz-rich layer is subnormal to the  $S_2$ -cleavage.

The grain orientation of quartz in the fold has been analysed at 17 positions as shown in Fig. 55. The results are illustrated in Fig. 56 and Table 13. The shape of the mean strain ellipsoid of quartz aggregate appears to be  $X \approx Y > Z$  at all places on fold knee, like in the case of the specimen XII. The strain picture in the fold is essentially the same as that in the fold of the specimen XII. The strain picture in question will be named Type VI.

It can be assumed that difference between the strain pictures of Type III and Type VI is due to the extent of which the quartz-rich layers being folded were elongated in a direction parallel to the fold axis, that is, the layers for the strain picture of Type

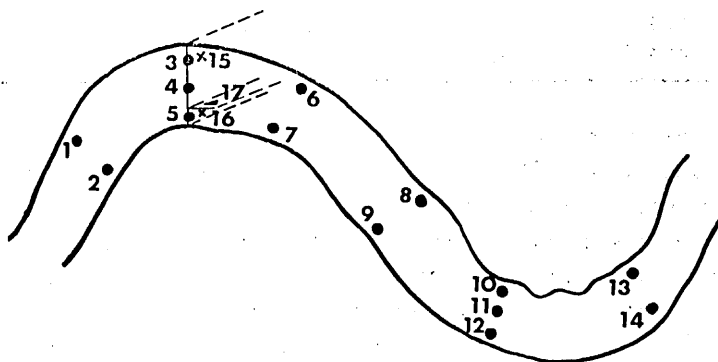


FIG. 55 Diagram showing the positions for the measurement of directions and degrees of grain orientation of quartz in the fold of the specimen XIII.

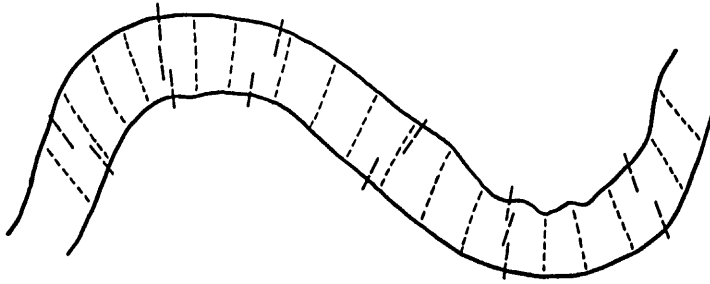


FIG. 56 Diagram showing the directions of preferred grain orientation of quartz on the ac-section for the fold of the specimen XIII and the trajectories of the principal axis X through the fold.

TABLE 13. Summary of grain orientation data for the specimen XIII.

Position Nos.	Vector Magnitude (%)	Probability	Significant	The angle between fold axis and vector mean (degrees)
1	63.2	$<10^{-5}$	Yes	
2	65.4	$<10^{-5}$	Yes	
3	42.4	$<10^{-3}$	Yes	
4	60.2	$<10^{-5}$	Yes	
5	89.0	$<10^{-15}$	Yes	
6	59.2	$\leq 10^{-5}$	Yes	
7	77.0	$<10^{-10}$	Yes	
8	64.8	$<10^{-4}$	Yes	
9	69.4	$<10^{-10}$	Yes	
10	83.4	$<10^{-10}$	Yes	
11	59.8	$<10^{-5}$	Yes	
12	42.2	$<10^{-3}$	Yes	
13	67.8	$<10^{-5}$	Yes	
14	58.4	$<10^{-5}$	Yes	
15	17.4	$<0.20$	No	88
16	15.2	$>0.30$	No	75
17	67.5	$<10^{-5}$	Yes	4

VI were more strongly elongated than those for the strain picture of Type III. According to RAMBERG's (1959), FLINN's (1962) and RAMSAY's (1967) works on rock folding and boudinage, generally, the extent of which during the folding a competent layer involved in a system may be elongated in a direction parallel to the fold axis appear to be determined by the orientational relation of the layer to the mean strain ellipsoid of the system, that is, the axial elongation of the folded layer would be maximum when oriented parallel to the principal axis X and minimum when oriented parallel to the principal axis Y. The hinge lines of the folds of quartz-rich layers, which show the strain picture of Type III, (Specimens VIII and XI), are inclined at

low angles to the  $L_{1-2}$ -lineation, while those of the folds, which show the strain picture of Type VI, (Specimens XII and XIII), are inclined at high angles to the  $L_{1-2}$ -lineation. Therefore, it may be concluded that the mean strain ellipsoid of the psammitic schist in the small domain in question is of the triaxial type and the principal axes Y and X are oriented approximately parallel to and normal to the  $L_{1-2}$ -lineation, respectively, as shown in Fig. 3.

Table 14 shows the dimensional orientation data of quartz in a quartz-rich layer in the psammitic schist of this domain which is parallel to the  $L_{1-2}$ -lineation and subparallel to the  $S_2$ -cleavage (Plate 7-4). It will be clearly pointed out that the strain ellipsoid of mean strain of quartz aggregate in the quartz-rich layer is of the triaxial

TABLE 14. Summary of grain orientation data for the specimen XIV.

Position of measurement	Vector Magnitude (%)	Probability	Significant	The angle between fold axis and vector mean (degrees)
ac-section	62.2	$<10^{-5}$	Yes	
section parallel to the layer	32.5	$<0.01$	Yes	86
section normal to the layer and ac-section	56.3	$<10^{-5}$	Yes	4

type and that the principal axis Y is parallel to the  $L_{1-2}$ -lineation and the principal axis X is normal to the lineation and parallel to the layer. This strain picture of the quartz-rich layer appears to be quite consistent with that of the psammitic matrix discussed in the preceding paragraphs.

From the above-described data, generally, it is clear that the mechanism of folding of competent layer is influenced by the orientational relation of the layer to the mean strain ellipsoid of the domain concerned. For folds of competent layers which are parallel or subparallel to the principal axis X in a domain, the mean strain ellipsoid at all position of the fold knee would be either of the axial type ( $X=Y$ ) or of the triaxial type, that being controlled by the shape of the mean strain ellipsoid of the domain. In the latter case, the principal axis X at fold knee may be frequently oriented parallel to the fold axis. And, at this time, the buckle folding of competent layer may be associated with the formation of the boudins perpendicular to the fold axis (cf. FLINN, 1962; RAMSAY, 1967).

#### V. DISTRIBUTION OF LAYER-THICKNESS IN BUCKLE FOLD

Generally, layer-thickness in folds formed by buckling is not constant, as pointed out by many authors. Variation in layer-thickness in buckle fold is the result of variation in the initial thickness of the layer and/or due to the deformation related to the formation of the fold. Therefore, following two problems must at least be examined on natural flexural folds: 1) the nature of the change of layer-thickness due to

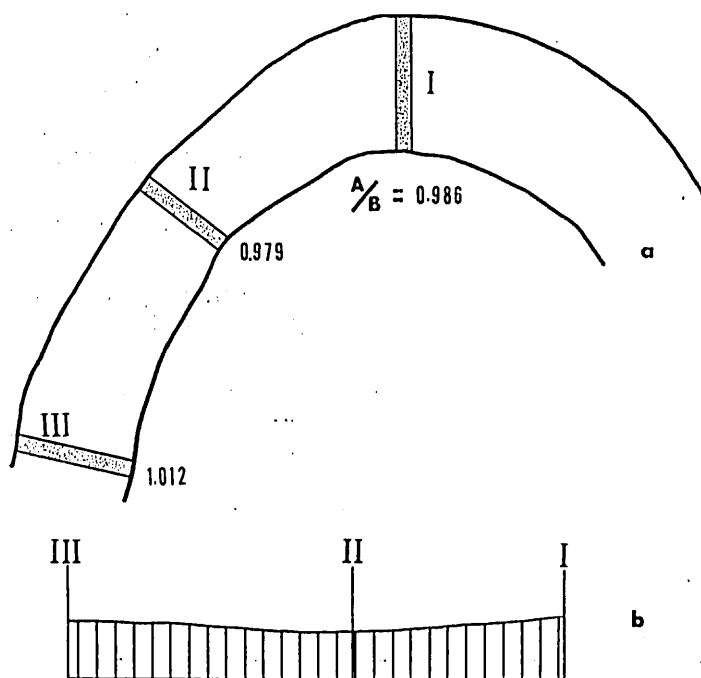


Fig. 57 Diagram showing the distribution of layer-thickness in the fold of the specimen IV.  
 a : the average  $A/B$  ratios for the domains I, II and III.  
 b : the result of the direct measurement of variation in layer-thickness in the fold.  
 I, II and III: positions of the domains I, II and III, respectively.

buckling, and (2) the relation of the initial thickness-variation to the location of fold hinge. However, only the former problem will be examined in this chapter.

The problem of the change of layer-thickness due to buckling has been examined on the folds of quartz-rich layers showing the strain pictures of Type I, Type II and Type IV by the following method; In three selected domains of a fold (domain I = column along the axial surface, domain III = column normal to the layer surface near the inflection and domain II = column containing the mid-point between the domains I and III and normal to the layer surfaces), which are placed on the plane normal to the fold axis, the over-all lengths of the individual grains parallel to and normal to the layer surface (normal to and parallel to the length of column) were measured. In each domain all the grains were measured without selection. The ratio of the two dimensions for each grain was calculated and then the average ratio for each domain. A and B are used to denote the axes of the grains parallel to and normal to the layer surface. The average  $A/B$  ratio for any domain will roughly be correlated with the change of layer-thickness in that domain which was produced by the deformation related to the formation of the fold. In the present cases, the change of dimension

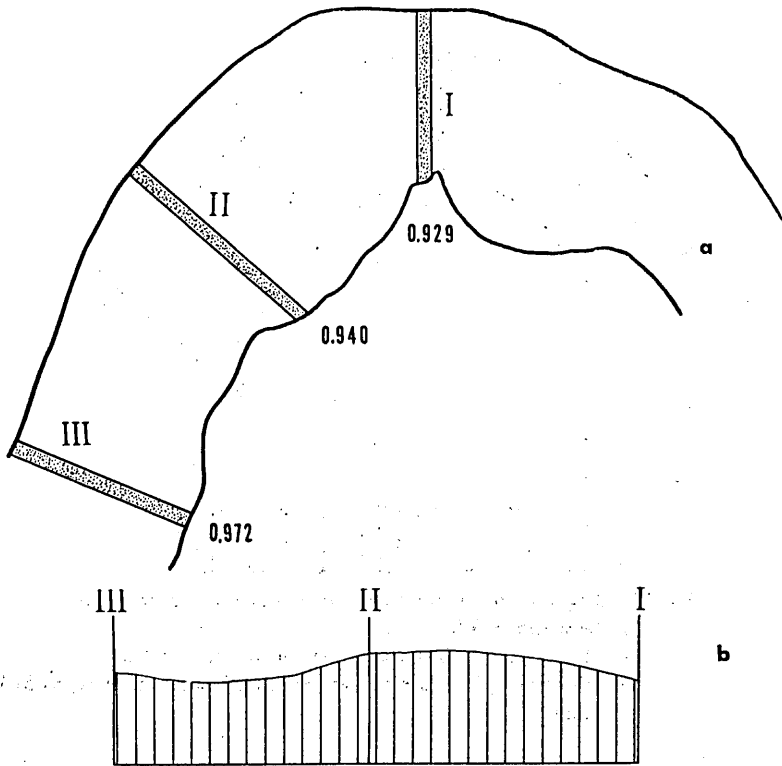


FIG. 58 Diagram showing the distribution of layer-thickness in the fold of the specimen I.

a: the average A/B ratios for the domains I, II and III.

b: the result of the direct measurement of variation in layer-thickness in the fold.

of quartz grain in a direction parallel to the fold axis is assumed to be negligible.

The data for the folds of quartz-rich layers showing the strain picture of Type I (Specimens I and IV) is shown in Figs. 57 and 58. It will be remembered that the neutral axis appears to be developed at the deeper portion of fold knee for the fold of the specimen IV than for the fold of the specimen I. For the fold of the specimen IV, the average A/B ratios for the domains I, II and III are 0.986, 0.979 and 1.012, respectively. Roughly speaking, they all approximate to 1.000, showing that the change of layer-thickness due to buckling appears to be negligible. The result of the direct measurement of variation in layer-thickness in the fold is also shown in Fig. 57.

The average A/B ratios for the domains I, II and III in the fold of the specimen I are 0.929, 0.940 and 0.972, respectively, (Fig. 58). The average A/B ratio for the domain I < that for the domain II < that for the domain III. Therefore, it will be pointed out that at any position of fold the quartz-rich layer was thickened during the deformation related to the formation of the fold, and that the amount of increase of the layer-thickness tends to increase progressively from the inflection zone of fold limb

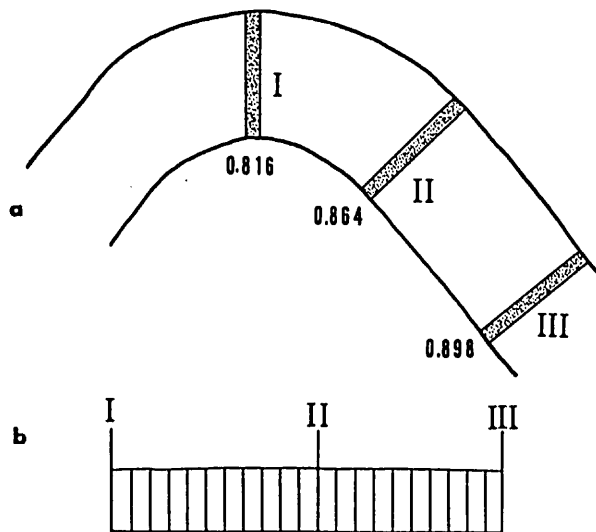


FIG. 59 Diagram showing the distribution of layer-thickness in the fold of the specimen VI.  
 a: the average A/B ratios for the domains I, II and III.  
 b: the result of the direct measurement of variation in layer-thickness in the fold.

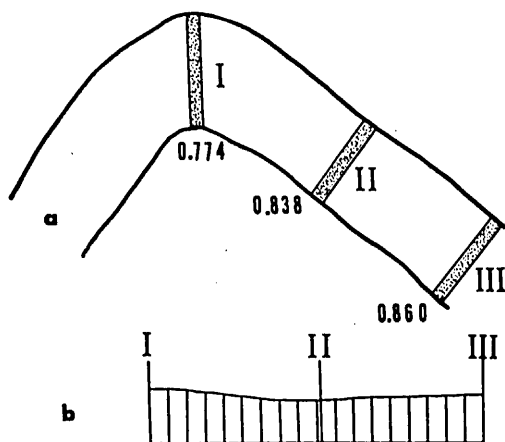


FIG. 60 Diagram showing the distribution of layer-thickness in the fold of the specimen X.  
 a: the average A/B ratios for the domains I, II, and III.  
 b: the result of the direct measurement of variation in layer-thickness in the fold.

to the axial zone.

Analogous relationship of the change of layer-thickness due to buckling appears to be also equally obvious for the fold of the specimen VI, which shows the strain picture of Type II, (the average A/B ratios for the domains I, II and III are 0.816, 0.864 and 0.898, respectively, Fig. 59), and for the fold of the specimen X, which shows the strain picture of Type IV and which among the observed folds in the Oboke psammitic schist shows the smallest value of the angle  $\beta$  when compared between the same interlimb angle, (the average A/B ratios for the domains I, II and III are 0.774, 0.838 and 0.860, respectively, Fig. 60). The results of the direct measurement of variation in layer-thickness in those folds are also shown in Figs. 59 and 60 respectively.

When the nature of the change of layer-thickness due to buckling is compared between the folds of the specimens IV (strain picture of Type I), I (strain picture of Type I), VI (Type II) and X (Type IV), which show the interlimb angles of between  $60^\circ$  and  $70^\circ$ , some important point can be found; With respect to the amount of thickening of quartz-rich layer in any domain, the fold of the specimen X > that of the specimen VI > that of the specimen I > that of the specimen IV (Fig. 61). Also with respect to the difference in the amount of thickening of quartz-rich layer between the domains I and III, X > VI > I > IV (Fig. 61).

The average A/B ratio for domain I+domain II+domain III in each fold may be roughly correlated with the average amount of the change of layer-thickness through the fold which was induced by buckling. The average A/B ratio for domain I+domain II+domain III in the fold of the specimens IV, I, VI and X is 0.992, 0.947, 0.859 and 0.826, respectively. With respect to the whole amount of shortening of quartz-rich layer through the fold, therefore, X > VI > I > IV.

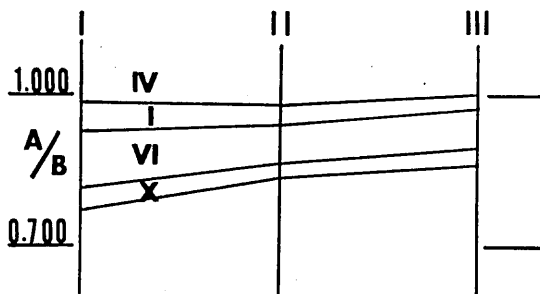


FIG. 61 Diagram showing the variation in the average A/B ratio from the domain I to the domain III for the folds of the specimens IV, I, VI, and X.  
I, II and III: the positions of the domains I, II and III, respectively.

Now, it may be generally pointed out that the nature of the change of layer-thickness due to buckling is closely related to the type of strain picture (Type I to Type V). Although the nature of the change of layer-thickness due to buckling is

not described for the folds with the strain pictures of Type III and Type V, the difference between folds with the strain pictures of Types I to V may be explained as follows: with respect to the whole amount of layer shortening, the amount of layer thickening at the axial zone and the inflection point, and the difference in the amount of layer thickening between those two positions, Type I < Type II < Type III < Type IV < Type V. This conclusion appears to agree with the theoretical prediction after RAMBERG (1964) which is for the relationship between the ratio of the rate of buckle shortening and the rate of layer shortening and the viscosity ratio of the related rocks. It may be roughly said that the layer shortening due to the folding for the strain picture of Type I is less than ca. 10 per cent, that it for the strain picture of Type II is between ca. 10 per cent and ca. 15 per cent, and that it for the strain picture of Type IV—Type V is larger than ca. 15 per cent, when interlimb angle becomes ca. 65°.

In the previous section, it has been clarified that at the initial stage of folding the axial surface develops commonly normal to the competent layer being folded and, when the folding proceeds to result in the fold with an acute form, the axial surface tends to rotate toward the principal plane XY of the mean strain ellipsoid of the system concerned. When a fold begins to show an acute form, therefore, the layer of both limbs of the fold may be oriented within the extension zone of the mean strain ellipsoid and consequently may begin to be thinned.

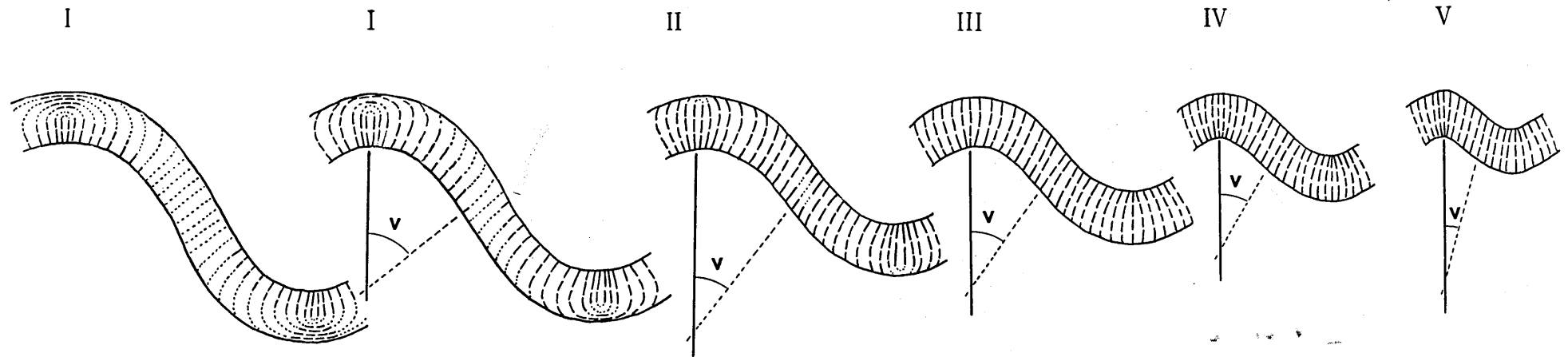
#### REFERENCES

- BIOT, M. A. (1957): Folding instability of layered viscoelastic medium under compression. *Proc. Roy. Soc. (London)*, Ser A, **242**, 444-454.
- (1961): Theory of folding of stratified viscoelastic media and its implication in tectonics and orogenesis. *Geol. Soc. Am. Bull.*, **72**, 1598-1620.
- (1964): Theory of internal buckling of a confined multilayered structure. *Geol. Soc. Am. Bull.*, **75**, 563-568.
- (1965a): Theory of similar folding of the first and second kind. *Geol. Soc. Am. Bull.*, **76**, 251-258.
- (1965b): Further development of the theory of internal buckling of multilayers. *Geol. Soc. Am. Bull.*, **76**, 833-840.
- (1965c): *Mechanics of incremental deformations*. John Wiley, New York.
- BIOT, M. A., ODÉ, H. and ROEVER, W. L. (1961): Experimental verification of the theory of folding of stratified viscoelastic media. *Geol. Soc. Am. Bull.*, **72**, 1621-1632.
- BRACE, W. F. (1955): Quartzite pebble deformation in Central Vermont. *Am. Jour. Sci.*, **253** 129-145.
- (1961): Mohr construction in the analysis of large geologic strain. *Geol. Soc. Am. Bull.*, **72**, 1059-1077.
- CARTER, N. L., CHRISTIE, J. M. and GRIGGS, D. T. (1964): Experimental deformation and recrystallization of quartz. *Jour. Geol.*, **72**, 687-733.
- CURRIE, J. B., PATNODE, H. W. and TRUP, R. P. (1962): Development of folds in sedimentary strata. *Geol. Soc. Am. Bull.*, **73**, 655-674.
- FAIRBAIRN, M. W. (1949): *Structural petrology of deformed rocks*. Addison-Wesley Press.
- (1950): Synthetic quartzite. *Am. Min.*, **35**, 735-748.
- FLINN, D. (1956): On the deformation of the Funzie conglomerates, Felter, Shetland. *Jour. Geol.*, **64**, 480-505.
- (1962): On folding during three dimensional progressive deformation. *Geol. Soc. London Quart. Jour.*, **118**, 385-433.
- GHOSH, S. K. (1966): Experimental tests of buckling folds in relation to strain ellipsoid in simple shear deformations. *Tectonophysics*, **3**, 169-185.

## Geometry and Internal Structures of Flexural Folds

- HARA, I. (1963): Petrofabric analysis of a drag fold. *Geol. Report Hiroshima Univ.*, **12**, 463-492.
- (1965): Quartz fabrics in a kink band. *Jour. Sci. Hiroshima Univ.*, Ser. C, **5**, 1-12.
- (1966a): Movement picture in confined incompetent layers in flexural folding-Deformation of hetelogeneously layered rocks in flexural folding (I). *Jour. Geol. Soc. Japan*, **72**, 363-369.
- (1966b): Strain and movement pictures in competent layers in flexural folding-Deformation of hetelogeneously layered rocks in flexural folding (II). *Jour. Geol. Soc. Japan*, **72**, 413-425.
- (1966c): Dimensional fabric of quartz in a concentric fold. *Jap. Jour. Geol. Geogr.*, **37**, 123-139.
- (1967): A note on Concentric folding of multilayered rocks. *Jour. Sci. Hiroshima Univ.*, Ser. C, **5**, 217-239.
- HARA, I. NISHIMURA, Y. and ISAI, T. (1966): On the difference in deformation behaviour between phenocryst and groundmass quartz of deformed rhyorite in the Oboke conglomerate schist. *Jour. Sci. Hiroshima Univ.*, Ser. C, **5**, 179-216.
- IWASAKI, M. (1963): Metamorphic rocks of the Kōtsu-Bizan area, Eastern Shikoku. *Jour. Facult. Sci. Univ. Tokyo*, Sec. II, **15**, 1-90.
- KOJIMA, G. (1951): Stratigraphy and geological structure of the crystalline schist region in Central Shikoku. (In Japanese). *Jour. Geol. Soc. Japan*, **57**, 177-190.
- KOJIMA, G. and MITSUNO, C. (1966): Geological map of Kawaguchi, Tokushima Prefecture, with an explanatory text (in Japanese). Geol. Surv. Japan.
- KNILL, J. L. (1960): A classification of cleavages, with special reference to the Craignish district of the Scottish Highlands. *Internat. Geol. Cong, 21st, Copenhagen, Rept.*, **18**, 317-325.
- MCBIRNEY, A. R. and BEST, M. (1961): Experimental deformation of viscous layers in oblique stress field. *Geol. Soc. Am. Bull.*, **72**, 495-498.
- MIYASHIRO, A. (1965): *Metamorphic rocks and metamorphic belts*. (in Japanese). Iwanami.
- OFTENDAHL, C. (1948): Deformation of quartz conglomerate in Central Norway. *Jour. Geol.*, **56**, 476-487.
- RAMBERG, H. (1959): Evolution of pygmatic folding. *Norsk Geol. Tidssk.* **39**, 36-46.
- (1960): Relationship between length of arc and thickness of pygmatically folded veins. *Am. Jour. Sci.*, **258**, 36-46.
- (1963): Fluid dynamics of viscous buckling applicable to folding of layered rocks. *Am. Assoc. Petrol. Geol. Bull.*, **47**, 484-505.
- (1964): Selective buckling of composite layers with contrasted rheological properties, a theory for simultaneous formation of several orders of fold. *Tectonophysics*, **1**, 307-341.
- RAMSEY, J. G. (1967): *Folding and fracturing of rocks*. McGraw-Hill. New York.
- SEKI, Y. (1961): Geology and metamorphism of Sanbagawa crystalline schists in the Tenryu district, Central Japan. *Sci. Rep. Saitama Univ.*, Ser. B. 75-92.
- SITTER, L. U. de (1956): *Structural geology*. McGraw-Hill, New York.
- TURNER, F. J. and WEISS, L. E. (1963): *Structural analysis of metamorphic tectonites*. McGraw-Hill. New York.
- WILLIAMS, E. (1961): The deformation of confined, incompetent layers in folding. *Geol. Mag.*, **98**, 317-328.
- WILLSON, G. (1946): The relationship of slaty cleavage and kindred structures to tectonics. *Proc. Geol. Ass. London.*, **57**, 63-300.

IRUO HARA: INSTITUTE OF GEOLOGY AND MINERALOGY,  
FACULTY OF SCIENCE,  
HIROSHIMA UNIVERSITY, HIROSHIMA JAPAN,  
SEIJI UCHIDAYASHI:            //  
YUJI YOKOTA:                    //  
HAYAO UMEMURA:               //  
MASANOBU ODA: DEPARTMENT OF FOUNDATION ENGINEERING,  
SAITAMA UNIVERSITY, URAWA JAPAN



EXPLANATION OF PLATE IV

Schematic diagram showing the relationship between the strain pictures of Type I, Type II, Type III, Type IV and Type V.

I, II, III, IV and V: Strain pictures of Type I, Type II, Type III, Type IV and Type V, respectively.

Dashed lines: Trajectories of principal axis X.

Dotted lines: Domains in which material does not show available distortion.

$v$ :  $\beta/2$ .

## EXPLANATION OF PLATE V

FIGS. 1 and 2    Folded and non-folded quartz-rich layers in the psammitic schist of the small domain in the hinge zone of the Kobokey syncline.

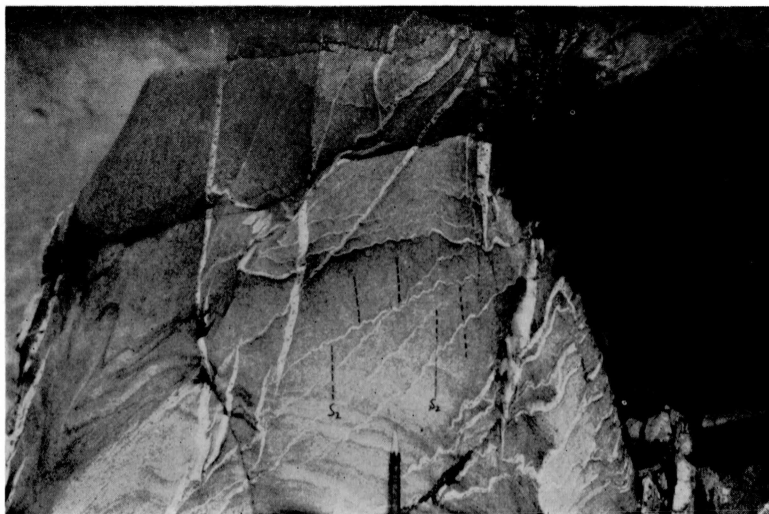


FIG. 1

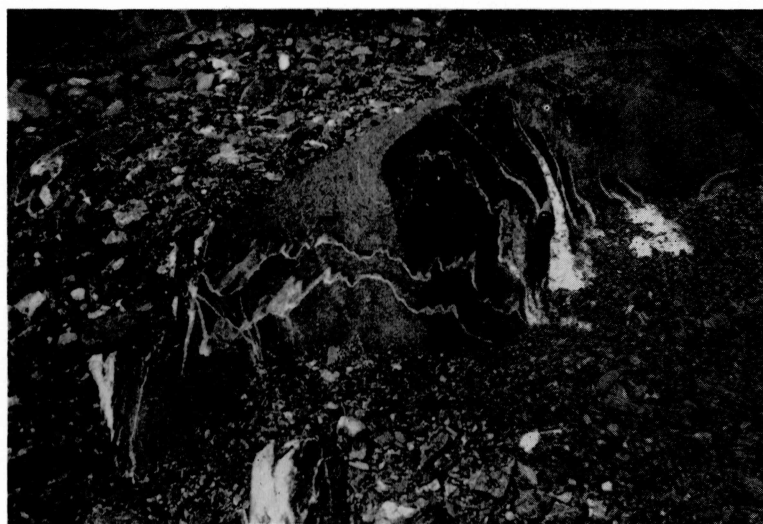


FIG. 2

## EXPLANATION OF PLATE VI

FIG. 1 Cleavage of Type I found in the pelitic schist of the Kune district.

FIG. 2 Cleavage of Type II found in the pelitic schist of the Kune district.

FIG. 3 Cleavage of Type III found in the pelitic schist of the Kune district.

FIG. 4 Cleavage of Type III found in the pelitic schist of the Kune district.

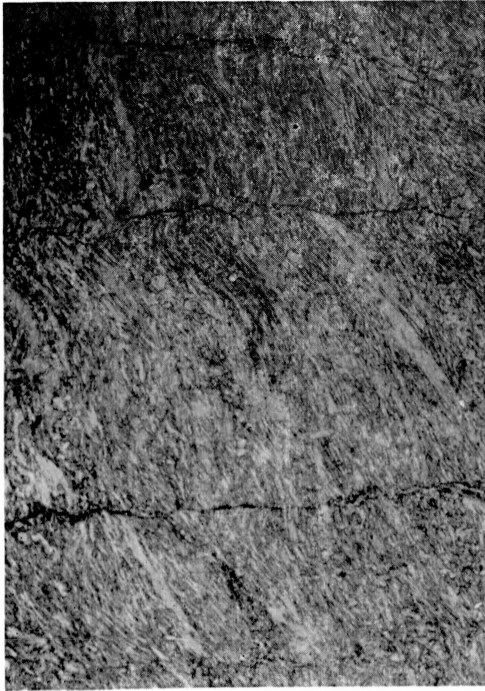


FIG. 1



FIG. 2



FIG. 3



FIG. 4

## EXPLANATION OF PLATE VII

- FIG. 1 Cleavage of Type IV found in the pelitic schist of the Kune district.
- FIG. 2 Cleavage of Type IV found in the pelitic schist of the Kune district, showing transition of the cleavage to the foliation-schistosity.
- FIG. 3 Cleavage of Type IV found in the pelitic schist of the Kune district, showing transition of the cleavage to the foilation-schistosity.
- FIG. 4 Preferred grain orientation of quartz in a quartz-rich layer which is slightly oblique to the  $S_2$ -cleavage (the principal plane XY of the mean strain ellipsoid) in the psammitic schist of the small domain in the hing zone of the Koboke syncline.

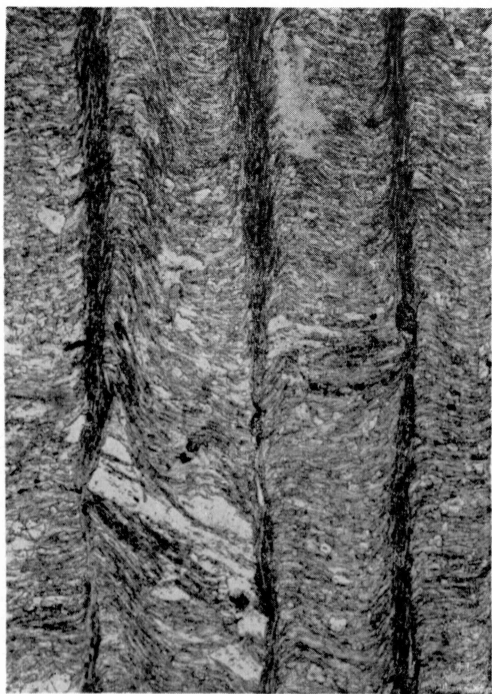


FIG. 1



FIG. 2

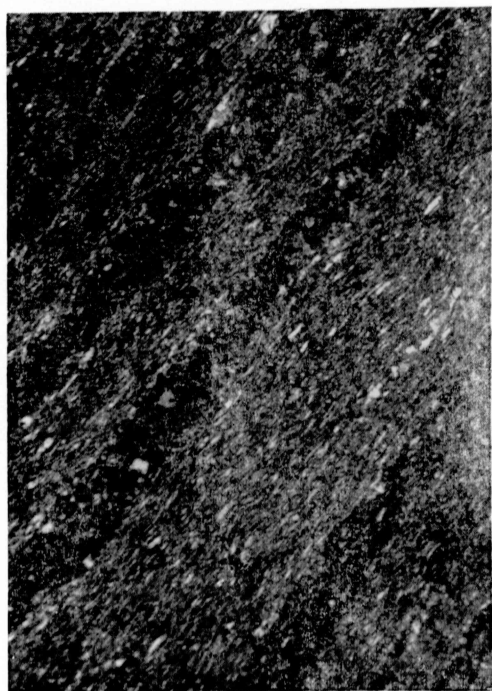


FIG. 3

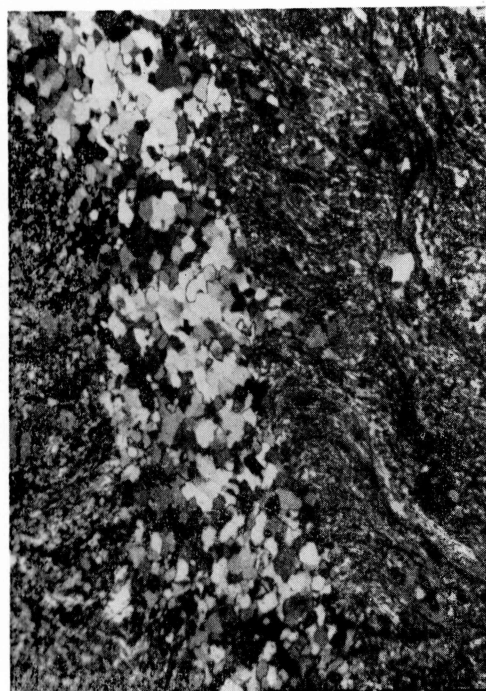
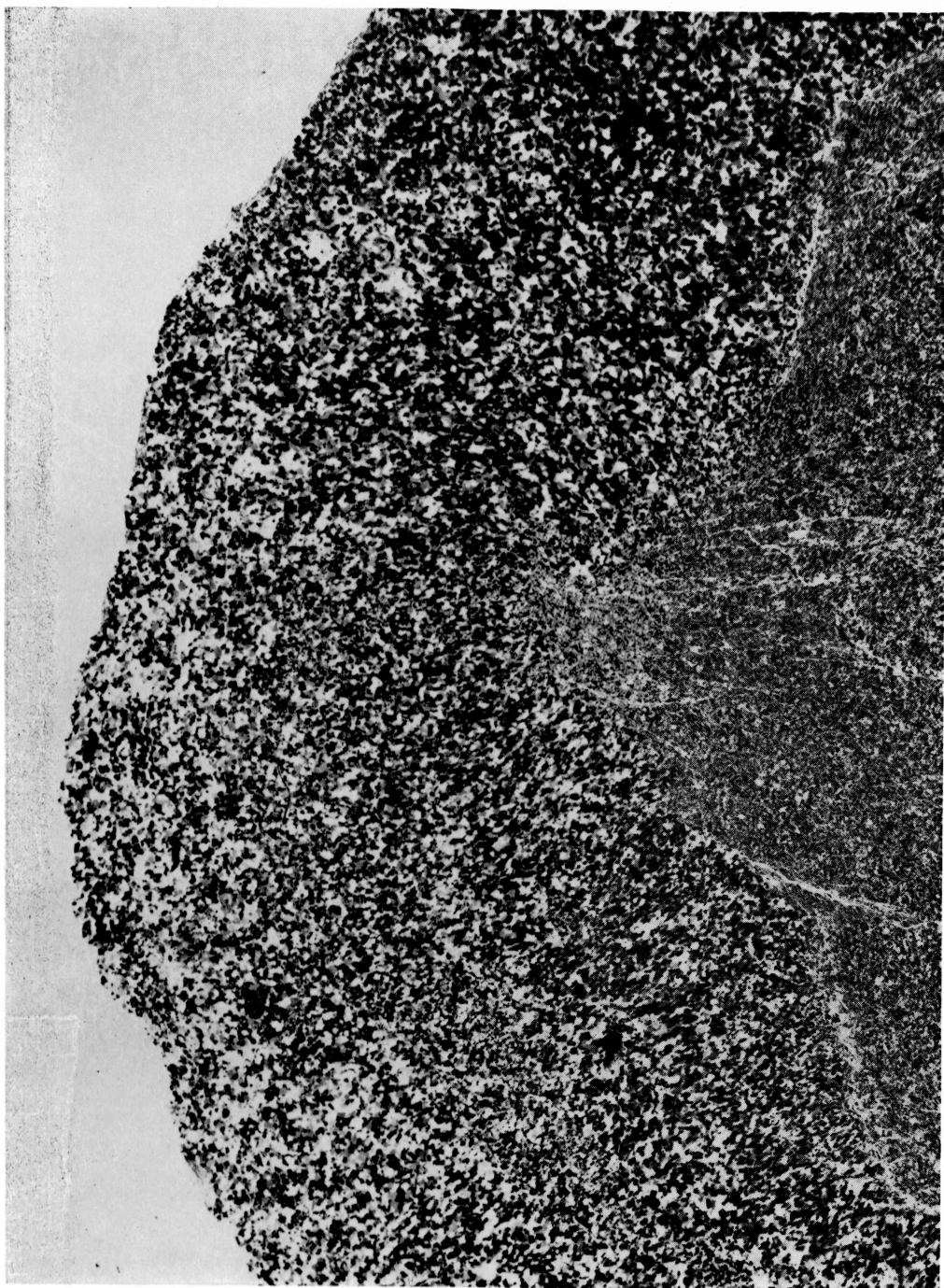


FIG. 4

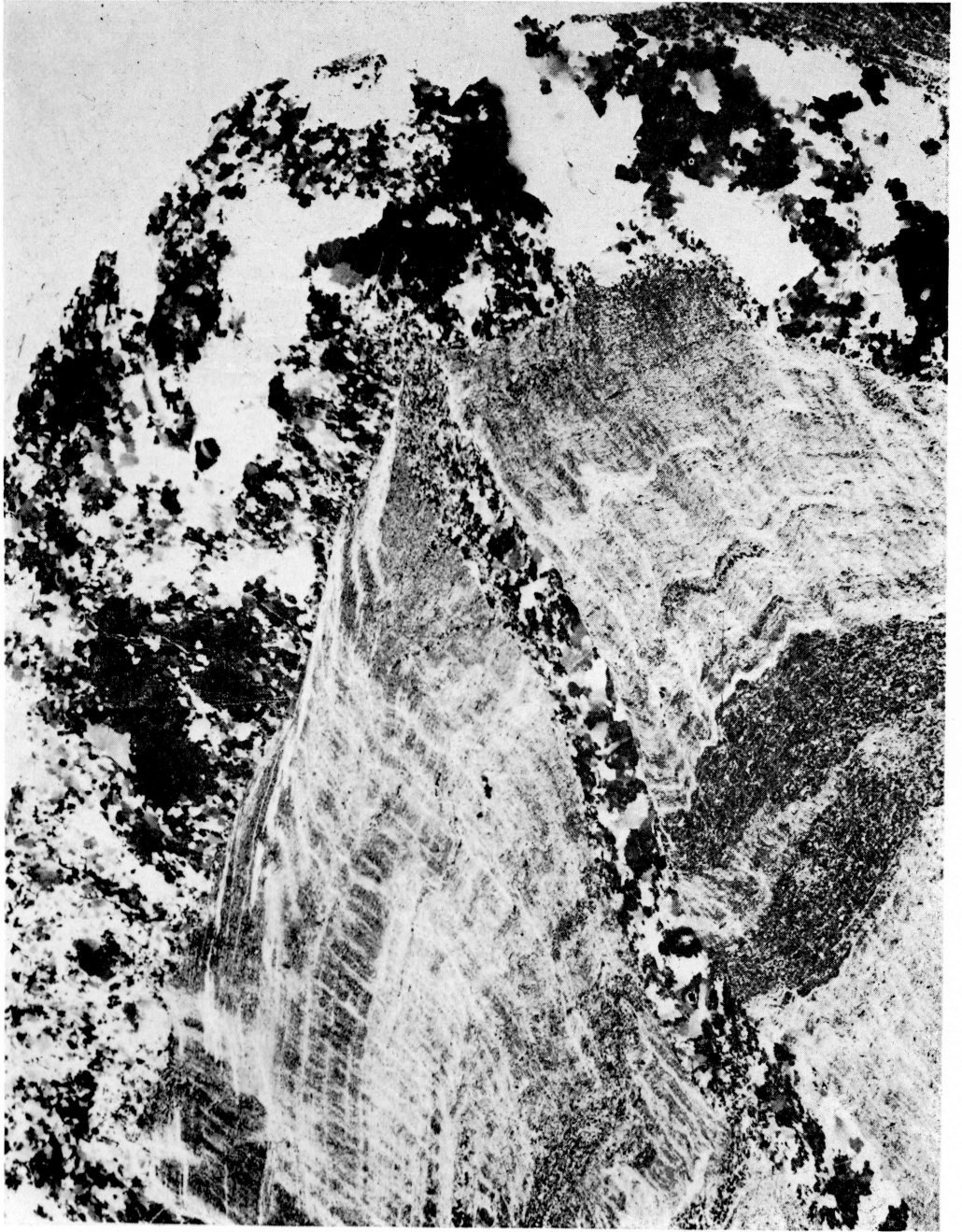
## EXPLANATION OF PLATE VIII

Grain orientation of quartz in the fold of quartz-rich layer in the specimen I.



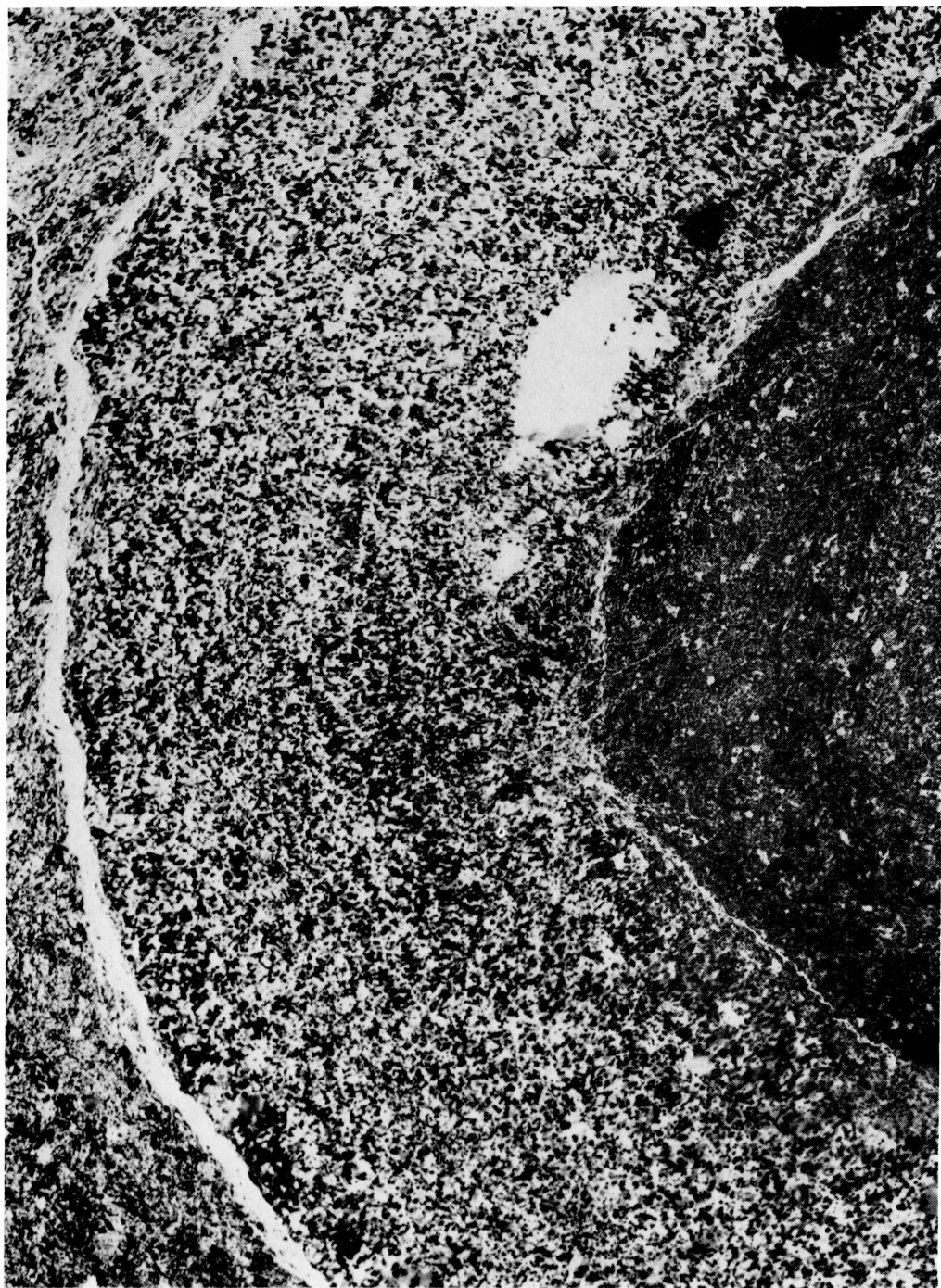
## EXPLANATION OF PLATE IX

Grain orientation of quartz in the folded and non-folded quartz-rich layers in the specimen V.



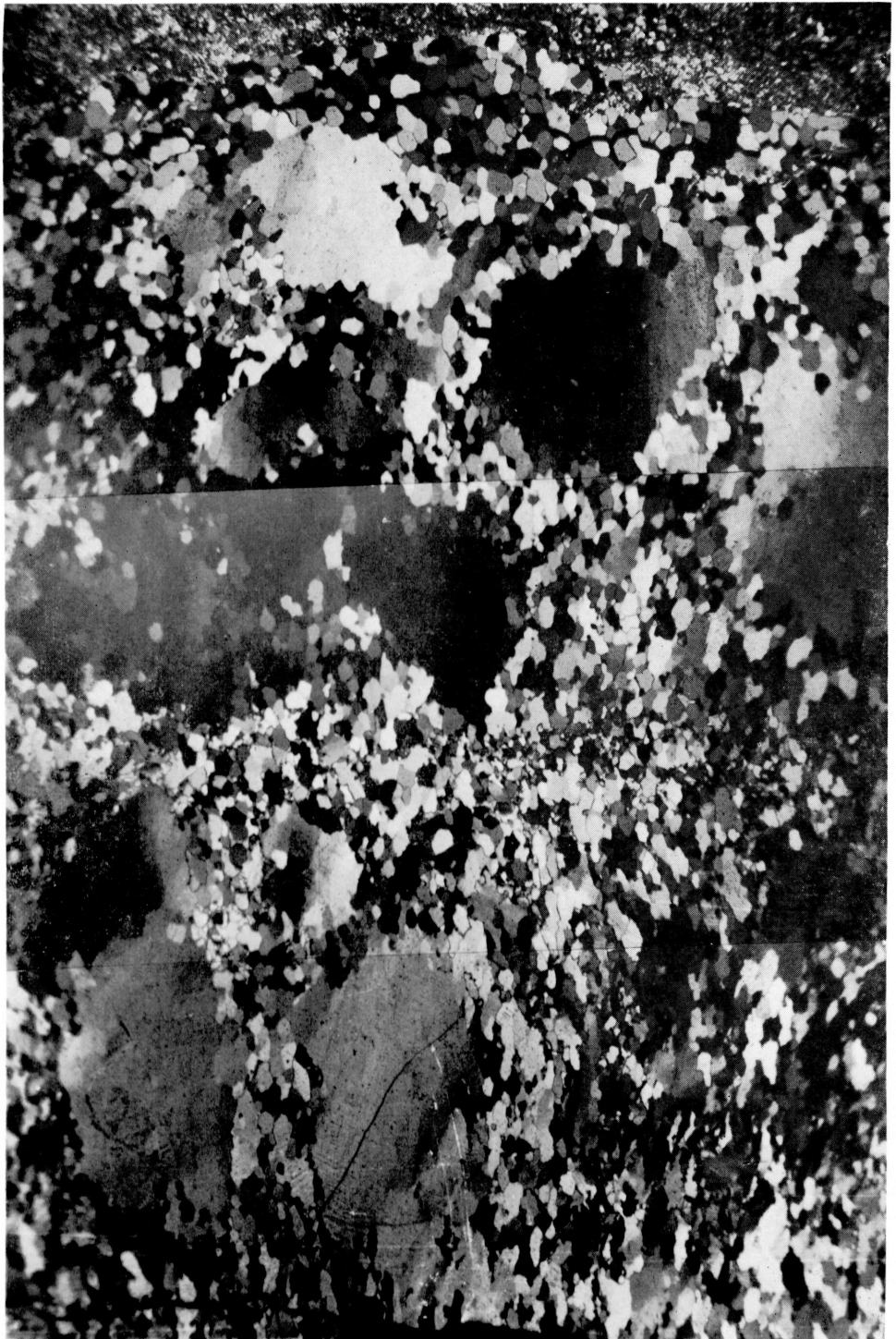
EXPLANATION OF PLATE X

Grain orientation of quartz in the fold of quartz-rich layer in the specimen VI.



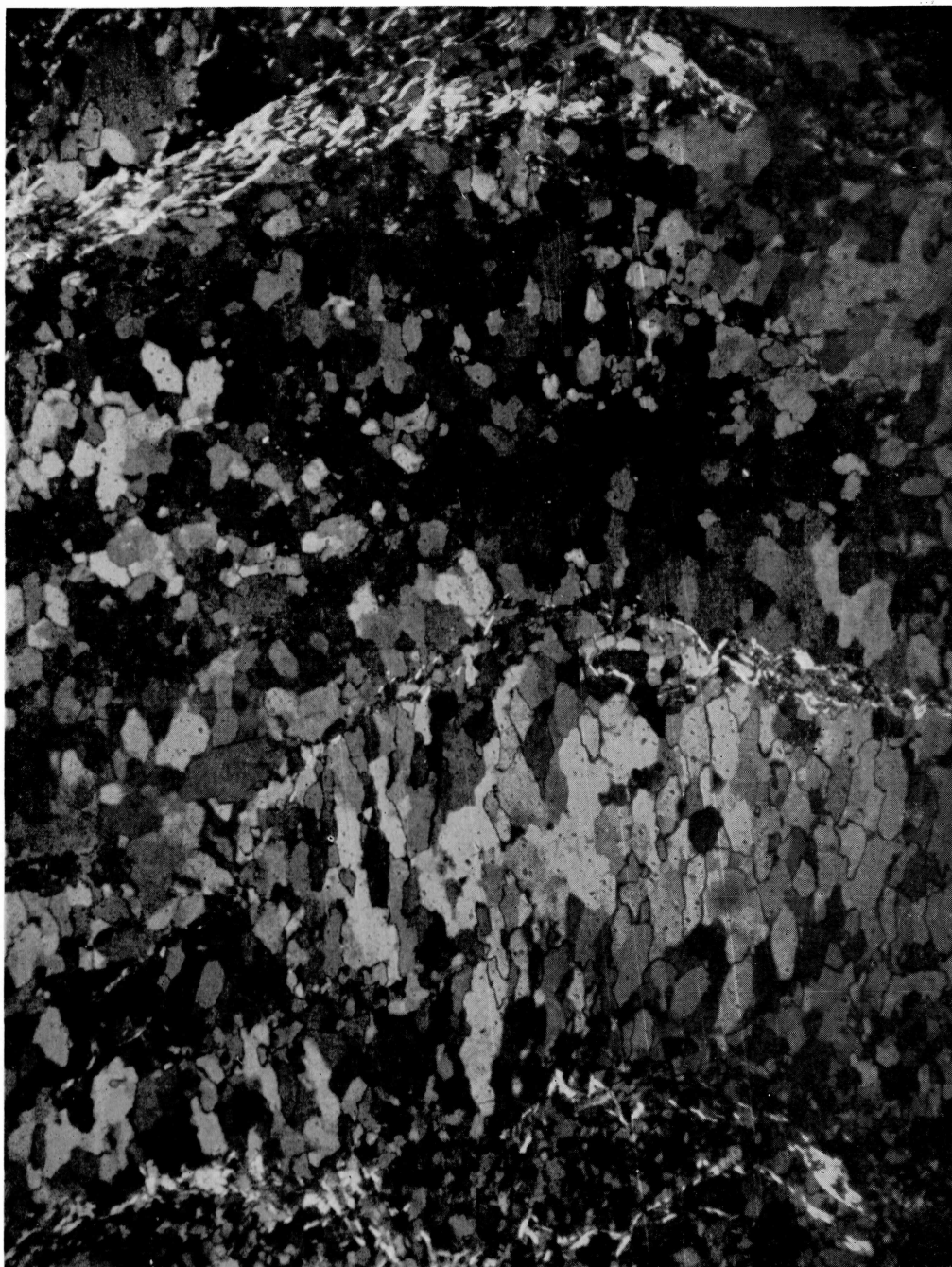
EXPLANATION OF PLATE XI

Grain orientation of quartz at the hinge zone of fold of quartz-rich layer in the specimen VII.



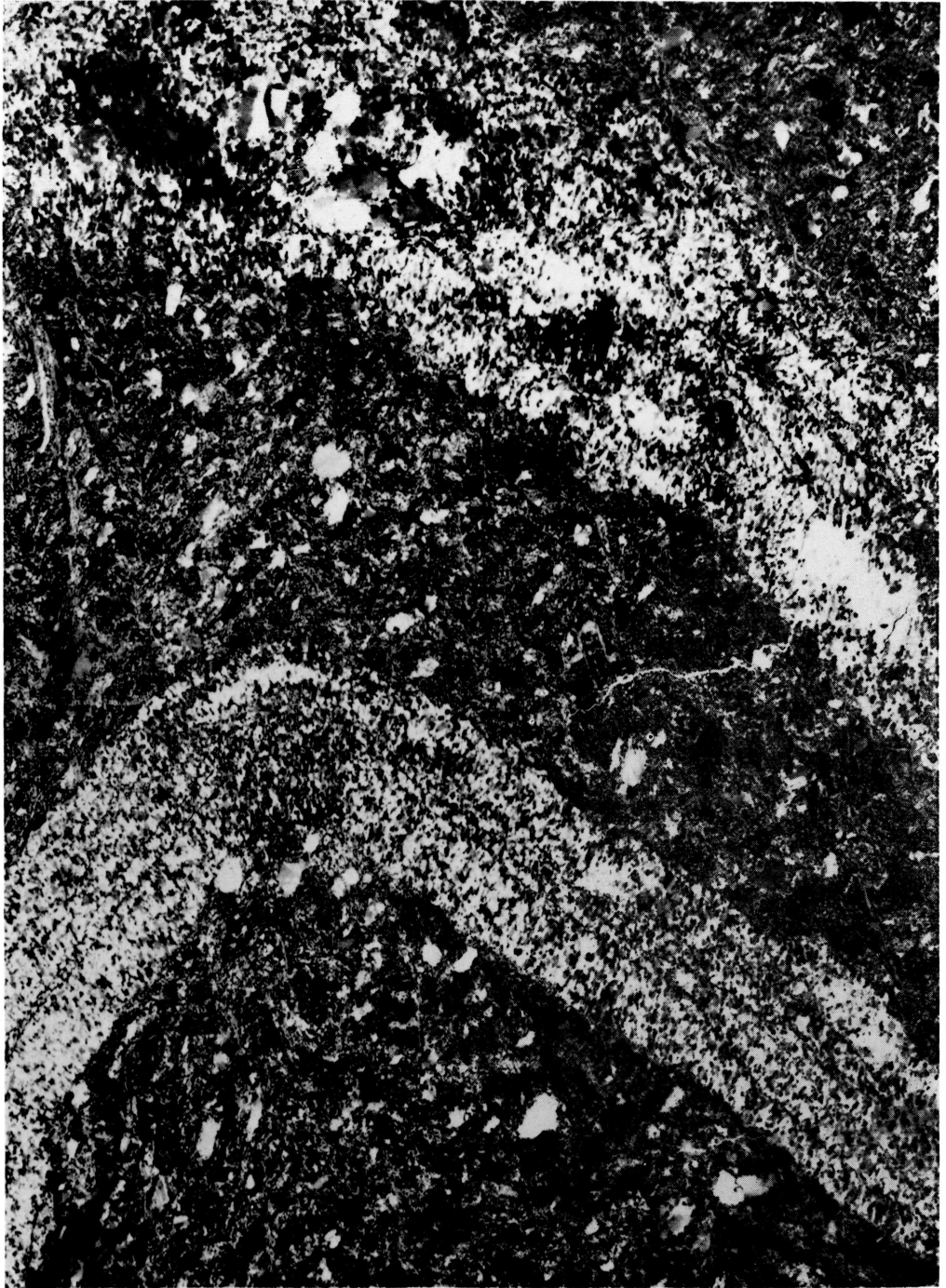
## EXPLANATION OF PLATE XII

Grain orientation of quartz in the hinge zone of fold of quartz-rich layer in the specimen IX.



### EXPLANATION OF PLATE XIII

Grain orientation of quartz in the fold of quartz-rich layer in the specimen X.



## EXPLANATION OF PLATE XIV

Grain orientation of quartz in the hinge zone of fold of quartz-rich layer in the specimen X.

